CLEARINGHOUSE FOR FEDERAL SCIENTIFIC AND TECHNICAL INFORMATION CFSTI
DOCUMENT MANAGEMENT BRANCH 410.11

LIMITATIONS IN REPRODUCTION QUALITY

ACCESSION #

☐ 1. LEGIBILITY OF THIS DOCUMENT IS IN PART UNSATISFACTORY. REPRODUCTION HAS BEEN MADE FROM THE BEST AVAILABLE COPY.

☐ 2. ORIGINAL DOCUMENT CONTAINS COLOR OTHER THAN BLACK AND WHITE AND IS AVAILABLE IN LIMITED SUPPLY. AFTER PRESENT STOCK IS EXHAUSTED, IT WILL BE AVAILABLE IN BLACK-AND-WHITE ONLY.

☐ 3. THE REPRODUCIBLE QUALITY OF THIS DOCUMENT IS NOT ADEQUATE FOR PUBLIC SALE. AVAILABLE TO CUSTOMERS OF THE DEFENSE DOCUMENTATION CENTER ONLY

☐ 4. DOCUMENT AVAILABLE FROM CLEARINGHOUSE ON LOAN ONLY (TECHNICAL TRANSLATIONS).

PROCESSOR:

TSL-107-12 64

TROPICAL PROPAGATION RESEARCH

Semi-annual Report No. 1

JULY 1962 — DECEMBER 1962

Prepared for

U.S. ARMY ELECTRONICS RESEARCH AND DEVELOPMENT LABORATORY

Signal Corps Contract
DA 36-039 SC-90889

JANSKY & BAILEY
A Division of Atlantic Research Corporation
Washington, D. C. Alexandria, Va.

TROPICAL PROPAGATION RESEARCH

Semi-Annual Report No. 1

July 1962 - December 1962

Prepared for

U.S. ARMY ELECTRONICS RESEARCH
AND DEVELOPMENT LABORATORY

Signal Corps Contract
DA 36-039 SC-90889

Approved by

Frank T. Mitchell, Jr.
Director, Research and
Engineering Division

L. G. Sturgill
Project Director

TABLE OF CONTENTS

ABSTRACT

This report describes the work performed by Jansky & Bailey, A Division of Atlantic Research Corporation under Signal Corps Contract DA 36-039 SC-90889 during the six month period from July 1962 to January 1963.

The basic concepts of the theoretical and experimental studies of radio propagation in jungle environments are reviewed. Results of a survey of literature pertaining to radio propagation in tropical areas and propagation over rough terrain are included. The details of a site survey are presented and describe, to a certain extent, the environment in which the proposed tests will be conducted.

A discussion of the tests planned includes a description of the measurements, test equipment and measurement techniques. The theoretical studies required to fulfill the requirements of the contract are summarized and presented along with the results accomplished to date. A theoretical analysis of the quadrant dipole antenna is included in the appendix.

LIST OF ILLUSTRATIONS

LIST OF ILLUSTRATIONS (con't)

1.0 INTRODUCTION

The Jansky & Bailey Division of Atlantic Research Corporation, Alexandria, Virginia, is engaged in a program to conduct theoretical and experimental studies of radio propagation in jungle environments. The purpose of this program is to obtain information that will serve as guidance (1) for the more efficient use of presently available radio equipment and (2) for the design and development of new equipment which is intended to provide short range tactical communications through tropical jungles. Under the direction of the U.S. Army Electronics Research and Development Agency (USAELRDA) this work is being carried out through Contract DA-36-039-SC-90889 and in accordance with Signal Corps Technical Requirement SCL-4379A, dated 13 July 1962, which has been specified in this contract.

Contract Modification 1, dated 29 August 1962, directed the contractor to carry out the Primary Field Tests of this program at a location in Thailand and to integrate the technical objectives and experimental results of this program into the Southeast Asia Communications Research Project (SEACORE). Under the over-all management of the Advanced Research Project Agency (ARPA), work on Project SEACORE is being conducted in both the United States and Southeast Asia. In Thailand, ARPA has established the ARPA Research and Development Field Unit to coordinate Project SEACORE and other research and development field efforts which are being applied in that area of Southeast Asia. The SEACORE objective with which Jansky & Bailey is primarily concerned is that of obtaining the theoretical and experimental knowledge of radio propagation in tropical jungle terrain necessary to develop improved communications techniques and devices needed by friendly indigenous forces in Southeast Asia.

2.0 GENERAL DISCUSSION

The communication engineer concerned with the employment of tactical radio systems in a tropical jungle environment is confronted with a wide variety of problems and limitations which arise from difficulties in propagating a radio wave through the lossy jungle growth. These problems and limitations can, perhaps, be brought into focus more clearly by a brief reference to the transmission loss equation, commonly written in the following form:

$$P_t = L_b - G_t - G_r + S/N + F_a + R_p + P + K \text{ (db)} \qquad (2.1)$$

where

P_t = minimum power required for satisfactcry transmission

L_b = basic transmission loss, or path loss

G_t = the transmitting antenna power gain

G_r = the receiving antenna power gain

S/N = the required receiver signal-to-noise ratio

F_a = the local noise grade, when it is applicable

R_p = the factor introduced for reliability reasons

P = polarization alignment factor, generally 0 db

K = lumped losses due to transmission lines, etc.

In the above equation, the only factors which are not associated directly with the performance of the transmitting and receiving equipments are L_b and F_a. The factor L_b is associated with the propagation mechanism and F_a with the geographical location. Of these two, L_b presents much the greater difficulty with which to deal.

In the cases of the more conventional modes of propagation over a smooth earth (such as the conventional ground wave, line-of-sight, etc.) the behavior of path loss, L_p, as a function of distance from the transmitting antenna and as a function of frequency is fairly well understood through the continual accumulation

of pertinent data over the years which have been analyzed and refined. Consequently, under these circumstances, the above equation can be applied to systems using these modes to predict system performance and to indicate directions toward system improvement, with a small uncertainty in the results.

However, when the propagation path involves a rough boundary (such as an irregular terrain or terrain covered with foliage), the natural behavior of L_b is statistical in both time and space. A graphic example of this behavior in relation to rough terrain is provided by Figure 2.1 which was taken from work previously done by this contractor. Therefore, to deal constructively with the parameter, L_b, and its effect in the cited transmission equation requires the language and techniques of statistical methods and probability theory.

The somewhat deterministic concepts of radio propagation loss are gradually giving way to the concepts which relate the system parameters in the transmission equation to some probability distribution of a successful signal reception at the receiver. More often, today, the questions are asked, "What is the probability that a given transmitter-receiver system will communicate at a certain range in a particular mode of propagation?"; "What is the probability that two transceivers can communicate when separated a distance, d, in a Thailand jungle?"; "How does the statistical distribution of terrain elevation affect this probability?"

To answer these questions as they apply to radio wave propagation requires a quantity of data representing samples, or measures, of the propagation phenomena, L_b, which have been observed over an interval of time and space with the remainder of the system parameters in the preceding equation held ideally at a fixed state.

The principal Tasks presented in Signal Corps Technical Requirement SCL-4379A are appropriately aligned with the basic concepts discussed above and, in effect, these Requirements direct the contractor to obtain appropriate propagation data for all potentially useful modes associated with the jungle over major sample spaces or intervals. While the primary concern of this program is devoted to

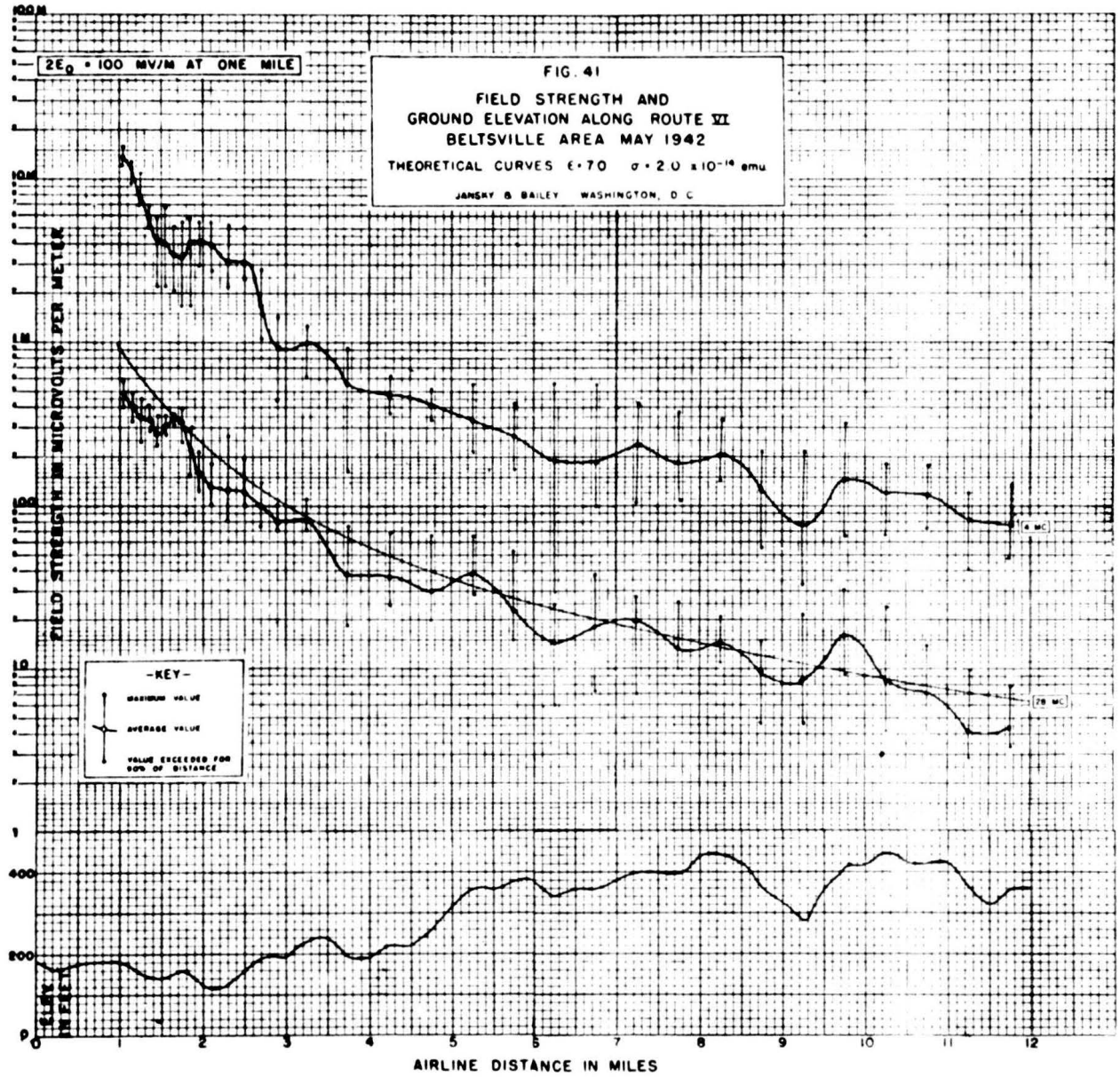

Figure 2 1. Field Strength Versus Distance Over Irregular Terrain

tropical jungle terrain, these Tasks, taken all together, constitute a program of considerable magnitude that may be expected to significantly advance the ability to deal with the more general problems associated with radio propagation over a non-smooth imperfect earth commonly encountered in the engineering of short-range vehicular and man-packed communication systems.

For convenience, the following descriptions of these Tasks, condensed from the Technical Requirement, are summarized.

> Task I - Primary Field Tests. This Task shall consist of field tests conducted in a dense jungle environment in Thailand. These tests shall be designed to experimentally measure all the pertinent factors which influence the propagation of radio waves in dense jungle areas during both wet and dry seasons. The tests shall be primarily concerned with distance ranges up to thirty miles and with ranges greater than thirty miles where necessary for the measurement of a particular mode of transmission (for example, the ionospheric mode). Measurements shall be made over various types of terrain and over a frequency range which covers the MF through VHF bands, and desirably will be extended into the LF band. In these frequency and distance ranges the path loss will be measured for all practical modes of propagation, including a measurement of short term variations, diurnal variations, seasonal variations, and atmospheric noise levels. The effects of polarization and the effects of changing the transmitter and receiver antenna elevations shall be determined in terms of measured path loss for the various modes.
>
> Data reduction and preliminary analysis of the data from the field tests shall be performed in Thailand, and the preliminary results of this work shall be submitted to the COTR in that area.

Task II - Statistical Terrain Studies. This task is concerned with the statistical correlation of propagation information obtained from the field tests with the tropical terrain characteristics, such that a relationship can be determined between the physical and the electromagnetic properties of the jungle. This Task shall include a detailed study of the characteristics and variations of tropical terrain, types of vegetation, and weather conditions generally encountered in jungle environments. A systematic nomenclature and descriptive terminology shall be developed to promote easy identification of jungle types regardless of geographic location. The results shall be analyzed with the objective of developing procedures for siting and frequency selection in all varieties of tropical terrain.

Task III - Secondary Field Tests. This Task shall consist of additional field tests at locations other than those used in Task I for the purpose of confirming and extending the results of Tasks I and II.

Tasks IV and V - **Instrumentation and Test Facilities.** These Tasks consist of the design, procurement and assembly of instrumentation and portable test facilities. These requirements are necessary to carry out Tasks I and III. All equipments shall be complete, calibrated, and checked out prior to shipment to the test location.

It may, therefore, be considered that the major technical objective of the Primary Field Tests is to obtain the data required under Task I above, and to provide a preliminary reduction and analysis of these data for the use of the ARPA R&D Field Unit in Thailand. All data will be sent to the Jansky & Bailey laboratory for the more detailed and extensive analysis involved in the performance of Task II.

It is obvious from the descriptions of Tasks I and II that a very large amount of reliably measured field data, covering

a relatively large jungle area, will have to be acquired in a short period of time (approximately ten months) in order to obtain a sufficiently large statistical sample for use in the performance of Task II.

The fundamental planned approach to this measurement program in Task I is simple and direct. First, the location of a jungle area approximately thirty miles square, having appropriate terrain characteristics, is to be established. Next, transmitters covering the frequency range of interest will be set up at a base site in this area. These transmitters will be sufficiently powerful to place a measurable signal level throughout most of the area for the various frequencies and modes of propagation to be measured. Then, a system of measuring sites will be established along at least three radial sectors extending into the area in different directions so as to give path profiles differing in roughness. Measurements of field strength and atmospheric noise levels are then carried out at these measuring sites for the different frequencies and propagation conditions involved. Since the measuring sites must be immersed in the jungle foliage, they must be situated so that they are accessible by the existing trails and cart tracks in the area. The field strength measurements at the measuring sites will be supplemented by continuous recordings of field strength taken in the vehicles as they move from one measuring site to the next. The over all effect of this entire procedure is to measure the spatial distribution of the test signals as a function of horizontal distance from the transmitter, and as a function of heights up to eighty feet above the ground, for the various frequencies and modes of propagation to be investigated during this program.

The sections which follow in this document describe in some detail the work performed during the reporting period July 1962 to January 1963. This work included a review of existing literature and information on jungle propagation, a site survey, the preparation of a field test plan, a series of studies required in preparation of the data analysis, and the theoretical analysis of an antenna suitable for short distance ionospheric circuits.

3.0 LITERATURE REVIEW

At the outset of the Tropical Propagation Research Program a review of existing literature and other information on jungle propagation was initiated. The purpose of this review was to familiarize project personnel with the procedures, results and conclusions of previous propagation experiments conducted in jungle environments before preparing the test plan for this program. Three significant reports prepared by Herbstreit and Chrichlow, 1943; Whale, 1945; and Busch, 1962, were reviewed and given consideration in the preparation of the test plan for this program. Summaries of these reports are included in this section.

Other reports describing the effects of temperate forests and irregular terrain on radio waves were also reviewed in order to determine whether techniques used in existing mathematical models for predicting foliage attenuation and the effects of irregular terrain might be applicable in this program. Included in this group of reports are those prepared by B. Trevor, 1940; Jansky & Bailey, 1943; K. Bullington, 1947, 1950; Saxton and Lane, 1955; J.J. Egli, 1957; H.T. Head and O.L. Presthold, 1960; H.T. Head, 1960; Dr. H.R. Reed, 1962; P.L. Rice, 1962; and H.H. LaGrone, 1963. Summaries of several of these reports are given in this section. A modification of the propagation model presented by P.L. Rice is given in a later section.

3.1 Measurement of Factors Affecting Jungle Radio Communication

In 1943, Herbstreit and Chrichlow reported the results of field strength measurements on signals propagated through jungle vegetation at frequencies of 2, 6, 44, and 99 Mc. The attenuation was found to be so great that for communication greater than approximately one mile, the ground wave which is normally employed for these ranges was practically useless for the equipment used in the test. It was concluded that communications over distances greater than one mile necessitate either (1) treetop-to-treetop or hill-to-hill transmitter and receiver sites at very high frequencies so that the transmission path is mainly above the top of the jungle; or, (2) use of skywave transmission at high frequencies wherein

the transmission is up to the ionosphere and back to the ground.

The test transmitters were Signal Corps SCR-694, SCR-511, SCR-300, and an AN/TRC-1. Vertical whip antennas near the ground were used on all frequencies except 99 Mc. At this frequency a half-wave dipole mounted on an 18-foot mast was used with both vertical and horizontal polarization.

In order to compare the attenuation over a dense jungle path with that obtained over a non-jungle path in the same area, field strength measurements were made over flat open ground with measurable ground conductivity and dielectric constant. These measurements were also used to estimate the radiated power of the transmitters.

A base station for the transmitting equipment was set up in a small jungle clearing about 150 feet from a highway. Measurements of field strength versus distance were made at four frequencies along the same radial jungle path. These measurements were obtained by driving down the highway and stopping at intervals of 0.1 mile to cut a path into the jungle. At each point the measuring equipment was carried at least 100 feet into the jungle. In addition to the point-to-point measurements made parallel to the highway, a continuous recording of field strength versus distance was made at 44 Mc along a trail through the jungle. The results of these tests at three frequencies are compared with the results of similar tests by Whale in a later section.

Figure 3.1 shows the foliage attenuation versus distance for four of the test frequencies. The data for these curves was obtained by comparing measurements over the non-jungle path with measurements over the jungle path at corresponding distances. For each curve on this figure, the attenuation increases as a function of distance but increases at a decreasing rate. A similar trend was noted by H. Head, 1960, while conducting experiments in a wooded area near Salisbury, Maryland.

It was found that considerable difference in both jungle attenuation and field strength variation existed between horizontal and vertical polarization. The vertically polarized fields were

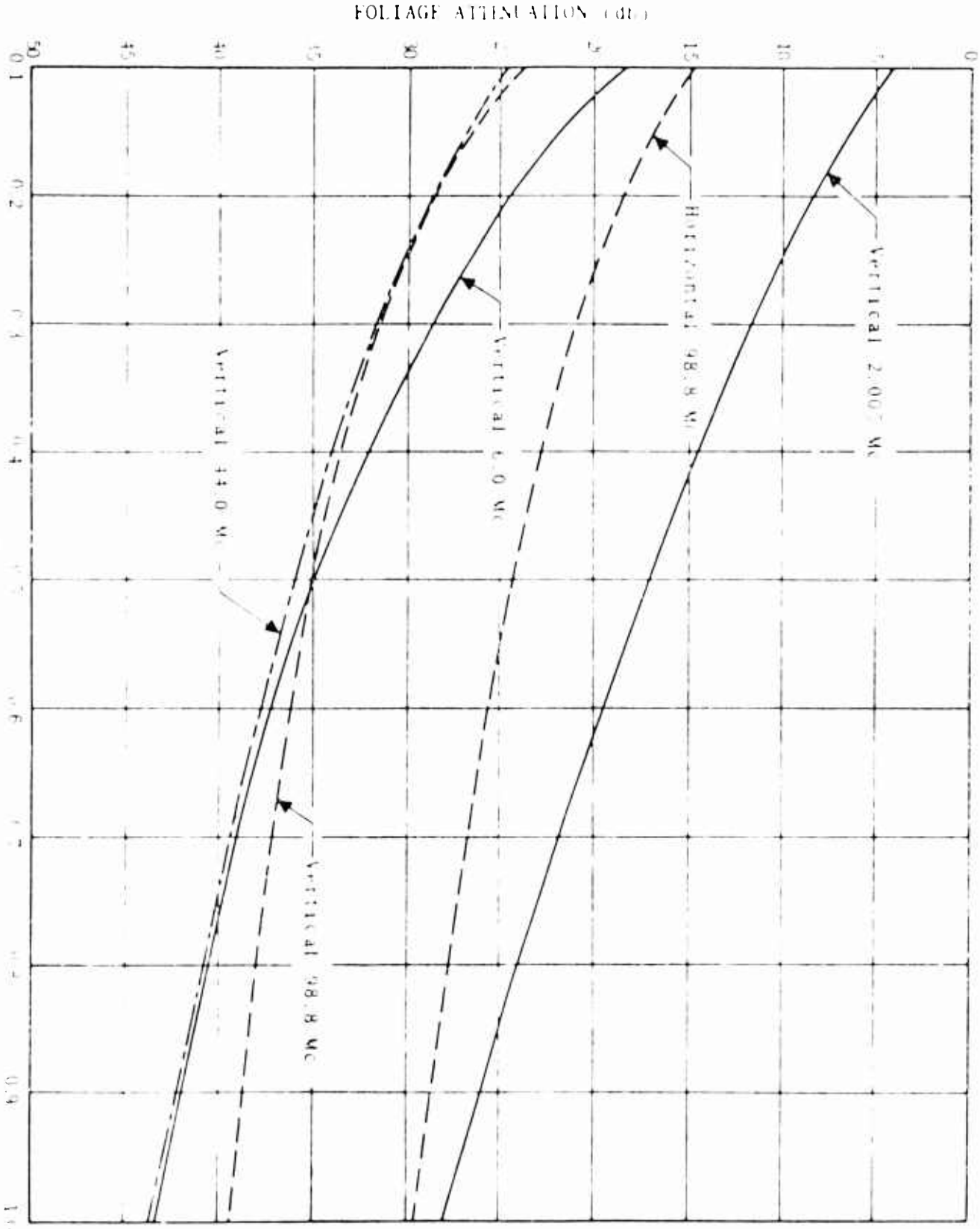

Figure 3.1 Foliage Attenuation Versus Distance

attenuated more rapidly and showed more variations in field strength than did the horizontally polarized fields. For example, at one mile, the horizontally polarized fields were attenuated approximately 15 db less than the vertically polarized fields at 98.8 Mc.

The measured field strengths at 44 Mc and 0.4 mile were increased approximately 12 db by elevating one of the terminals in a 50-foot tree, the average height of the intervening jungle growth being approximately 50 feet. When both terminals were elevated, one to 50 feet, the other to 70 feet, an increase of approximately 23 db over the field when both sets were on the ground was obtained.

3.2 Radio Propagation Through New Guinea Rain Forest

In 1945, a report titled "Radio Propagation Through New Guinea Rain Forest" was published as part of a thesis by Dr. Whale. This report describes a series of tests which were conducted in order to obtain some reliable figures on the magnitude of attenuation due to heavy jungle so that it would be possible to correlate the power output of a military communications set to it's expected range.

The investigation covered the case of equipment operating in the jungle with vertical antennas not extending above the top of the vegetation. In order to confine the measurements solely to the effect of the vegetation on radio wave propagation, the experiments were conducted in flat, uniformly dense jungle. Under these conditions, it was found by previous experience that the main factor affecting attenuation is the density of the foliage and that the ground constants of the ground underneath the foliage make but a secondary contribution. In order to compare the effects of vegetation of different density, measurements were made over paths in a coconut plantation as well as in the heavy jungle.

The jungle selected averaged about 60 feet in height and was so dense that in most parts the sky could not be seen overhead. The denseness of the foliage increased slightly with height. In order to provide access to the transmitting site in the jungle and to the various points chosen for the field strength measurements, a narrow trail was cut through the undergrowth and marked at 25 yard intervals.

The transmitter was set up in a chosen location and calibrated in the direction of the narrow trail. The field strength was then measured at various marked locations along the trail. The series of measurements were then repeated after moving the transmitter some distance along the trail and thus covering a different stretch of jungle. The field strength curves given in this report are deduced as an average of the two or more runs made at a given frequency.

A second series of tests were conducted in a coconut plantation. In this case the field strength meter was set up in a jeep for these tests, and all the measurements were made along a road skirting the plantation.

The transmitter was set up along a side road close to the edge of the plantation, and measurements were made along the road where the transmission was entirely through the plantation. The receiver was not actually amongst the trees for these measurements but only at their edge. It was found that moving from the road into the trees made a negligible difference to the measured field strength.

Figures 3.2 through 3.4 show the results of the New Guinea measurements and the results of Herbstreit's Panama measurements at three corresponding test frequencies. The New Guinea curves, which are the result of an elaborate smoothing process, were taken directly from Whale's thesis. This smoothing process was especially necessary for the measurements made in the jungle because the very close vegetation often caused false readings on the field strength meter. Consequently these curves give the probable average field strength at a given location. The field strengths are given in db above one microvolt per meter and have been corrected to an unattenuated field ($2E_o$) of 10^{-2} v/m at one mile. This field corresponds to a radiated power of 2.9 watts from a short vertical whip. The Panama data were obtained from Herbstreit's report, corrected to the same unattenuated field, and replotted. In order to show the attenuating effect of the vegetation on propagation, theoretical open-country curves are also shown. These curves are based on ground constants of $\epsilon = 15$ and $\sigma = 0.05$ mho-m/sq. m given by Whales. Differences between the measured curves may be attributed to differences in foliage density.

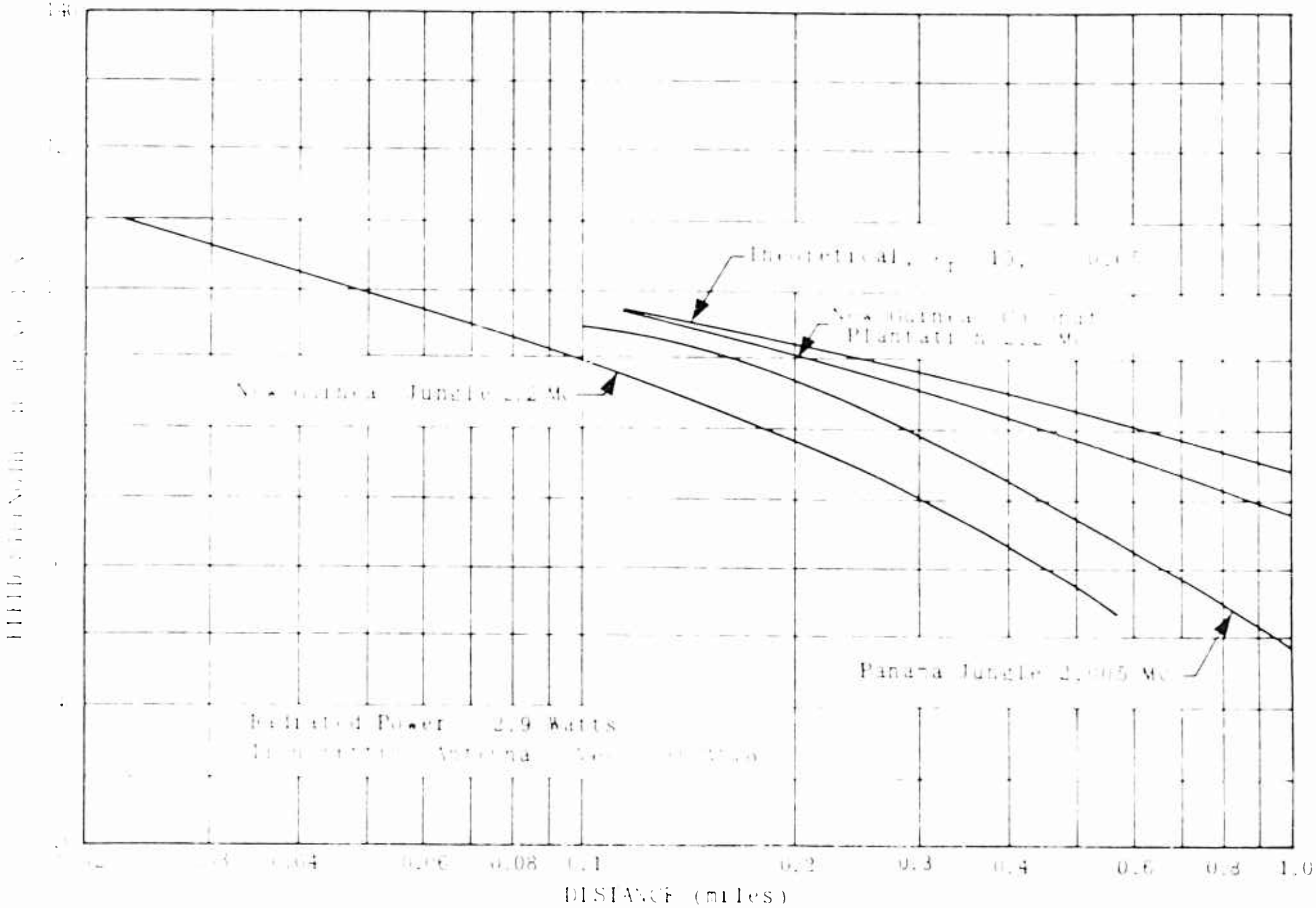

Figure 3.2. Comparison of Field Strength Versus Distance for Different Jungle Environments.

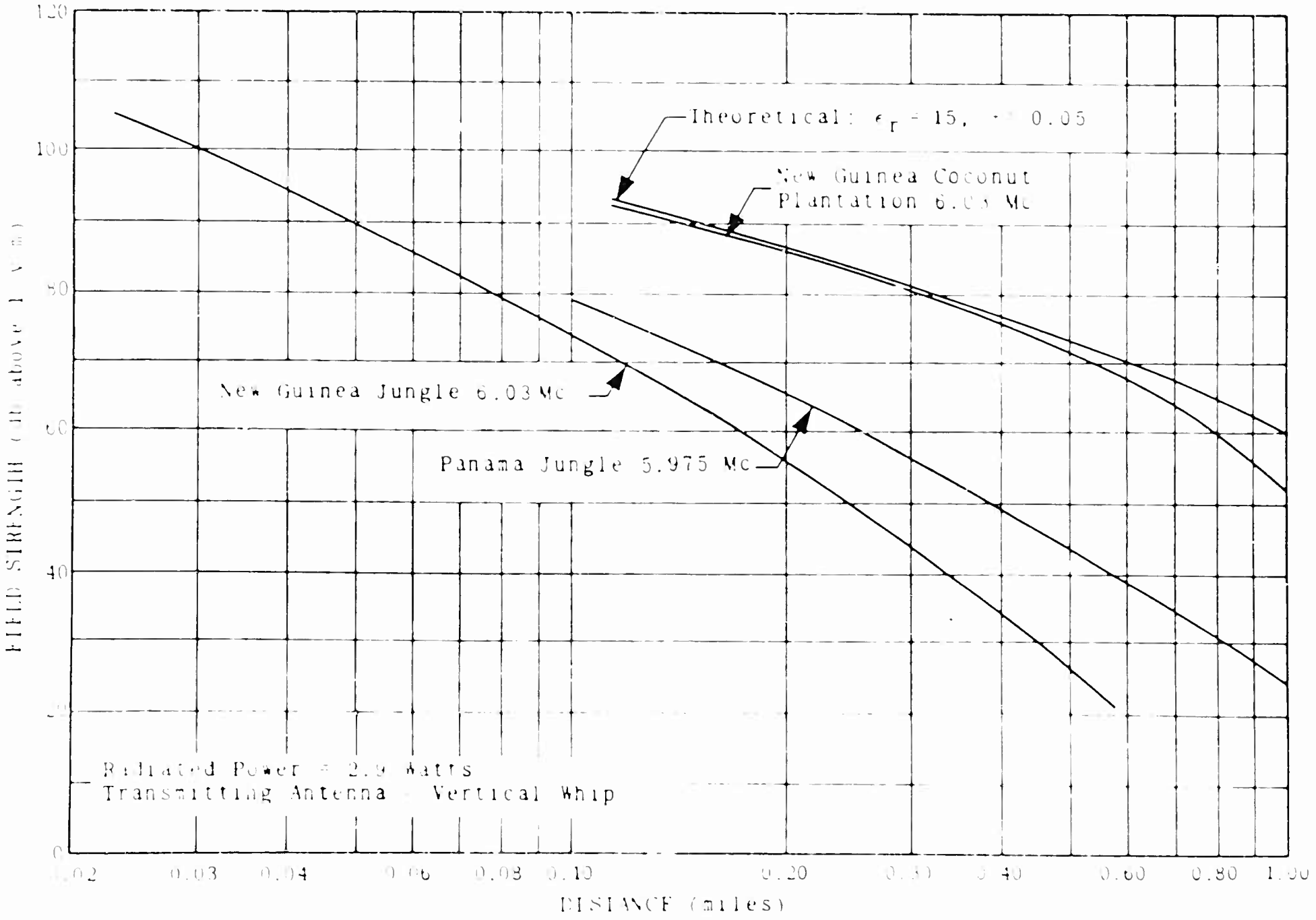

Figure 3.3. Comparison of Field Strength Versus Distance for Different Jungle Environments.

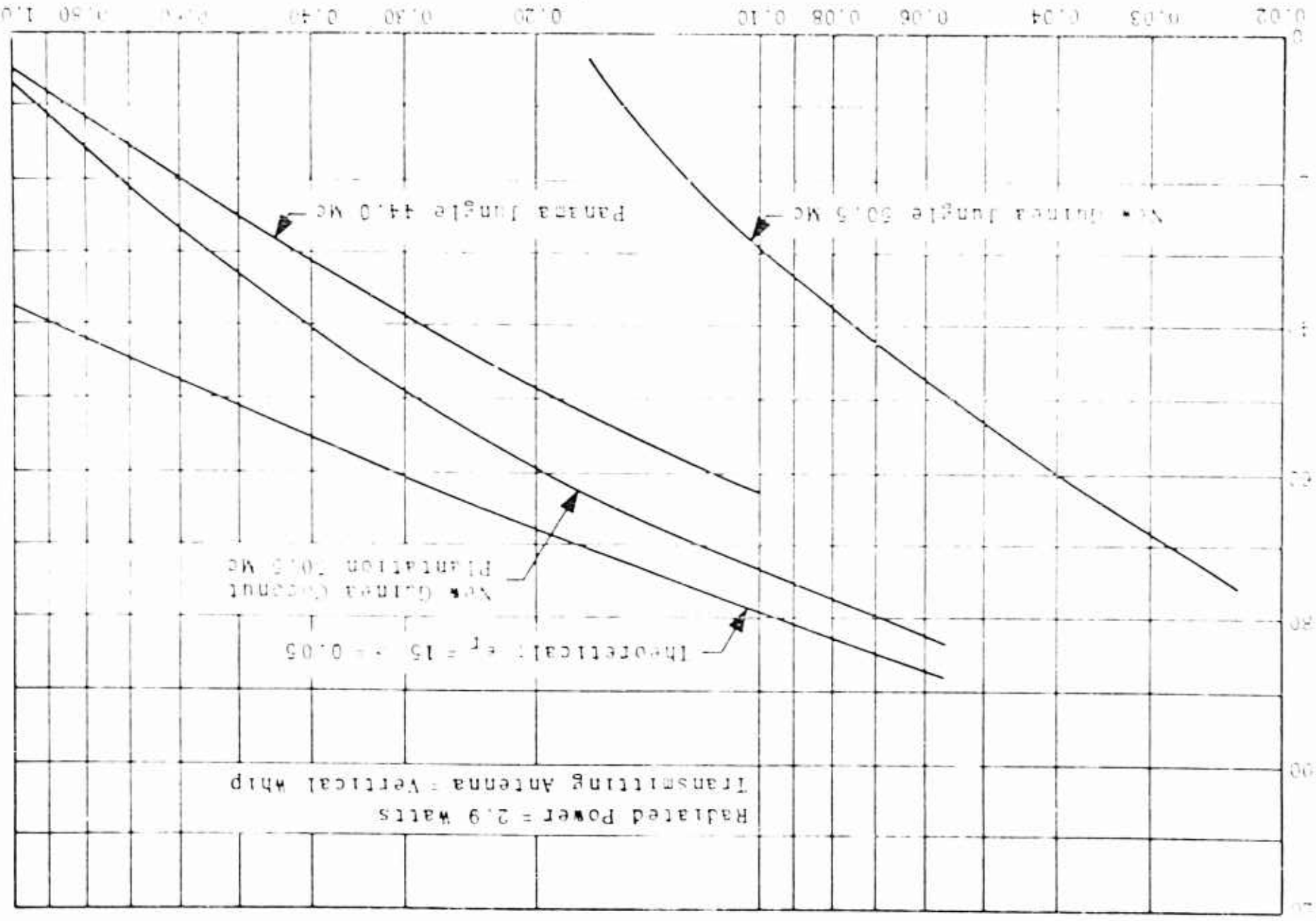

Figure 3.4. Comparison of Field Strength Versus [illegible] Type B [illegible] Jungle Paths.

3.3 Project Yo-Yo Field Experiments

In September 1962, a report titled "Project Yo-Yo Field Experiments" was prepared under the sponship of ARPA Order #299-62 and Contract NOnr-2507(00) for the Office of Naval Research by H.F. Busch, ACF Electronics Division. The primary objective of Project Yo-Yo was to measure under the field conditions of Southeast Asia the characteristics of skywave signals between two sites separated by a distance of 30 to 50 kilometers of dense jungle foliage and mountainous terrain or various combinations of these obstructions

Four preliminary tests preceded the primary tests. The first two tests, a spectrum survey and a direction finding test, were made in order to determine that any proposed location for the transmitting site had a minimum of man-made interference. In the third test, samples of information on local ionospheric behavior were used in the selection of the optimum operating frequencies. Test four involved the use of pulse transmissions for sounding the ionosphere.

In the primary tests three separate paths were used to prove the basic feasibility of establishing two-way communications over obstructed ground paths of about 30 to 50 kilometers in length In all cases, the transmitting antennas were Yo-Yo antennas erected 3 meters above the ground. Initially, simple doublet antennas were used at the receiving terminals. Later tests were designed to provide comparisons between simple dipole receiving antennas and a 16-element planar array at several frequencies.

The spectrum occupancy tests indicated the few signals which possessed interference potential in the 2 Mc to 4 Mc portion of the HF spectrum were within the confines of recognized medium wave international broadcast bands The spectrum between 4 Mc and 6 Mc contained a larger number of signals capable of serious interference, but again, these signals were concentrated within the international broadcast bands Above 6 Mc, skywave transmissions from more distant sources were present and produced interference of severe proportions.

Pulse soundings of the ionosphere from mid-February through April confirmed the expected behavior of critical frequencies and layer height variations. The F region critical frequency occasionally fell below 3 Mc for short intervals during the 0400-0530 pre-dawn period in the early part of the program. During the later months, however, the pre-dawn minimum critical frequency increased so that successful continuous transmission of signals at 4.6 Mc was demonstrated over several 24-hour test periods.

The communications feasibility tests were successful and indicated the skywave transmission mode can support communications over various combinations of mountainous terrain and densely foliaged jungle at the distances tested. In all cases, Yo-Yo antennas were employed for transmitting, and successful reception of signals for several frequencies between 2 Mc and 4 Mc was obtained with short and resonant dipoles and a 16-element zenith directional planar array at the receiving terminal. The transmitter power ranged from a few milliwatts to 20 watts, depending on the experimental techniques employed.

The receiver input voltages obviously depended on the frequency, time of day, and antenna. The 4 Mc fields received at night were as much as 30 db greater than those received during the day. The same magnitude difference occurred between the 4.4 Mc and 2.6 Mc transmissions at midday. Day-to-night variations in the 2 Mc signal strengths averaged 40 db. At night there was no significant difference between the 2 Mc and 4 Mc signal strengths since ionospheric absorption at night is minimal.

A comparison of the receiving antennas showed the resonant dipole produced a 12 db improvement over the 0.1 λ level and 0.1 λ high dipole when at the same height. The 16-element planar array produced an additional 10 db improvement.

The antenna comparison tests were analyzed for information concerning spherics activity. The results of this analysis agreed with previous measurements made in 1957-1958 by Chrzchlow of the National Bureau of Standards in Singapore. A diurnal variation, asymmetric about noon with a peak in the early afternoon, was obtained.

In addition to the review of literature on propagation in tropical areas, a number of reports concerned with propagation over rough terrain or propagation in temperate forests have been reviewed. As it is impractical to include a summary of each report reviewed and listed in the bibliography, the summaries of three reports are included here. Each of these reports offers a type of mathematical model which may be utilized later in the program.

3.4 Radio Propagation Above 40 Mc Over Irregular Terrain

In the report "Radio Propagation Above 40 Mc Over Irregular Terrain," by J.J. Egli, the effect of irregular terrain on radio propagation is analyzed as a function of frequency, antenna height, polarization, and distance. The prediction process formulated is used to estimate the percentage of locations at a prescribed distance one would expect to cover with a satisfactory service for a given radiated power.

A large portion of the data on which this report is based was originally collected by the Federal Communications Commission. These measured field strength data were compared to those one would expect over a plane earth (Equation 3.1) rather than over a curved earth since the best median field strength data fit for distances up to 30 or 40 miles show that the inverse distance squared trend for plane earth is better than the curved earth field, at least for low antenna heights.

$$E = \frac{h_{t(ft)}\ h_{r(ft)}\ f_{(mc)}}{95\ d^2_{mi}} \sqrt{P_{t(watts)}} \quad \frac{\text{Microvolts}}{\text{meter}} \tag{3.1}$$

The difference between the predicted plane earth field and the measured field was used to evaluate a median deviation or terrain factor. The median field is then defined as

$$E_{50} = E_{theor} - \text{Terrain factor (db)} \tag{3.2}$$

The terrain factor is shown in Figure 3.5 where it may be concluded that

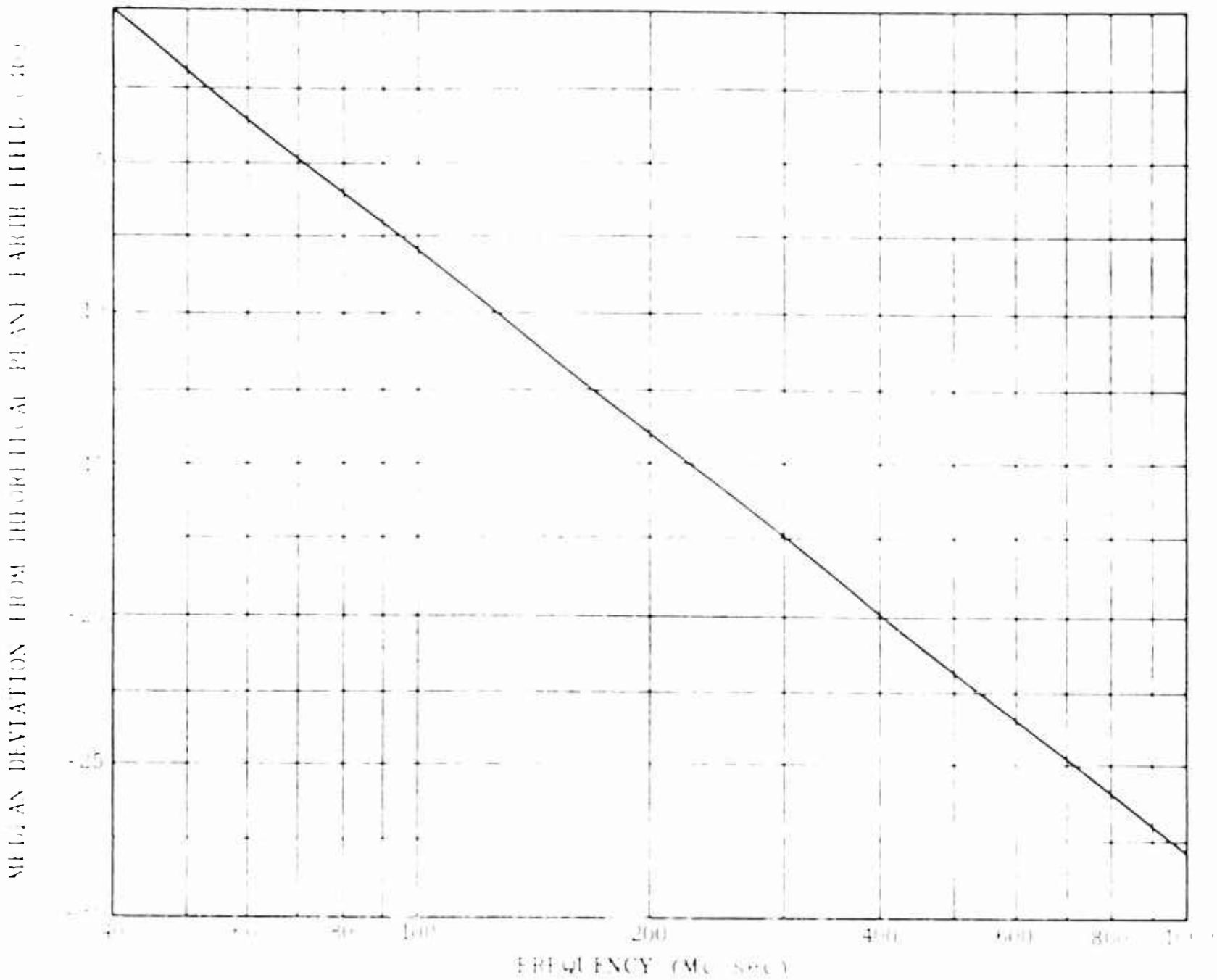

Figure 3.5. Median Terrain Factor for Fixed-to-Land or Mobile Service.

(1) The deviation from the plane earth field strength varies inversely with frequency.

(2) The deviation from the plane earth field strength is independent of distance.

(3) The variation with frequency is with respect to 40 Mc.

Based upon these conclusions, the median field at the 50 percentile locations is given by

$$E_{50} = \frac{h_1 \; h_2 f}{95 \; d^2} \sqrt{P_t} \times \frac{40}{f}$$

or

$$E_{50} = \frac{40 \; h_1 \; h_2 \sqrt{P_t}}{95 \; d^2} \qquad (3.3)$$

and is independent of frequency.

Further data analysis indicated the terrain factor distribution was log normally distributed. Consequently, this distribution will appear linear on probability paper and may be described by its median value and standard deviation. The result of this analysis is shown in Figure 3.6 where correction factors which must be applied to E_{50} when received field strengths to other than the 50 percentile locations are given. Figure 3.7 gives the information shown in Figure 3.6 on a power basis.

For all practical purposes, the data analysis confirmed that the received field strength increased linearly with transmitting antenna height. However, the field strength variation with receiving antenna height was proportional to the square root of the antenna height for heights less than 30 feet and varied linearly for heights greater than 30 feet.

The wave polarization appeared to have negligible effect on the transmissions above 40 Mc over the irregular terrain. While vertically polarized waves gave better results at locations within the shadow area behind hills, horizontally polarized waves gave better results in back of but away from the shadow area. In wooded areas the attenuation was less for horizontally polarized transmission.

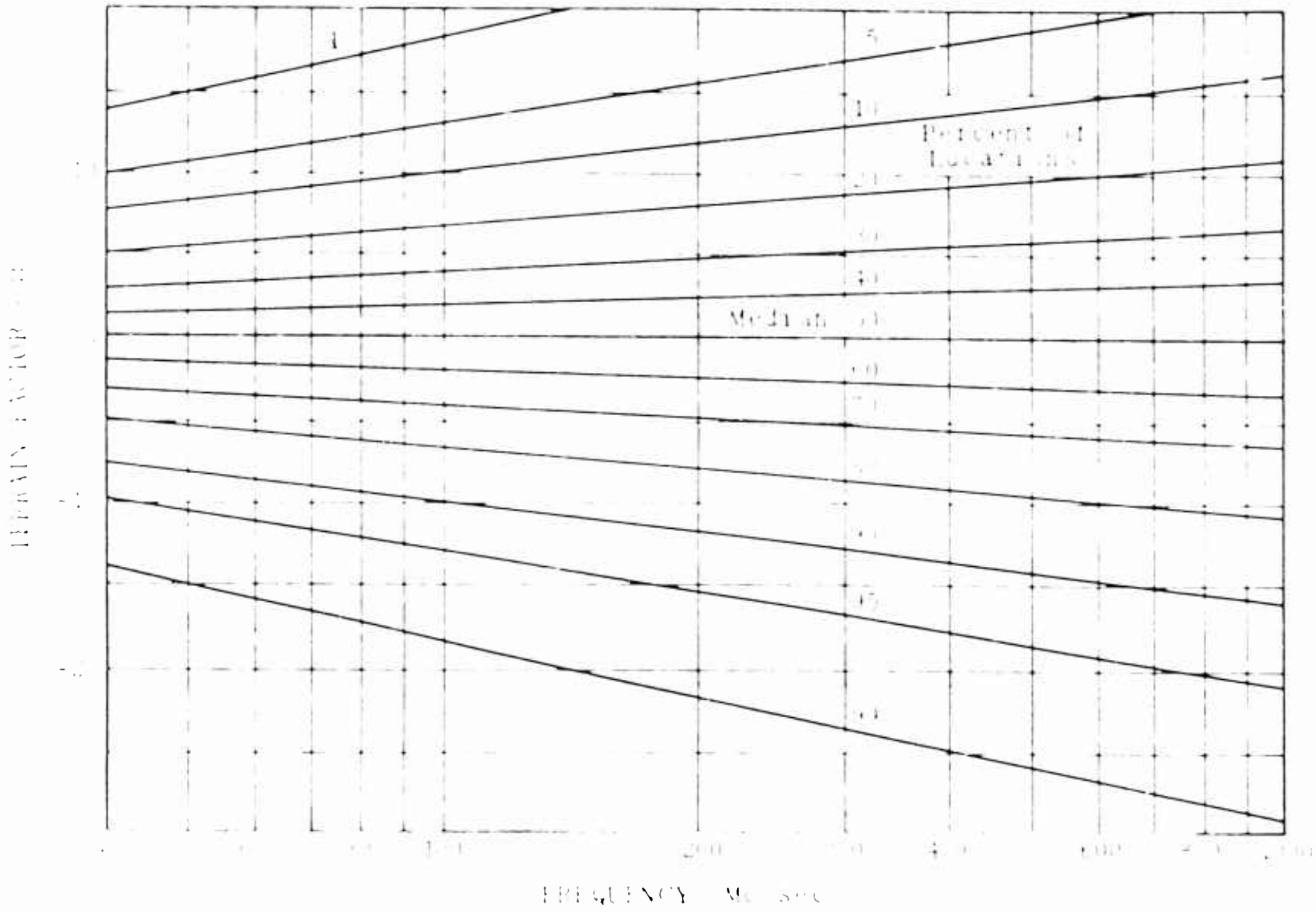

Figure 3.6. Fixed-to-Vehicular or Mobile Service Field Strength Terrain Factor.

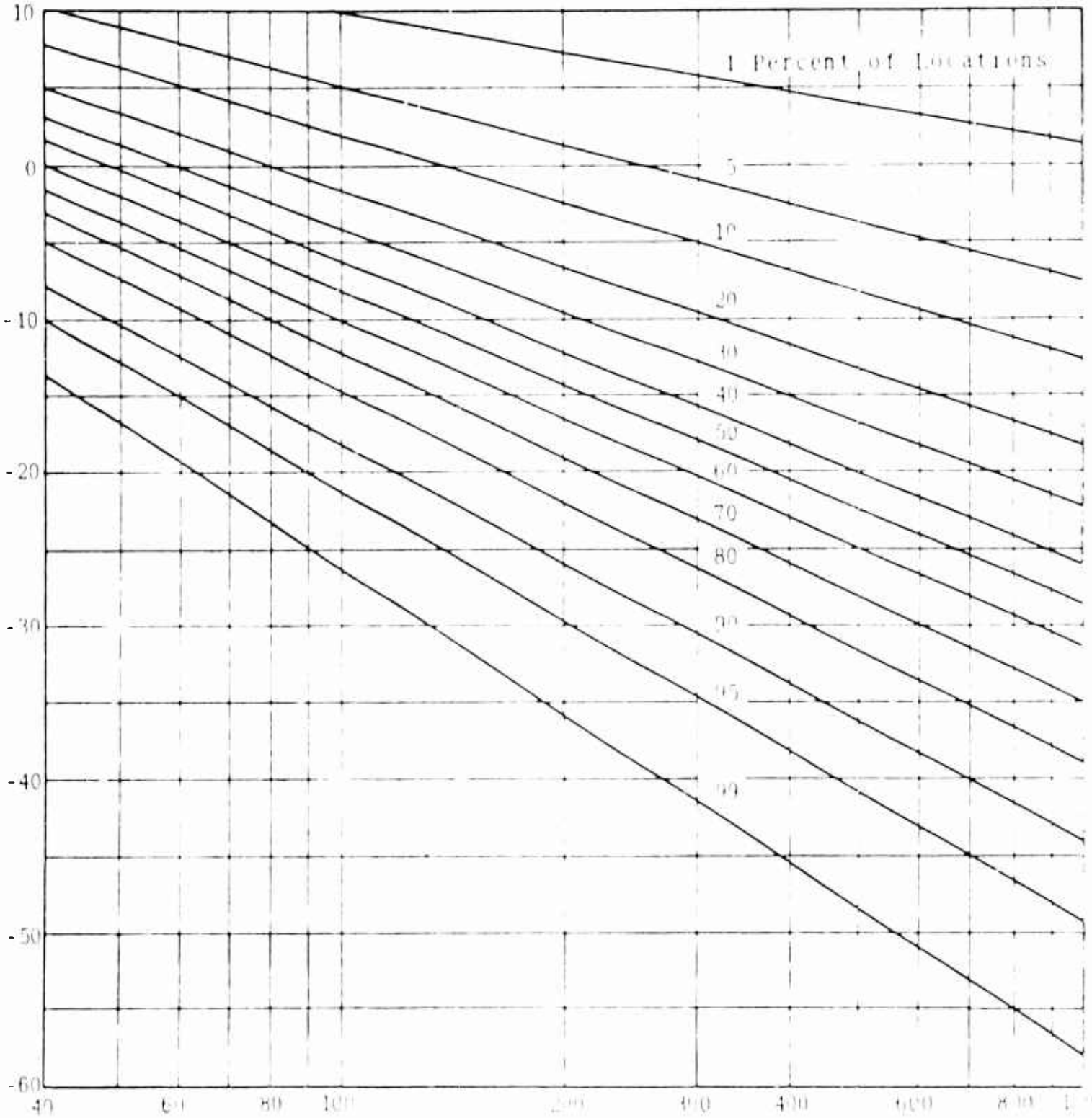

Figure 3.7 Received Power Terrain Factor for Fixed to-Vehicular or Mobile Service

Additional sections of this paper discuss, "Small Sector Field Strength Variation," "Wide Modulation Bandwidth Effects," "Indigenous Noise," and "Vehicular-to-Vehicular Transmissions." A numerical example is included to illustrate the practical application of the prediction method.

3.5 The Influence of Trees on Television Field Strength at Ultra-High Frequencies

The results of an experimental program designed to evaluate the effect of trees on VHF transmissions are discussed in a report prepared by H.T. Head for the June 1960 issue of the Proceedings of the Institute of Radio Engineers. Field strength measurements of a local television signal were made over flat terrain with woodland cover in the vicinity of Salisbury, Maryland, during December 1958 and January 1959. For each observation there was determined the depression value of the measured field below the smooth-earth value (Δ_{SE}), the depression of the field below the free-space value (Δ_{FS}), and the ratio of the obstruction of the trees in the first Fresnel zone to the radius of the zone at the point of maximum obstruction (H/H_o). Graphs of these values were plotted and compared with attenuation curves representing various modes of diffraction.

A plot of Δ_{SE} versus H/H_o did not show an acceptable correlation with the theoretical diffraction curves. More encouraging results were obtained when Δ_{FS} versus H/H_o was plotted. The measured points tended to fall in the general region of the theoretical curves for diffraction around a smooth sphere having a reflection coefficient of -1.0 and a value of Bullington's[1] parameter of M of 300 when the Fresnel zone clearances were greater than -1.0. The standard deviation of the observed values from this theoretical curve is 3.4 db. By assuming an edge effect of 10 feet which reduced the apparent average height of the trees from 55 feet to 45 feet, recomputing H/H_o and assuming diffraction around a sphere having a radius equal to 4/3 of the earth radius, the standard deviation of the observed values from the theoretical curve is 2.9 db for Fresnel zone clearances greater than -0.6.

---

1. K. Bullington, "Radio Propagation Fundamentals," Bell System Tech. Journal; May 1957.

The analysis of certain measurements indicated the received signal had "leaked" through the treetops, often in an erratic fashion. These measurements were analyzed for any evident trends. An examination of eight observations of leakage field at distances ranging from 12.0 miles to 22.5 miles from the transmitter indicated the average signal level below the calculated smooth earth field to be more-or-less independent of distance. In these measurements, the average depression of the field below the smooth earth field was approximately 30 db.

On the basis of these observations and conclusions, Head has proposed a model to account for the loss due to trees. Figure 3.8, which illustrates this model, shows the profile of a transmission path over smooth terrain. Between the transmitting antenna and the first woods at D_1, the received fields are those predicted by smooth-earth theory. Beyond D_1 (in the woods), the received signals are those which travel through the woods and the attenuation increases rapidly with woods' thickness until the leakage field level is reached at D_2. Under this concept, the attenuation cannot exceed that corresponding to the leakage level, and thus, any additional woods' thickness does not result in further depression of the signal.

Beyond the distance D_3, where the far edge of the woods is reached, the received signals recover with distance in an approximately logarithmic fashion until the clearing depth is sufficient that the smooth-earth values are once again approached. This logarithmic recovery, which is noted in Figure 3.9, can be shown to follow as a consequence of diffraction.

It is interesting to note that data published by Herbstreit and Chrichlow do not contradict the model proposed by Head. Figure 3.1 shows a plot of the jungle foliage attenuation as a function of distance for the frequencies of 6, 44, and 99 Mc, vertical polarization. For each curve on this figure, the slope decreases as the distances increase, indicating, if the same trend exists at greater distances, that at some greater distance a maximum foliage attenuation is approached. The portion of the curves shown would correspond to the attenuation between D_1 and D_3 in Figure 3.8. Although the available data do not contradict the model, it is insufficient to justify any conclusions.

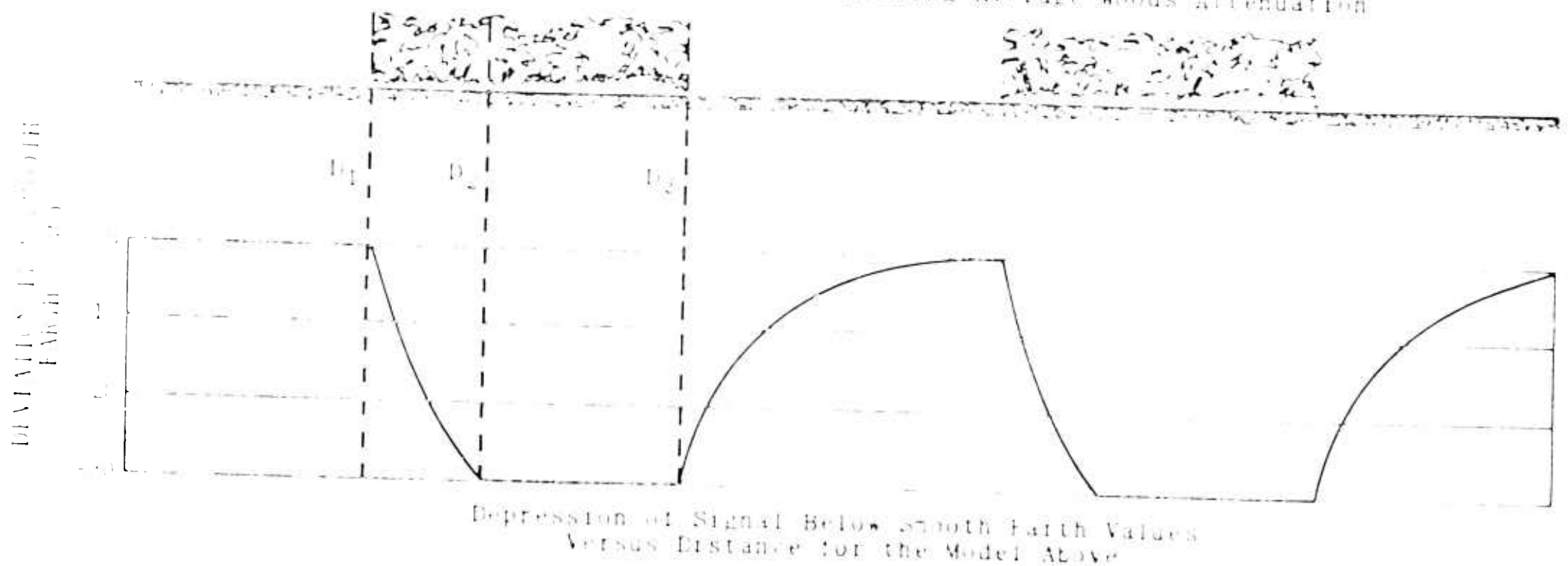

Figure 3.8. Model for Estimating Average Woods Attenuation.

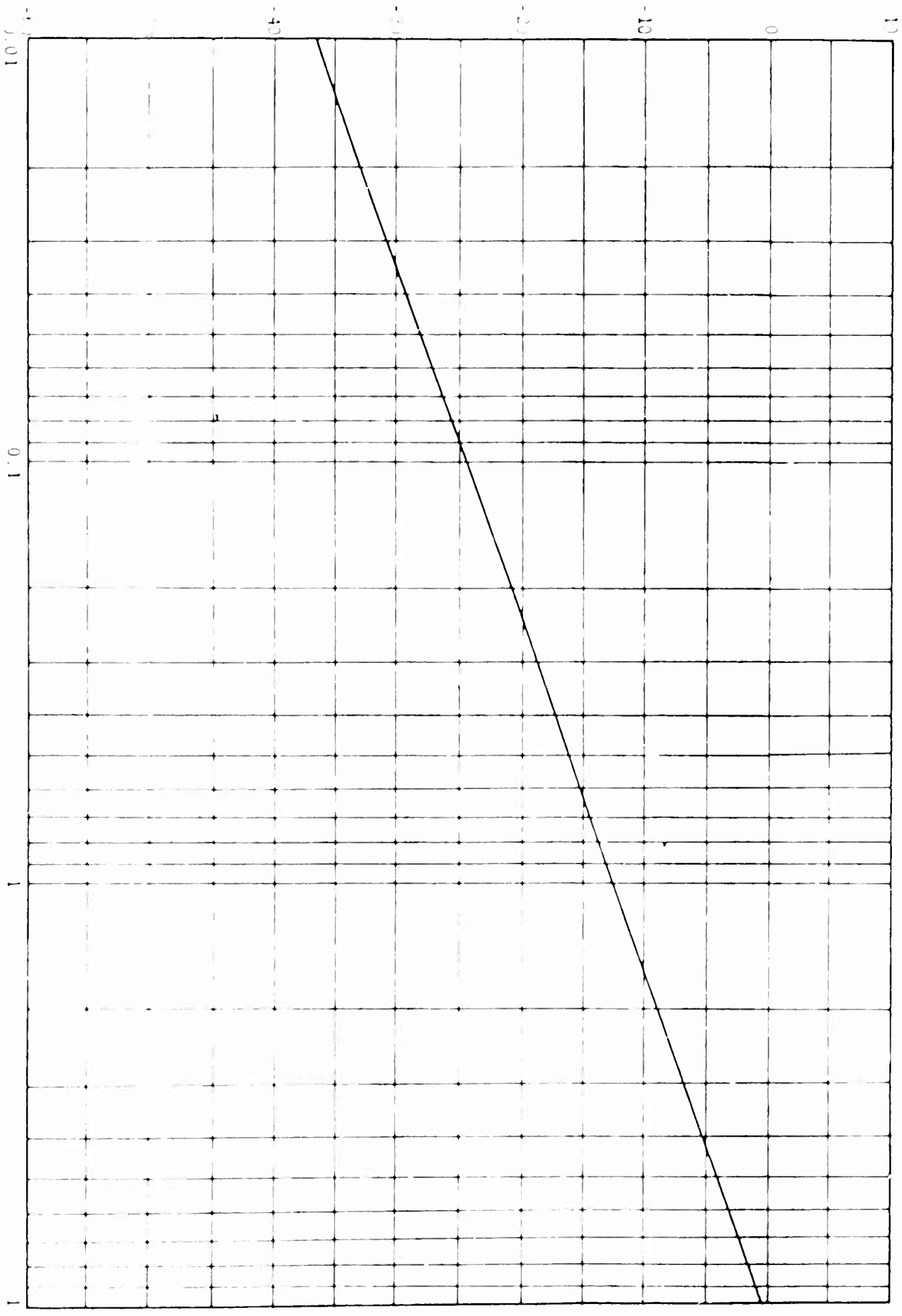
dB FROM SMOOTH EARTH FIELD
-40
-20
-10
0
10
0.01
0.1
1
1
HEIGHT (miles)

3.6 Height Gain Measurements at VHF and UHF Behind a Grove of Trees

More recently, a report, "Height Gain Measurements at VHF and UHF Behind a Grove of Trees," was published in the IEEE Transactions on Broadcasting by A.H. LaGrone, P.E. Martin, and C.W. Chapman. This paper presents the results of measurements at frequencies of 81.75, 209.75, 633.25, 1280, and 2950 Mc behind a grove of live oak and hackberry trees in full leaf. Horizontal polarization was used and vertical height-gain runs from 5 to 60 feet at various distances from the trees.

Signal strength versus height curves for the five frequencies at clearance distances behind the trees of from 15 to 365 feet are presented. Theoretical curves were computed for propagation over a smooth spherical earth and for a plane wave diffracting over a knife edge and are presented for comparison with the measured curves.

Commercial stations in San Antonio were used as signal sources at 82, 210, and 633 Mc. Laboratory transmitters were used at 1280 and 2950 Mc. The receiver site was located near Boerne, Texas, about 40 miles from the transmitters. The measuring procedure was to raise the telescoping pole to its maximum height of 60 feet and to take continuous signal strength recordings as the pole was lowered. The lowest height at which measurements could be made continuously was 23 feet. At this height the antenna was removed from the telescoping pole and placed on a section of pole. The receiver truck was moved about 90 feet away in a direction along the path radial and measurements were made at fixed heights of 23, 18.5, 14, 9.5, and 5 feet.

A typical set of curves (Figures 17 and 18 in the original paper) are shown in Figure 3.10. Curves for the other four frequencies and various distances are presented and discussed in the paper. The greater average absorption at 210 Mc suggests that the effective diffracting height and the effective distance of the trees might be nearer to the observed tree height and true distance to the trees than that at 82 Mc. Accordingly, knife edge heights of 25 and 30 feet were assumed, and the knife edge diffracted signal

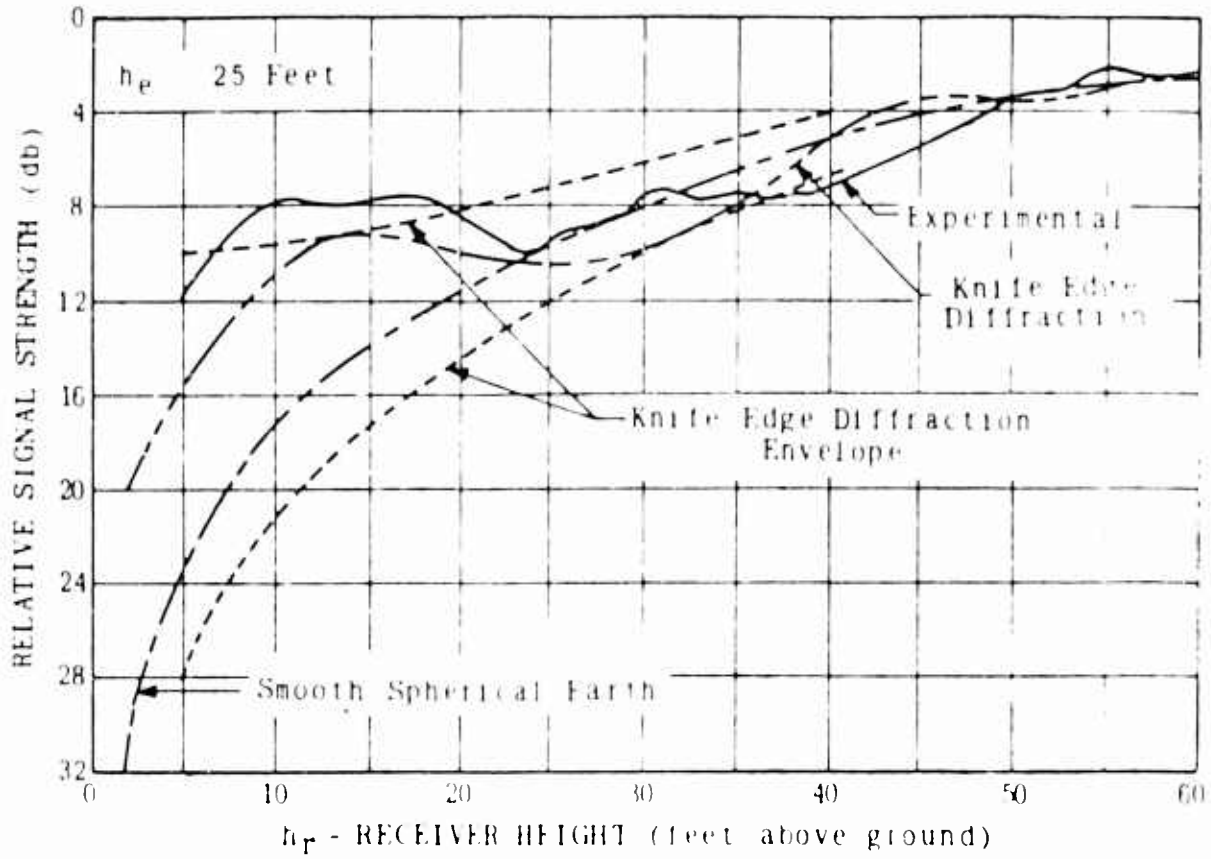

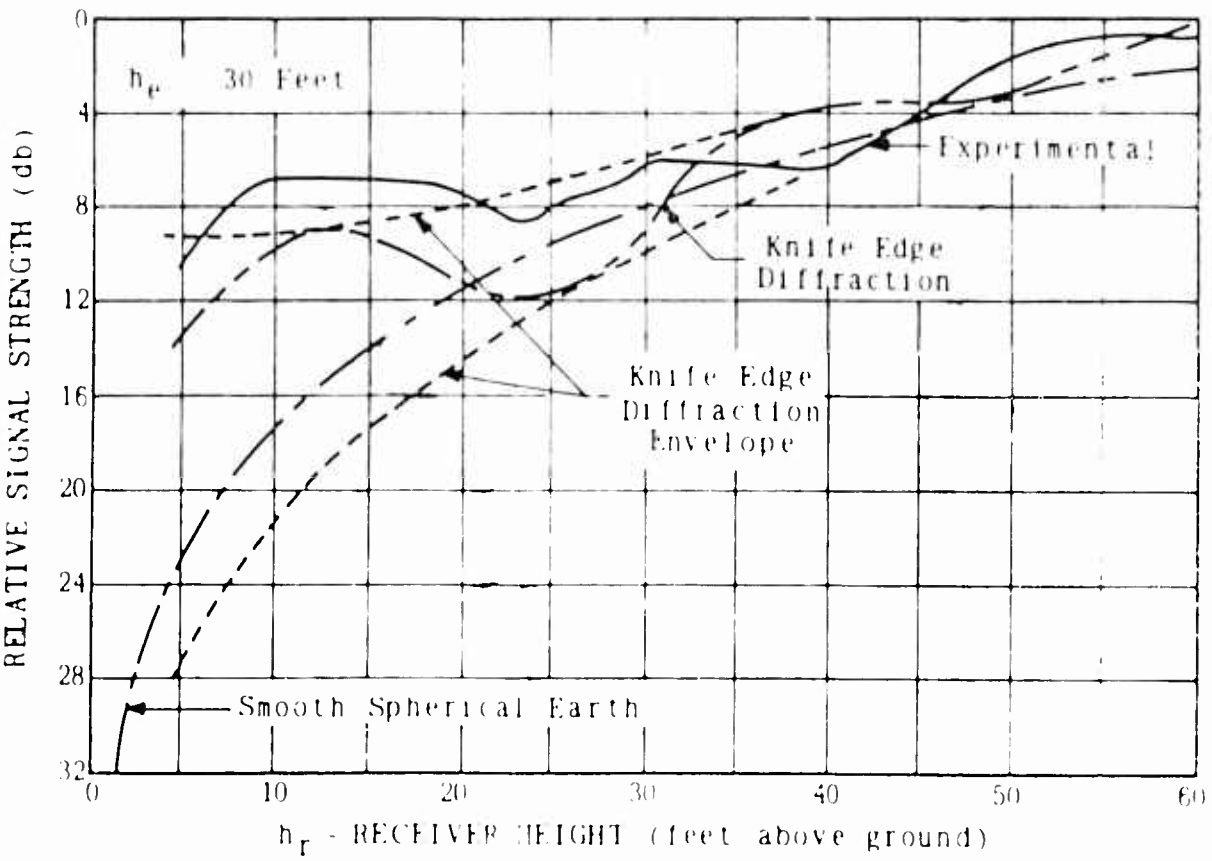

Figure 3.10. Comparison of Measured Signals with Theoretical Signals at 210 Mc (d = 365 feet).

computed assuming two components. These are shown for a receiver distance of 365 feet in Figure 3.10. In this figure, the knife edge diffraction curve of 25 feet fits the measured data rather well and clearly shows the lobe structure found in the measured data. This strongly suggests the effect of trees cannot be neglected at this frequency.

The comparison of the field measured height gain curves with theoretical height gain curves suggests that the field at VHF and UHF found behind a grove of trees has characteristics that most resemble those of a plane wave being diffracted over a knife edge type of obstruction. At large distances, greater than about five times the tree height (30 feet) for the measurements reported in this paper, the diffracting edge appears to be approximately the same height as the trees and the same distance away.

At shorter distances, significant propagation through the foliage takes place reducing the effective height of the diffracting edge to something less than the physical height of the trees and increasing the effective distance of the diffracting edge from the receiver to something greater than that of the near edge of the grove.

REFERENCES

Bullington, K., "Radio Propagation at Frequencies Above 30 Mc," Proc. IRE; October 1947.

Bullington, K., "Radio Propagation Variations at VHF and UHF," Proc. IRE; January 1950.

Busch, H.F., "Project Yo-Yo Field Experiments." Work performed for the Office of Naval Research under Contract NOnr-2507(00). ARPA Order No. 299-62 by ACF Electronics Division of ACF Industries September 1962.

Egli, J.J., "Radio Propagation Above 40 Mc Over Irregular Terrain," Proc. IRE; October 1957.

Head, H.T., "The Influence of Trees on Television Field Strengths at Ultra-High Frequencies," Proc. IRE; June 1960.

Head, H.T. and Presthold, O.L., "The Measurement of Television Field Strengths in the VHF and UHF Bands," Proc. IRE; June 1960.

Herbstreit, J.W. and Chrichlow, W.Q., "Measurement of Factors Affecting Jungle Radio Communication," Office of Chief Signal Officer, Operation Research Branch, ORB-2-3; November 1943.

Jansky & Bailey, Inc., Washington, D.C., "Radiotelephone Communication Between Mobile Units," Final Report, Contract No. OEMsr-174; 1943.

LaGrone, A.H., "Forecasting Television Service Fields," Proc. IRE; June 1960.

Reed, H.R., "Propagation Data for Interference Analysis," Contract No. AF 30(602)-1934, Jansky & Bailey Division of Atlantic Research Corporation; January 1962.

Rice, P.L., "Within the Horizon Paths," Case II, CCIR DOC V/23-E; 1962.

Saxton, J.A. and Lane, J.A., "VHF and UHF Reception - Effects of Trees and Other Obstacles," Wireless World; May 1955.

Trevor, B., "Ultra-High Frequency Propagation Through Woods and Underbrush," RCA Review; July 1940.

Whale, H.C.T., "Ground Aerials," M. Sc. Thesis; 1945.

4.0 SITE SURVEY

During the months of November and December 1962, a site survey team was sent to Thailand for the major task of selecting a suitable jungle area in which to carry out the primary field tests. Members of the team included L. G. Sturgill, F. T. Mitchell, C. B. Sykes, and G. V. Graves, Jansky & Bailey; H. L. Kr[illegible]s and Major J. A. Krantz, U. S. Army Electronics Research and Development Agency; and B. Bergman, ARPA Research and Development Fi[illegible] Unit. The technical objectives of the primary field tests are such that the area selected would have to meet the following requirements: (1) be approximately 30 miles square and contain dense jungle growth that is peretrable by means of an existing system of roads and cart tracks, (2) offer appropriate variations in topographic features, and (3) is not so remote that logistic support and supply from Bangkok is excessively difficult and expensive.

From a study of a Thai Forestry Service map provided by the ARPA R&D Field Unit, it was determined that the jungles in Thailand are disposed in more-or-less distinct areas that tend to be distributed along the chains of hills and mountains. Later, another map was provided by the J-2, USMAG, which correlated closely with the original Forestry Service map but defined the jungle areas more exactly. This latter map is shown in Figure 4.1.

While map study undoubtedly provided a considerable amount of information about some characteristics of the foliage in a given area, the actual foliage density and nature of the undergrowth could not be evaluated by map study alone. With the cooperation of JUSMAG effort was made to use existing aerial photographs, obtained for other purposes, to aid in the selection of an appropriate test area. However, it soon became apparent that the assemblage and study of these photographs for the purposes of this task would be inordinately time consuming and expensive with the possibility of leading to a sound selection of a suitable area highly doubtful.

Since map and photo study could not provide sufficient information about the foliage density and trail conditions in the various areas to allow a sound choice of area, it was necessary to

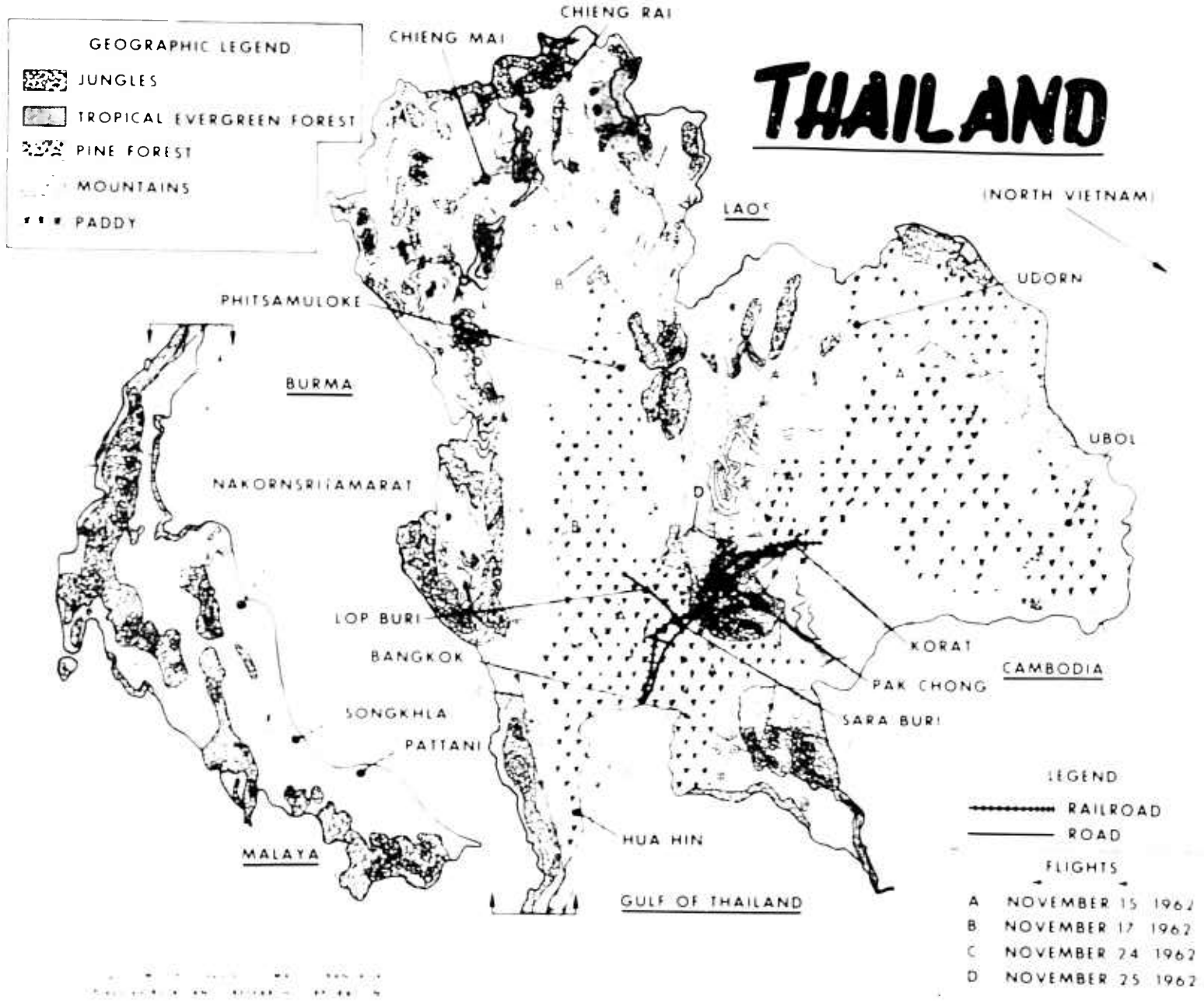

Figure 4 1 Map of Jungle Areas in Thailand

make an initial appraisal by means of aerial observations. It is known from experience that the question of whether a particular area of dense foliage extends over a range of some 30 miles cannot be answered from ground observations alone. Therefore, it was of paramount importance that aerial observations of a particular area be carried out before attempting a ground survey of that area.

Accordingly, aerial observations of nearly all significant areas in Thailand were carried out. This work was accomplished in four days of flying. The approximate flight paths are shown on the map in Figure 4.1. During these flights, the pilots were requested to fly over the areas in question at an altitude of 1500 to 2000 feet. The general characteristics and approximate extent of jungle growth was visually determined. Photographs were taken for records of the flight as well as for later detailed study leading to a methodology for describing jungle growth in more definitive terms.

The flight paths A and B at first may appear to be peculiarly related to the areas of jungle under observation. However, this is due to the fact that the aircraft was carrying out other assigned missions during these flights in addition to the subject observations.

The results from the four flights shown in Figure 4.1 may be summarized as follows. The only significant jungle area revealed by Flight A was in the vicinity of Pak Chong, south of Friendship Highway. Although observations during this flight were limited by several factors, this area appeared to offer the desired foliage density and terrain characteristics for the test area.

The areas along the west leg of Flight B were mountainous and, generally, were not heavily forested (especially on the slopes). The undergrowth did not appear to be dense, and there was little evidence of trails or cart tracks into these areas. The two jungle areas in the vicinity of Phitsamuloke exhibited dense tree growth with heavy undergrowth over terrain that varied from hilly to mountainous. Although some trails and roads were evident in these two areas, large portions appeared to be almost impenetrable by vehicular means.

The purpose of Flight C was to examine the areas on the peninsula along the Malayan border. Below Hua Hin, the foliage density appeared to increase markedly, with tree heights averaging about eighty feet. The undergrowth appeared to be somewhat more dense than that observed in the middle and northern areas. The terrain was generally mountainous and few access trails into these areas were observed.

The last loop of Flight C was over the area south of Friendship Highway and also encompassed the area east of Bangkok, adjacent to the border of Cambodia. During this flight, the area south of Friendship Highway appeared to offer the most desirable characteristics for a possible test area from among those areas examined thus far by aerial observations. The area east of Bangkok did not exhibit the dense tree growth and undergrowth desired for the field tests. The portion of this area nearer to the Cambodian border was not examined since the conduct of tests in this area would likely be complicated by a sensitive border situation.

During Flight D, the area north of Friendship Highway was further examined. While portions of this area exhibited dense growth over rolling terrain, the over-all extent of this area was not sufficiently large for the planned tests.

Based on the results from the observation flights, the best choice for a test area appeared to be south of Friendship Highway, in and around the Thai National Forest. An expanded scale map of this area is shown in Figure 4-2. During the last week in November, this area was examined by a ground party traveling by jeep on the existing trails. The area was penetrated from Friendship Highway to Mount Khao Khieo and to the villages of Sap Takhian and Ban Pong Chanuan. Considering that these trips were made during the dry season, the trails found in this area accommodated slow travel by jeep, with only an occasional delay when the vehicles became stuck in soft spots or whenever brush and trees had to be removed from across the trail. During the rainy season it is expected that these trails will deteriorate considerably, thereby seriously affecting mobility. To overcome this difficulty, it is planned to precondition these trails sufficiently to allow the use of

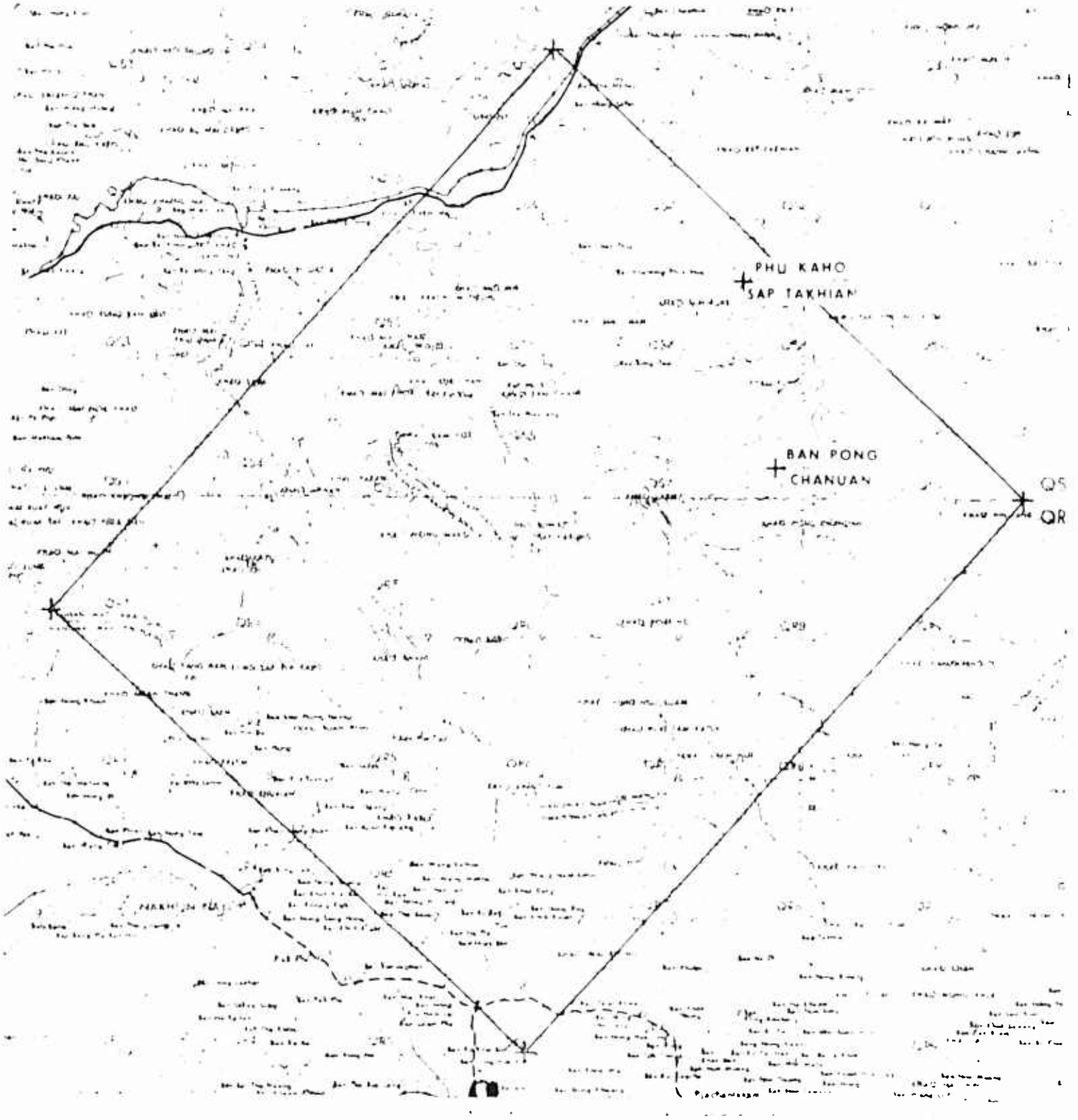

Figure 4 2 Jungle Propagation Test Area.

conventional types of vehicles, such as jeeps or landrovers, to transport the measuring teams during the rainy season. This approach is in contrast to that of attempting to locate and procure special purpose vehicles, such as tracked vehicles or Gamma Goats, which would negotiate these trails with a better degree of mobility under wet weather conditions. The fact that these vehicles are not available in Thailand, and the economics of obtaining them in that country, makes the latter approach impractical.

In summary, the reasons for choosing the test area shown in Figure 4.2 are as follows:

a. Among all the areas examined, the terrain features and foliage density of this area are best suited to the requirements of this program.

b. A usable trail system exists in the area

c. Operation in this area can be supported logistically from Bangkok with much less expense of time and money than in the other areas.

In the course of conducting the ground survey in the area shown in Figure 4.2 it became evident that the locations of the trails existing now in this area do not agree with those shown on maps currently known to be available. This is perhaps explained by noting that the last complete aerial mapping survey of this area was evidently done in 1955 Presumably, new trails have come into existence and old trails have been abandoned since the last survey was made.

Since it is essential that an accurate trail map be used in the process of laying out the system of radials required for these field tests, the ARPA R&D Field Unit was requested to obtain aerial photographs of this area. The flight mission to obtain these photographs has been completed After the trail information from these photographs has been transferred to a topographic map of the area, the best locations for the transmitting site and the radials can be determined

5.0 TEST PLAN

The objectives of the primary field tests and the general approach to attain these objectives are given in Sections 1.0 and 2.0 of this report. This section describes the parameters to be measured, the measurement equipment, the measurement techniques and the data reduction to be performed in Thailand.

In developing the test plan, first considerations were given to the various modes of propagation which (1) will exist in a jungle environment and (2) will be feasible for tactical communication systems. Five propagation modes were defined according to such parameters as frequency, path profile, and antenna height. These modes are:

A. Surface Wave Mode

The surface wave is that mode which is propagated along the surface of the earth and depends upon the boundary effect of the earth's surface for its existence. Conventional use of this mode is limited to frequencies below approximately 20 MHz and to vertical polarization. The path loss is a function of parameters such as frequency, antenna height, distance, polarization, earth conductivity, earth dielectric constant, and in a jungle environment, foliage attenuation.

B. Treetop Mode

This mode is analogous to the surface wave mode except that the lower boundary will consist of treetops rather than the earth's surface.

C. Line-of-Sight Mode

The line-of-sight mode is defined as that mode which exists when the intervening terrain profile is such that the transmitting and receiving antennas are intervisible. Jungle foliage may obscure visibility, but this is not a factor in the definition. Parameters affecting the received signal include frequency, antenna heights, polarization, distance, path profile, and foliage attentuation.

D. Diffraction Mode

The diffraction mode exists when the transmitting and receiving antennas are not intervisible. Parameters affecting the received signal include those listed for the line-of-sight mode.

E. Ionospheric Mode

The short range communications circuits which are supported by the E, the F_2, or the sporadic E layers are included in this mode. The path loss for a circuit having one ionospheric reflection is given by

$$L_b = L_{fs} + A_a + K$$

where

L_{fs} is the free space loss

A_a is the atmospheric absorption

K is the conversion factor between calculated and measured median values.

In general, there is for any fixed distance of transmission an upper limit of frequency which can be both transmitted and received. The existence of this upper frequency limit depends on the fact that the ionization in the atmosphere will reflect only waves of frequencies less than a certain critical value, called the maximum usable frequency (MUF). If the operating frequency is above the MUF, the wave will not be reflected. As the operating frequency is decreased below the MUF in the daytime, the atmospheric absorption increases. At night the condition of the ionosphere is such that the absorption is negligible even though the MUF is lower than during the day.

Over the short paths (0 to 30 mi.) under study in this program the maximum usable frequency will be approximately equal to the MUF at vertical incidence or zero distance. These MUF's vary with season, time of day and sunspot number at a given location. Typical values of F_2-layer MUF's in megacycles at a location near Bangkok are,

Sunspot Number	F_2-zero-MUF @ Local time	F_2-zero-MUF @ Local time
25-50	10.0-12.5 1400-1700	2.5-4.5 0500-0600

Zero distance maximum usible frequencies for the E layer range from 1.0 to 3.5 Mc with the maximum value occuring near 1200 hours local time.

The atmospheric absorption A_a is determined as

$$A_a = \frac{C15.5 \sec \phi (\cos 0.881 \chi)^{1.3} (1 + 0.0037 S)}{(f + f_H)^{1.98}}$$

ϕ is the angle at a 100 kilometer height between a perpendicular to the earth and the ray path

χ is the zenith angle of the sun

S is the 12 month running average sunspot number

f is the operating frequency in megacycles

f_H is the gyro frequency at a 100 kilometer height

The 100 kilometer height is used here because it roughly corresponds with the theoretical absorption heights. Typical absorption values for a gyro-frequency of 1.1 Mc, sunspot number of 34, and zenith angle of 70° for short paths (0 to 30 mi.) as a function of frequency are 28.0 db (2.0 Mc), 10.4 db (4.0 Mc), 5.4 db (6.0 Mc), and 3.4 db (8.0 Mc).

An additional loss factor that might be significant over a path in a jungle environment and about which there exists little data is the added attenuation a signal would experience traveling through the overhead canopy and jungle foliage. It may be assumed that this loss will vary as a function of antenna height, the loss decreasing with increasing antenna height. This measurement program will include measuring the ionospheric path loss as a function of receiving antenna height.

The approximate frequency range for each of the five modes is shown in Figure 5.1

5.1 Description of Measurements

Ten test frequencies were selected within the range of interest (0.1 Mc to 425 Mc) and are shown in Figure 5.1 These

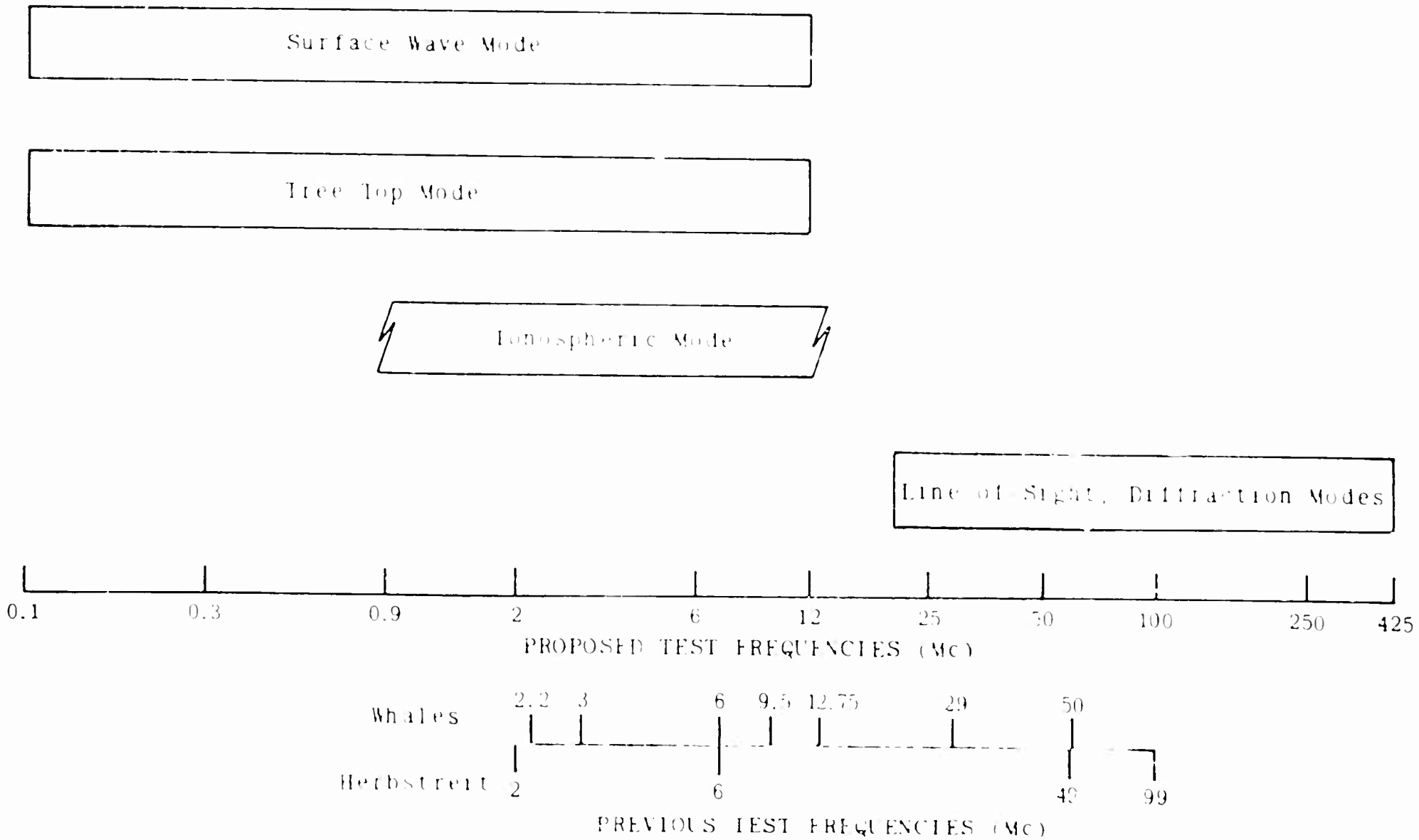

Figure 5.1. Proposed Test Frequencies.

selections were made in order (1) to obtain an even distribution across the range of interest, (2) to assure at least three frequencies per propagation mode, and (3) to verify previous experimental works performed independently by Herbstreit and Whale in jungle environments.

Transmitting antenna heights for horizontal polarization and vertical polarization at 25 Mc and above will be located above ground level (10 feet) between the ground and treetop height (45 feet) and above the treetop level (80 feet). Ground based vertical whips will be used for vertical polarization between 2 Mc and 25 Mc. Ground based top loaded antennas will be used from 100 kc to 900 kc. Table 5.1 shows the contemplated antennas for each test frequency. A block diagram of the transmitter facilities is shown in Figure 5.2.

Field strength measurements will be made along a maximum of three radials. A maximum of 12 receiving sites (field points) will be established on each radial. Within the limits of practical accessibility, these points will be distributed as follows:

(1) Four field points 0 to 1 mile from the source.
(2) Four field points 1 to 10 miles from the source.
(3) Four field points 10 to 30 miles from the source.

At each field point, the vertical distribution of field strength will be measured. Recordings will be made while the receiving antenna is raised from the ground level to 8[illegible] eet above ground. This will place the antenna above all but a few sparsely scattered tall trees. Height notations made on the recordings will relate the field strength data with antenna height. During data analysis, the total height will be divided into small (5 to 10 feet) sectors and field strength values will be determined for maximum, median, and the level exceeded 90 percent of the height. This procedure will be repeated at each field point for the various frequencies and polarizations. Because of the work involved in moving and erecting the antenna tower, as many as four different transmission conditions will be measured during one visit to a field point. For example, one measurement could involve radiation at MF with vertical

Table 5.1

TRANSMITTING ANTENNAS

Test Frequency (Mc)	Vertical Polarization Antenna Type	Horizontal Polarization Antenna Type
0.1	80-foot top loaded vertical whip, base tuned	
0.3	"	
0.9	"	
2.0	50-foot vertical whip, base tuned	λ/2 horizontal wire dipole (supported between two towers)
6.0	"	"
12.0	21-foot vertical whip	"
25.0	λ/2 vertical dipole, tower supported, and 21-foot vertical whip	λ/2 horizontal dipole (self-supporting on one tower)
50.0	λ/2 vertical dipole, tower supported	"
100.0	"	"
250.0	"	"
400.0	"	"

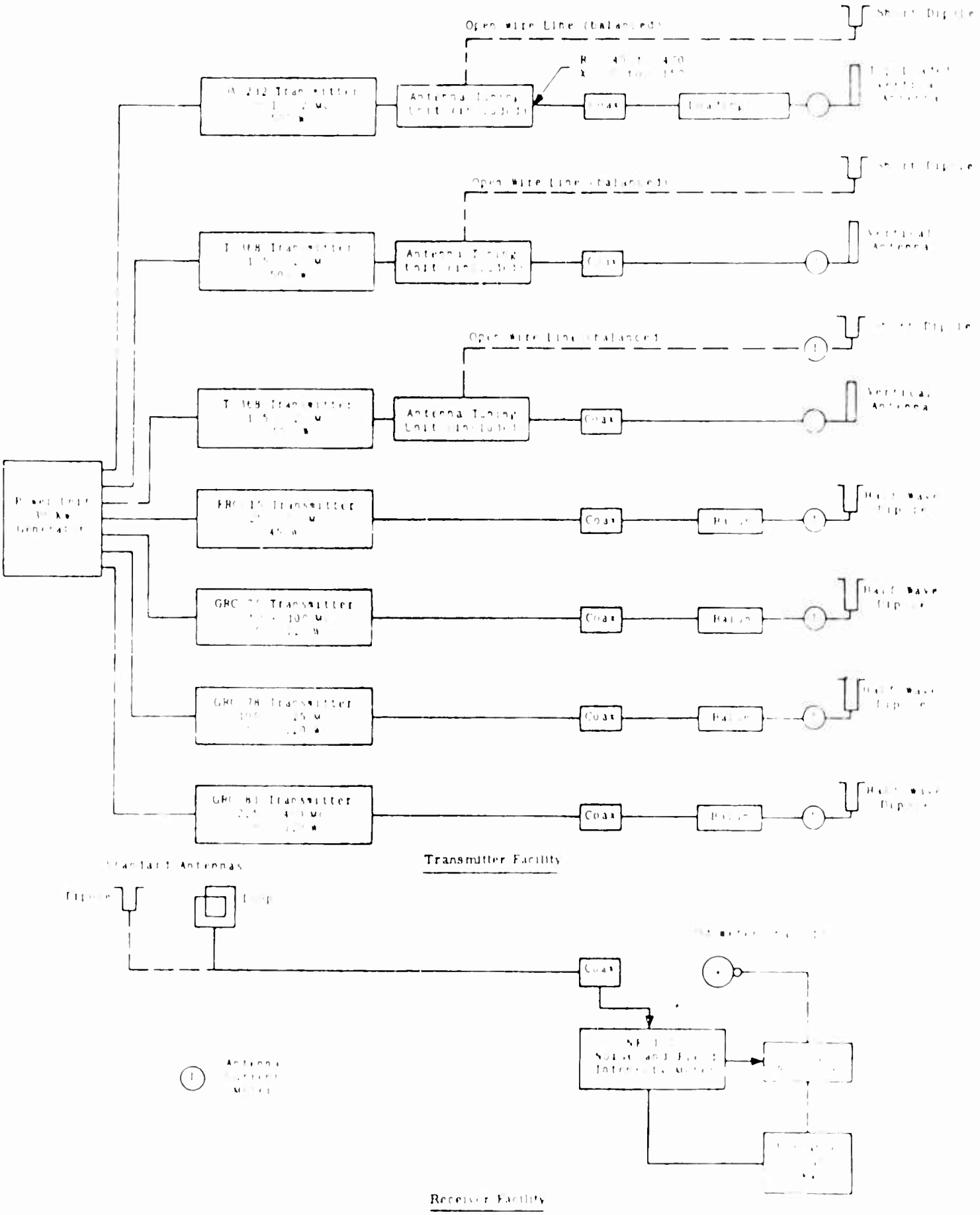

Figure 5.2. Overall Block Diagram of Measurement Facilities.

polarization, another at HF with horizontal polarization, and two others at UHF with vertical and/or horizontal polarization. The receiving antenna for each of these conditions will be different, requiring that the antenna be raised and lowered for each test with the necessary antenna changes made between tests. After the field strength has been recorded at a field point, ambient noise levels will be recorded at specific frequencies near the test frequency.

In addition to the vertical distribution of field strength at selected points, investigations will be made of the spatial distribution at ground level along the radial. Recordings of field strength will be made while progressing along the radial from one field point to the next. Only one transmission test condition can be measured at a time, so the distance must be traversed several times for each set of transmission conditions. During the recording, distance information must be carefully noted on the chart to allow data analysis for small distance sectors along the radial. In these cases, the field strength values will be determined for maximum, median, and the level exceeded for 90 percent of the distance for each of these sectors. These data, plotted versus distance, will show the spatial distribution of field strength along the measuring radial.

The measurements of the field strength via the ionospheric mode will be made in order to determine the path loss variation as a function of distance, antenna height and time on frequencies of approximately 2, 4, 8, and 12 Mc. Measurements will be made simultaneously at three receiver sites located 1-5 miles, 15 miles, and 30 miles from the transmitter. At each site the signal will be measured for 10 minutes at a constant antenna height of about 40 feet. The antenna will then be raised to 80 feet and the signal recorded for two minute intervals at height increments of 10 feet as the antenna is lowered to about 10 feet. At this point the transmission frequency will be changed and the measurement process repeated. After the field strength has been measured at each of the four transmission frequencies, the process will be repeated until 24 hours have elapsed. The measurement sequence will be repeated once each month for the duration of the program.

Two atmospheric conditions will be recorded each day. First, the daily amount of rainfall will be recorded once each day. Second, measurements of the dry bulb temperature, wet bulb temperature and atmospheric pressure, the parameters required to calculate the radio refractivity, will be made three times a day or more often if the diurnal variation requires. All of these measurements will be made at the transmitter site and will be assumed to be indicative of conditions along the transmission path.

5.2 Description of Test Equipment

Test Transmitters

The general requirements for the primary field tests state that propagation measurements are to be made over a frequency range of 100 kc to 400 Mc out to a distance of 30 miles. Transmitters have been selected from military communications equipment which cover this frequency range and provide output power of 45 to 500 watts. The table below shows the selected transmitters plus some of their characteristics.

TEST TRANSMITTERS

Quantity	Type	Frequency (Mc)	Power (Watts)
1	OA-232/GR	0.1 to 2	500
2	T-368/URT	1.5 to 20	500
1	AN/FRC-15	25 to 50	45
1	AN/GRC-75	50 to 100	50-1[illegible]
1	AN/GRC-78	100 to 225	50-[illegible]
1	AN/GRC-81	225 to 400	50-

Complete equipments have been requested for the first three types. This includes the transmitters plus a set of spare parts. The complete equipment in the case of the remaining three types includes power generators, and antenna systems, in addition to the transmitters. For each of these, the equipment lists were reviewed and only the units essential to operation per the test requirements were requested. Common power will be provided at the transmitter site. Special antennas designed for the propagation tests will be used rather than the military communication antennas

It is not anticipated that any modifications will be required within the various transmitters. The only changes will be in the operational procedures and possibly in the interconnections. In the event that internal modifications are required it is planned that the units would be restored to their normal condition at the completion of the program.

Two of the T-368/URT transmitters have been requested because three planned test frequencies are within the 1.5 to 20 Mc frequency range. To expedite the measurements, it will most probably be necessary to operate simultaneously on several frequencies. This can readily be accomplished by using two of this type transmitter plus one each of the other types.

Transmitting Antenna Systems

Antennas must be provided at the main site for test transmission and for communications purposes. Test transmission antennas will consist of vertical whips, dipoles and long wire antennas. The communications antennas will be a yagi array and a vertical whip Multiple antennas must be provided for test transmission purposes to allow simultaneous operation at several frequencies.

TEST ANTENNAS

Frequency	Antenna	Polarization	Height
100 kc	80 ft. Whip Top Loaded	Vertical	Ground
300 kc	80 ft. Whip Top Loaded	Vertical	Ground
900 kc	80 ft. Whip Top Loaded	Vertical	Ground
2 Mc	50 ft. Whip	Vertical	Ground
6 Mc	50 ft. Whip	Vertical	Ground
12 Mc	21 ft. Whip	Vertical	Ground
25 Mc	21 ft. Whip	Vertical	Ground
2 Mc	Horizontal Dipole	Horizontal	to 80 ft. max.
6 Mc	Horizontal Dipole	Horizontal	to 80 ft. max.
12 Mc	Horizontal Dipole	Horizontal	to 80 ft. max.
25 Mc	λ/2 Dipole	Vert. & Hor.	to 80 ft. max.
50 Mc	λ/2 Dipole	Vert. & Hor.	to 80 ft. max.
100 Mc	λ/2 Dipole	Vert. & Hor.	to 80 ft. max.
250 Mc	λ/2 Dipole	Vert. & Hor.	to 80 ft. max.
400 Mc	λ/2 Dipole	Vert. & Hor.	to 80 ft. max

The 50 and 80-foot whip antennas will be insulated and guyed towers. They will be assembled using 10-foot tower sections which are available commercially. By using this short section type construction they can be transported to the site and assembled and erected without the use of special equipment. The guy wires can be used for the top loading and isolated from the tower when operating on frequencies which do not require the top loading. It is planned that the communications antenna array also be mounted on the top of this tower.

The 21-foot whip would be a telescoping tubular whip mounted on an insulating base. This would be guyed and its total height can be adjusted by changing the extension of the telescoping sections.

The horizontal wire antenna would be supported by two towers which can be raised to a maximum of 80 feet or any height lower than this. Several firms build such a tower. Apar Manufacturing Corporation has one which extends from 12 to 85 feet. The horizontal wire antenna would be fastened to two of these towers, and its height above ground adjusted by raising the tower. The wire length will be adjusted using appropriately spaced insulators which can be shorted.

Dipole test antennas can be mounted on the top of the two adjustable towers. Resonant length adjustments and changes from horizontal to vertical polarizations can be made by lowering the towers.

To summarize, a total of three towers and one whip will be used for the test antenna system. Five test conditions are available with this arrangement. Vertically polarized transmission may be made at one frequency from 100 kc to 6 Mc and one frequency from 6 to 12 Mc. Horizontally polarized transmissions may be made at one frequency from 2 to 12 Mc. Vertical or horizontal polarization may be selected for two frequencies from 25 to [illegible] Mc.

Antenna matching units are to be located at the base of the antenna. Coaxial transmission lines are to be used to connect the transmitter to these matching units. In most cases antenna

matching networks furnished as part of the transmitter are adequate for the intended use. In some cases, particularly at the low frequencies where the whip antennas are short, modifications will have to be made to match the high reactance antennas.

Field Measuring Equipment

Equipment for the field intensity measurements will consist of a field intensity meter, receiving antennas, antenna supporting tower, recorder and power unit. Other support equipment will consist of vehicles to transport equipment and personnel, communications equipment for contact with the transmitter site, plus miscellaneous tools and equipment required for movement and work within the jungle environment. To expedite the measurement program within a ten-month period it is planned to use three measuring teams making it necessary to have three complete sets of field measuring equipment.

Field Intensity Meters

The field intensity meter selected for use on this program is the NF-105, manufactured by Empire Devices, In This meter measures over the frequency range of 14 kc to 400 Mc with one single instrument plus four plug-in tuning units. The NF-105 consists basically of a receiver, calibrating circuits, indicators and antennas. Maximum full scale sensitivity of 1 μv from 14 kc to 30 Mc, and 10 μv from 20 Mc to 400 Mc. Internal calibration is provided by an impulse generator and a sine wave calibrator. Its power supply requires 115 v 40 to 400 cps input, and produces regulated plate and filament voltage. Construction is for field use, in accordance with rigid military standards. A rubber gasketed cover is provided which renders the instrument waterproof and protects the controls and indicators.

Calibrated antennas furnished with the NF-105 consist of loops, rods and dipoles. A 36-inch diameter loop is used for measurements from 14 kc to 150 kc. From 150 kc to 25 Mc, a 41-inch rod with a matching transformer is used. Tuned dipoles with balun-matching transformers are used in the frequency range of 20 Mc to

400 Mc. Since transformers are used at the antennas, the length of the interconnecting coaxial transmission is not critical. Thirty-foot cables are supplied as standard. Longer lengths may be used provided a cable loss correction factor is applied to the results. The test plan procedures require measurements at heights up to 80 feet. The loss of the necessary length of transmission line must be measured versus frequency and applied to the measured data.

A second type field intensity meter is being provided which covers the frequency range of 550 to 1600 kc. This is a RCA type WX2E meter. It is battery operated and has a loop antenna which is a part of the instrument cover. It is very well adapted to portable use since it can be easily hand carried. This instrument was selected for its portability and will be used in the event it becomes desirable to measure in areas where it is impossible to penetrate with a vehicle.

Antenna Mounting

To investigate the horizontal distribution pattern of field strength it will be necessary to record measurements while the transporting vehicle is moving along the radial. For these measurements, the appropriate receiving antenna will be mounted on the vehicle at a convenient height above ground of 8 to 15 feet. The NF-105 and recorder plus power supply will be mounted and operated inside the vehicle. An antenna factor for the antenna mounted on the vehicle must be determined. This will be done by comparing the output of the mounted antenna with that of a standard antenna when immersed in identical fields. This calibration varies with frequency and will have to be repeated at all the test frequencies.

The other type of field intensity measurements are those which record vertical distribution of field intensity at selected intervals along the radial. To do this it will be necessary to erect a supporting tower for the receiving antenna and record field intensity as the receiving antenna is elevated from ground level to a height above the treetops. Because of the environment and the operational procedure, this tower must be lightweight, compact when collapsed, easily erected by several men in a reasonably short time, and be extendable up to a maximum of approximately 80 feet. It must

be constructed so as not to be adversely affected by the environment, must require a minimum number of guys and should be nonsusceptible to damage due to normal handling. Several types of these towers are available commercially, all of which will be investigated for possible use. The possibility of designing a tower is also being considered.

Recorders

A portable null balance type recorder manufactured by Emcee Electronics, Inc. has been selected to record the field intensity measurements. This unit operates on 115 v 60 cps power and uses a pressure sensitive paper. It employs a servo system and null balance which is more rugged than a type utilizing a meter movement. The pressure sensitive paper avoids the field problems inherent with an ink recorder. A special input amplifier is being provided by Emcee for use with the normal NF-105 output (100 μa into 1800 ohms). There are also provisions being made for moisture and fungus proofing the recorders. Four of these recorders, plus spare parts, are to be supplied. This number will provide backup equipment for failures as well as for recording purposes other than for field measurements.

Power Units

Portable gasoline engine driven power units are to be used to power the field measuring equipment. Hearth Industries, Inc. build a line of lightweight portable power units. The type selected is their Mark IA with an output of 1500 watts at 110 volts and weighing only 73 pounds. The generator employs axial air gap construction with permanent magnets which eliminate brushes and slip rings and reduces weight. Four of these units are to be ordered which will provide backup units and satisfy requirements for any other portable power uses.

Vehicles

All measuring equipments and personnel must be transported along jungle trails to the measuring points at a reasonable rate of speed. For this purpose, it is planned that an International

Harvester Scout or a Landrover (or equivalent vehicle) will be provided for each measuring team. The field intensity meter and recorder would be installed in the vehicle which is large enough to accommodate the equipment and operators.

Test Site Support Equipment

Power Generators

At the main test site, electric power for the test equipment and personnel's quarters will be produced by diesel-powered generators. Two each of 15 kw and 30 kw capacity are planned. The 15 kw units would provide 115 v AC power and the 30 kw units would be used to produce 230 v AC power. These voltages and power have been selected after evaluating the total power requirements. This combination provides maximum flexibility for load charges from maximum to minimum, and backup is accomplished by duplicating the units. The complete installation will include the generators with mounting pads and shelters, fuel storage tanks, and power switch panels plus the necessary distribution wiring.

Test Equipment Shelters

It is presently planned that four S-141()/G shelters will be used to house the test transmitters and to provide maintenance and conditioned storage facilities. The equipment mounting, bench and shelf space, power and lighting circuits, plus air conditioning equipment, will be installed at our laboratories in Alexandria, Virginia. These, plus all other equipments, would then be transported to Thailand where a minimum of work would be required to make the equipment operational. The shelter layouts have been planned for maximum operational efficiency and to provide suitable facilities for record keeping and maintenance work. Air conditioning has been incorporated in the design to protect the equipment in the hot humid jungle environment. After checking humidity conditions and heat loads, it was decided that two window-type air conditioning units rated at approximately 14,000 BTU would be adequate for each shelter. Each of these can be operated at two speeds which will

allow considerable variation in capacity to compensate for changes of heat loads within the shelters and also for external temperature changes. Two smaller units are being used rather than a single large unit because installation will be easier, cooling control will be more versatile, and outage of a unit will still allow some air conditioning in the shelter.

In the event that the delivery schedule of the communication shelters holds up the project schedule, it may prove necessary to change the plan and use another type of installation. It would then become necessary to build a building, or buildings, at the test site. All of the facilities included in the shelters would have to be incorporated in the building. The main difference would be in the air conditioning. For a building, it probably would be more economical to install a single large unit.

The building would be less desirable than the shelters for several reasons. All of the installation, wiring, air conditioning, and construction work would have to be done in Thailand at the test site. This would require the employment of various types of skilled labor, which could be a problem. At the end of the program, the equipment shelters could be moved easily to another location, whereas the building plan would not adapt itself to this mode of operation. In summary, it is felt that the shelters have numerous advantages. Every effort will be made to procure these structures without delaying the program.

RF Measuring Equipment

During the program, precision measurements of various transmission parameters must be made. These will include such parameters as antenna impedance, antenna input power, and frequency. Impedance measurements will be made using a General Radio Type 1606-A RF Bridge and Type 1602-B UHF Admittance Meter. The NF-105 Field Intensity Meter will be used as a detector. The General Radio Type GR 1330-A Bridge Oscillator or a Hewlett-Packard 606A or 608C Signal Generator would be used as the driver. Power measurements would utilize RF ammeters to measure line current together with the Sierra Model 164 Bidirectional Power Monitor. Frequency measurements will

be made using an AN/URM-32 Frequency Meter. These measurements will affect the accuracy of the program results, and the equipment was selected to assure the highest degree of precision and to be adaptable to use in the field. Other RF measuring equipment will be used primarily for maintenance pruposes and will be described in that section.

Calibration Equipment

To assure the degree of accuracy essential to the program, calibration checks must be made on the equipment at periodic intervals. Impedance measuring equipment will be checked by comparison with accurate standard RF components such as line terminating resistors. Field intensity meters will be calibrated against the output of Hewlett-Packard 606A or 608C Signal Generator and with standard coaxial attenuators. The signal generator accuracy will be checked using a Hewlett-Packard 431-B Power Meter. Using the above procedure plus other cross checking which is possible, the accuracy of the measuring equipment will be maintained throughout the entire program.

Maintenance Equipment

Equipment must also be supplied to trouble shoot and maintain the test transmitter plus the measuring and calibration equipment. Two oscilloscopes are to be provided, one a Tektronix 515A and the other a Hickok 675A. A 500-watt dummy load, Sierra Model 160-500 plus a Sierra Model 164 Bidirectional coupler will be used when checking transmitter operation and tuning. Measurements Corporation Model 59 Combination Megacycle Meter will be supplied to be used for general trouble shooting and RF circuit checking. Two Hewlett-Packard 410B Vaccum Tube Voltmeters are included as part of the maintenance equipment. An AN/USM-118 tube tester or equivalent will be supplied. In addition to these major items miscellaneous multimeters, RF fittings and probes and maintenance tools will be required to keep the equipment operational.

Meteorological Kit

Certain weather data must be measured and recorded throughout the measurement program. This would include, as a minimum, temperature, relative humidity, barometric pressure and rainfall. A meteorological kit has been requested as a GFE item.

Communications Equipment

For project coordination as well as for safety reasons it is imperative that radio communication links be established between the headquarter's office in Bangkok and the main field test site and between the test site and the measuring teams. The distance from Bangkok to the test site is in the order of 150 miles. The most suitable link would be one which utilizes the HF skywave mode of propagation. Usable frequencies must be calculated for the path over the measurement period and these must then be coordinated with the cognizant authorities in Thailand.

Communications within the jungle environment between the test site and the measuring teams present a much more difficult problem. There is a very distinct possibility that communications may not be possible at all times and locations. It is planned that one vehicle per measuring team be equipped with a portable type transceiver operating in the range of 150 Mc; a base station transceiver would be installed at the main test site. These would be used to the extent possible to coordinate the field test program. After some operational experience is gained the areas where two-way communications are possible will become known and utilized when communications are required. Field experience may also result in the necessity for changes in equipment or operational procedures.

Spare Parts

To assure reliable and continuous operation adequate spare parts must be included. This problem has been approached by providing spare equipments for critical items as well as spare components. The military type transmitters have been ordered with their normal complement of spare parts. Malfunctions in these units can be

diagnosed and repaired using components from the spare parts kits. Commercial facilities which are important to the operation of the program such as field intensity meters, recorders, power units and signal generators have been ordered to include spare units. This will allow measurements to continue while a disabled equipment is being repaired. Parts lists have been reviewed for all the commercial units, and a coordinated list prepared for such components as tubes, electrolytic capacitors and other items which experience indicates may fail. These parts will be provided for field repairs of the equipment. Additional maintenance support is also available via air from the original manufacturers in the event of a breakdown for which spare parts have not been provided. It has been estimated that ten percent of the price of the test equipment should cover the cost of the spare parts.

Equipment Environmental Protection

Protection of the equipment in the field environment is being approached in two ways. One way is to actually apply protective treatment to the equipment and the other is to control the environment. Moisture and fungus proofing will be applied to the commercial equipment insofar as practical. Shock and vibration isolation will be provided for vehicular-mounted equipment. At the transmitter site, the shelters or other enclosures housing the equipment will be air conditioned to control both temperature and humidity. All equipment will be stored in this conditioned environment when not in actual use. Much of the equipment will also be operated in this environment. The field intensity meters and recorders used in the field will be powered at all times in the field. Thus, internally generated heat will minimize humidity condensation inside the equipment.

5.3 Description of Measurement Techniques

The effects of jungle foliage upon other various modes of propagation will be determined after evaluating the basic transmission loss over each test path. The basic transmission loss[1,2], L_b,

1. Dr. H. R. Reed, "Propagation Data for Interference Analysis" Contract Number AF 30(602)-1934. Jansky & Bailey Division of Atlantic Research Corporation.
2. K. A. Norton, "System Loss in Radio Wave Propagation," N.B.S. Journal of Research, vol. 630, pp. 53-73, July-August, 1959

(sometimes called path loss), which is defined as the transmission loss expected between fictitious loss-free isotropic transmitting and receiving antennas at the same locations as the actual transmitting and receiving antennas, may be expressed as,

$$L_b = 36.57 + 20 \log f_{mc} + 20 \log E_o \frac{\mu v}{m} - 20 \log E \frac{\mu v}{m} \qquad (5.1)$$

where

E_o is the free-space field at one mile in microvolts per meter

E is the signal at the receiving antenna expressed in microvolts per meter.

Thus the path loss between a transmitter and receiver may be evaluated if the free-space field of the transmitting antenna and the field strength at the receiving antenna are known.

Two general or classical methods are available for measuring field strength. They are (1) the standard antenna and (2) the standard field methods. The first technique makes use of a standard antenna of known dimensions in which the relationship between the field strength of the radio wave and the voltage that it induces in the antenna is known. The second method involves comparison of the voltage induced in the antenna by the radiating field with that voltage induced in the same antenna by a known generated field. The standard antenna method will be used in this program.

Field Strength Measurements

The field strength measuring equipment will include an Empire Devices NF-105 Noise and Field Intensity Meter and associated antennas, a strip recorder, an antenna tower and transmission line, and a portable power generator. A block diagram of the receiver facility is shown in Figure 5.2.

The basic antennas associated with the NF-105 are the loop, whip, and dipole. Each antenna represents a "standard antenna" and, in conjunction with the NF-105, is calibrated directly in terms of field strength (volts/meter). The loop antenna will be used for

the lower frequencies up to 150 kc where the loop's electrical size is not appreciable. A 41-inch whip antenna will be used from 150 kc to 25 Mc. Dipoles will be used over the range from 25 Mc to 425 Mc. The antennas will be raised to any desired height up to 80 feet by a portable telescoping tower.

The output of the NF-105 Noise and Field Intensity Meter will be recorded directly on a portable strip recorder which is calibrated to allow the recorded values to be converted to units of field strength. The recorder will be calibrated using the NF-105 metered output circuitry. System accuracy is thus determined by the NF-105 characteristics.

In addition to field strength measurements at the selected field points, recordings of field strength will be made near ground level along the radial. The equipment will be the same as that used for the measurements at the fixed field points. In this instance, the NF-105 calibrated antenna for the measuring frequency would be mounted on the transporting vehicle. Since the vehicle will influence the antenna calibration, it will be necessary to calibrate the antenna when mounted on the vehicle. This is easily done by comparing the antenna and vehicle to the calibrated antenna only, and thus determining new antenna factors and directivity constants, if any exist. A calibration check such as this would have to be made at all test frequencies and for both horizontal and vertical polarization.

For these measurements, the field strength meter output will be recorded on a strip chart recorder driven by an odometer. Distance identification points along the radial must also be marked on the chart to provide positive position information at all times during the recording. Only one frequency and polarization can be recorded each time the radial is traversed.

Receiver Calibration

At any measurement point, it is important that the field intensity meter (NF-105) and recorder be accurately calibrated in terms of field strength. Since the NF-105 was designed for this purpose, it has an internal standard which is used for calibration. The strip recorder has built-in gain stabilization circuitry. A reference voltage derived from an internal mercury cell is applied

to the input and the meter input amplifier gain is adjusted for the standard deflection. This standardizes the gain so that a 100 μa signal (maximum NF-105 output) will deflect the meter pen to full scale on the chart. In this manner the NF-105 meter and the recorder indications are correlated. This calibration must be made and checked at intervals during the measuring periods. A single additional check must be made one time. This is the check which correlated the NF-105 output indications to the strip chart values. This will be done in the laboratory using an external signal source to vary the NF-105 over its metered output range. Recorder values would be measured and plotted versus the NF-105 output levels. This would constitute a calibration of the recorder values. The normal NF-105 antenna factors applied to the recorded information will then convert the data to field strength in microvolts per meter.

Transmitting Antenna Calibration

The free-space field referred to in Figure (5.1) will be evaluated by calibrating the transmitting antenna using the standard field method previously mentioned.

In this calibration, the field strength is measured at a finite distance from the transmitting antenna. A signal generator and its antenna are substituted for the transmitting source and the field strength again is measured. The free-space field strength, E_o, at the transmitting antenna is then determined by comparing the field strength, E, from the antenna under measurement with E′, produced by the standard field. (Refer to the following illustration.)

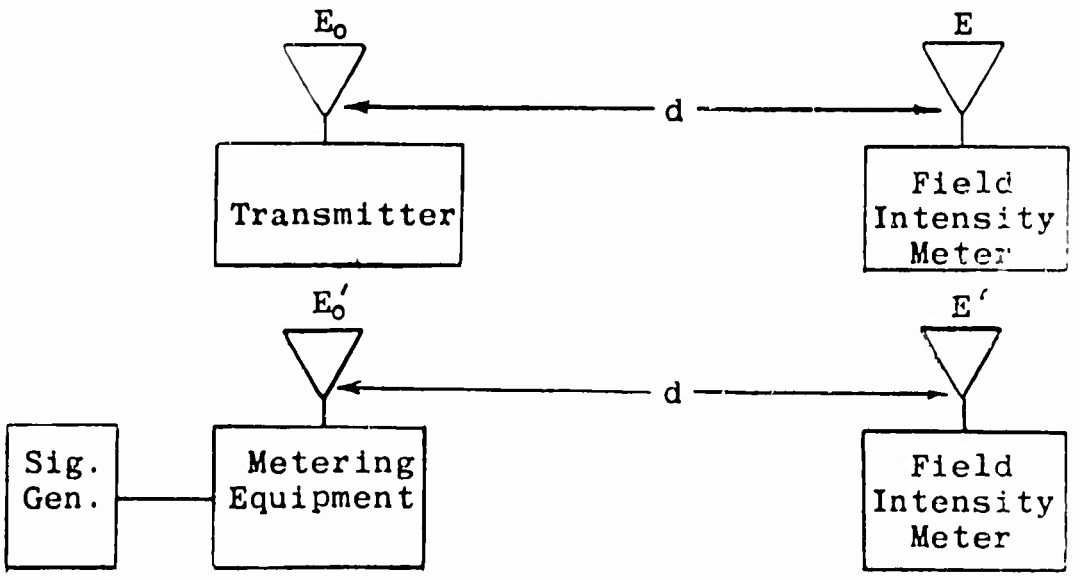

where

E' = radiation field in the plane of the loop at distance, d, on the earth's surface from standard field antenna

E_o' = free-space electric field strength in volts/meter in the plane of the loop

E = radiation field in the plane of the loop at distance, d, on the earth's surface from unknown antenna

E_o = unknown free-space field intensity

Then

$$E_o = E_o' \times \frac{E}{E}, \text{ volts/meter}$$

Distance, d, can be arbitrary; however, in most cases, it should be at least a wavelength at the measured frequency. At the lower frequencies, where the antennas are electrically short, d can be as small as one-half wavelength.

Since nearly all of the transmitting antennas are of a standard variety (i.e. whips and dipoles) the test transmitters and their associated antennas will be used as standard field generators. The current will be measured at the bases of the whip antennas and at the feed points for the dipole. When the antenna dimensions and current are known, the free-space field strength may be computed using the following relations.

Short top loaded vertical antenna carrying a uniform current:

$$E_o = \frac{60\pi}{d} \frac{H}{\lambda} I_a \qquad (H < \lambda/10) \qquad (5.2)$$

Center-fed horizontal or vertical antenna of any length:

$$E_o = \frac{60\ I_a}{d \sin \frac{\beta \ell}{2}} \left[1 - \cos \frac{\beta \ell}{2}\right] \qquad (d > \lambda/6) \qquad (5.3)$$

For a half-wave dipole this becomes

$$E_o = \frac{60\ I_a}{d} \qquad (5.4)$$

Vertical whip

$$E_o = \frac{60\ I_a}{d \sin \beta H} \left[1 - \cos \beta H\right] \qquad (H = n\ \frac{\lambda}{2}) \qquad (5.5)$$

E_o = field strength in volts/meter at distance d

d = distance in meters

λ = wavelength in meters

H = height of vertical antenna in wavelengths

ℓ = length of center-fed antenna in wavelengths

I_a = current at antenna base in amperes

Expressions (5.3) and (5.5) are derived assuming an infinitely thin antenna having a sinusoidal current distribution. For this antenna the base or terminal current is related to the loop current by

$$I_a = I_{loop} \sin \beta H \qquad (H = \frac{\ell}{2}) \qquad (5.6)$$

For antenna lengths for which H is a multiple of a half-wavelength, the assumed sinusoidal distribution gives a value of zero for the current at the feed point corresponding to an infinite input resistance. At these lengths the actual input current will be small but not zero, and the input resistance will be large but not infinite.

Therefore, the following expression for free space field strength will be used for values of H near n $\lambda/2$.

$$E_o = \frac{60\ I_{loop}}{d} \left[1 - \cos \beta H\right] \qquad (5.7)$$

where I_{loop} is determined from the following expression

$$I_{loop} = \left[\frac{P\ \eta_1\ \eta_2}{R_R}\right]^{\frac{1}{2}} \text{ amperes (rms)} \qquad (5.8)$$

where

η_1 = antenna efficiency

η_2 = transmission line and coupling efficiency

P = transmitter output power in watts

R_R = antenna radiation resistance referred to the loop

For H = $\lambda/2$, R_R = 100 ohms and η_1 = 0.95.

Measurement of Ionospheric Mode Path Loss

A pulse discrimination technique will be employed in order to eliminate the effects of signals received via other propagation modes when measuring short range ionosphere path loss. This technique utilizes the fact that the transmission time for the ionospheric path is much greater than for the ground wave. Thus, when pulses of shorter duration thanthe difference in propagation time between the modes are employed, the received signal may be separated into its components parts and undesired signals blanked out at the receiver. A general idea of the display of the received signal over one period is shown in the diagram below.

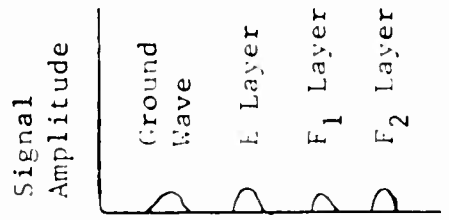

The following table shows the approximate propagation times to the various measuring points.

Distance	Ground Wave Prop. Time	E Layer Prop. Time	F_1 Layer Prop. Time	F_2 Layer Prop. Time
mi	ms	ms	ms	ms
5	0.016	0.734	1.33	2.00
15	0.050	0.734	1.33	2.00
30	0.117	0.734	1.33	2.00

In order to obtain the desired resolution for separating the signals, transmitted pulses should be of the order of 200 μs or less duration with a repetition rate of approximately 300-350 cycles.

The suggested instrumentation for this system is shown in Figure 5.3. The output of a pulse generator is used to pulse the exciter of the T-368 transmitter whose output is then a train of CW pulses. The signal is received by an NF-105 noise & field intensity meter whose detected output is gated such that the ground wave may be eliminated. The signal is then amplified and integrated to a dc level which is, in turn, plotted on a strip recorder. With calibration this dc level corresponds to a finite value of field strength.

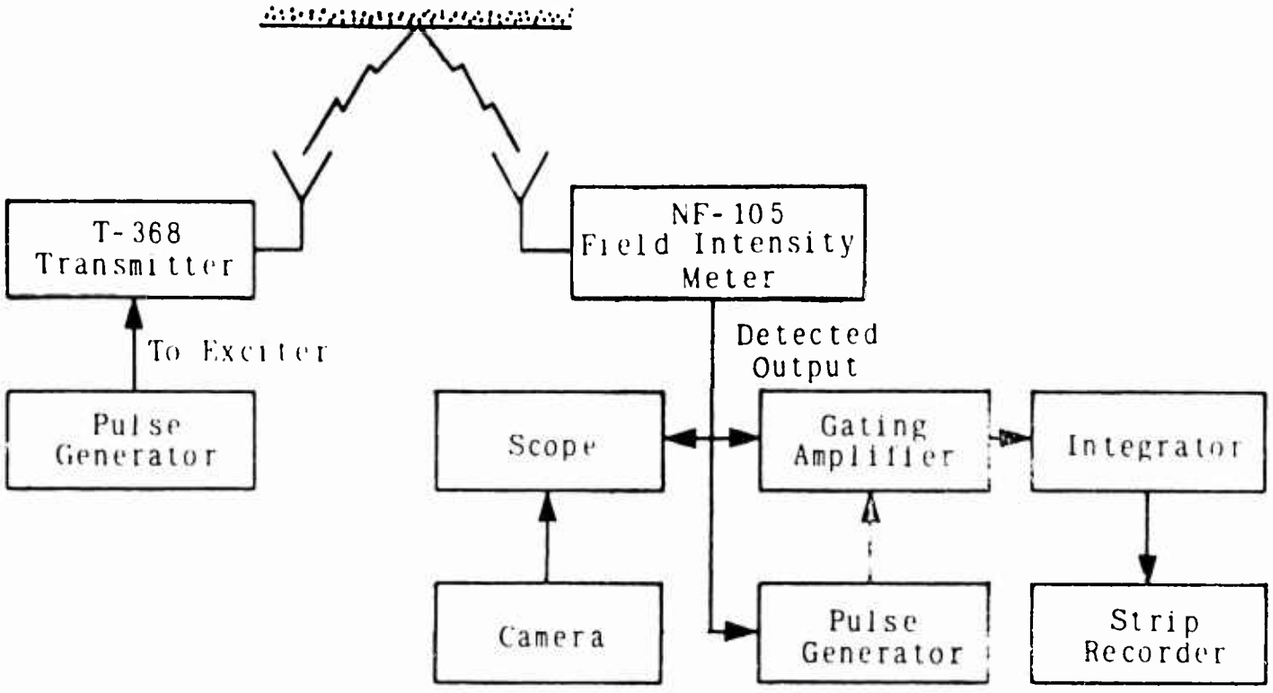

Figure 5.3. Instrumentation for Measuring Ionospheric Mode Path Loss.

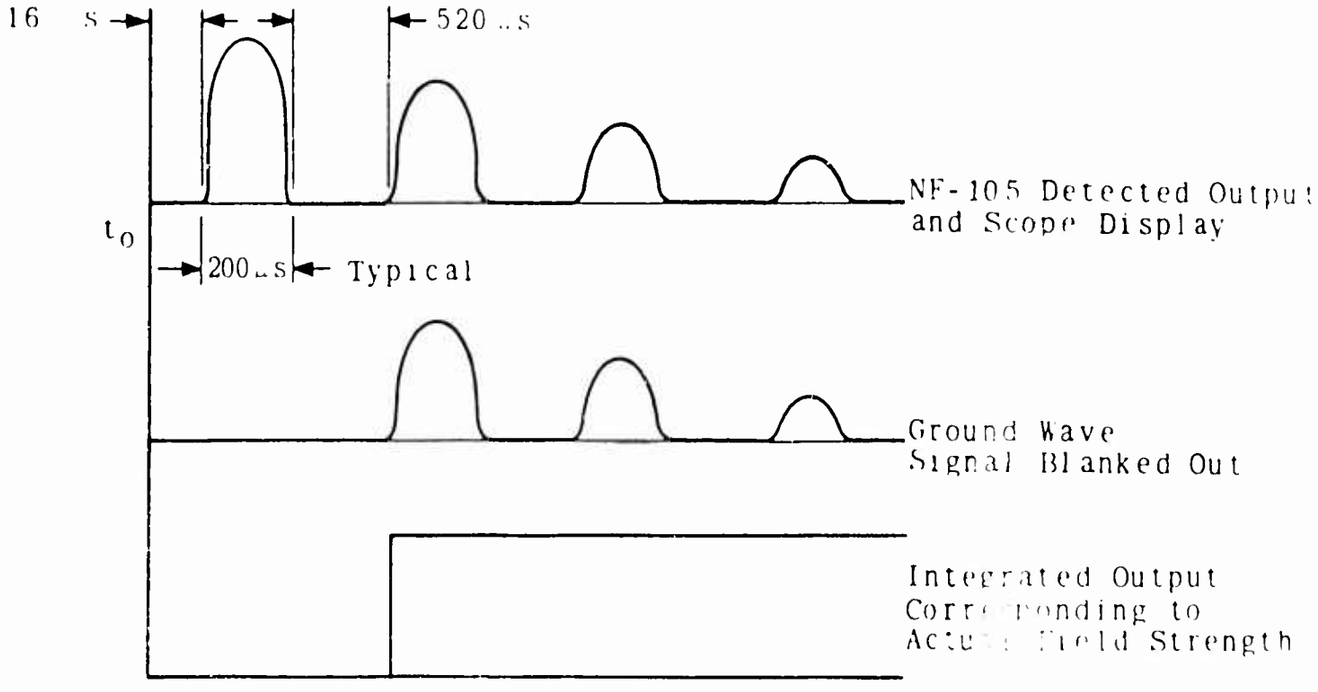

Figure 5.4. Instrumented Signal Waveforms.

The time difference between the various pulses may be measured when the NF-105 output is displayed on an oscilloscope. These measurements may be used to evaluate the virtual layer heights and the relative amplitude of each reflected signal.

Figure 5.4 shows the expected received signal waveforms observed with this instrumentation.

Measurement of Atmospheric Noise

Measurements of the ambient noise will be made in the same general manner as the field strength measurements. The noise level in microvolts per meter will be measured at discrete frequencies with the NF-105 Noise and Field Intensity Meter.

Weather Data

A meteorological kit has been requested in order to provide instruments to measure dry bulb temperature, wet bulb temperature, barometric pressure, and the amount of daily rainfall. The first three parameters are used to compute the radio refractivity and will be measured at least three times each day while tests are being conducted. Barometric pressure readings are also required for proper operation of a precision altimeter to be used for measuring field point elevations.

5.4 Field Data Reduction

The field strength recordings sent to the administrative office in Bangkok for data reduction will be of two forms. One form will show the measured field strength in microvolts per meter as a function of distance; the second will show the field strength in microvolts per meter as a function of height at a fixed distance. In both cases, time of measurement (date and hour), frequency, distance, antenna heights, polarization, weather conditions (rain, overcast, clear, etc.) and the radiated field at one mile will be printed on the original recordings.

The recordings resulting from the measurements that are made with the receiving equipment in the moving vehicles will show

the received signal as a function of distance which is determined in the following manner. The results of an aerial survey will be used to determine the location of the jungle trails and significant landmarks relative to the transmitter site. This information will be transferred to maps of the area. Concentric circles, centered on the transmitter, will also be drawn on the map every 0.2 mile from 0.6 to 3.0 miles and every 0.5 mile beyond 3.0 miles. Those points defined by the intersection of the boundaries of the distance sectors and the jungle trails will be marked along the trail. As a vehicle moves between field points, each distance sector boundary will be marked on the recording as the vehicle passes that point. A record of the distance traveled within the sector will also be noted on the chart.

Each sector of each recording will then be analyzed for three values of field strength: (1) the value exceeded for 10 percent of the distance within the sector, (2) the median value of field strength within the sector, and (3) the value of field strength exceeded for 90 percent of the distance within each sector. In all cases, the received field intensity will be adjusted to correspond to a free-space field of 100 millivolts per meter.

Figure 5.5 shows how an original recording for a distance sector between 3.0 miles and 3.5 miles might appear for the frequency and antenna heights indicated. The odometer scale below the recording shows that the vehicle traveled one mile within the sector boundaries and that the chart advanced at the uniform rate of five inches per mile. Ten percent of this distance, or 0.1 mile, corresponds to a horizontal chart length of 0.1 mile x 5 inches per mile. As shown on the figure, the field strength value exceeded for only 0.5 inch of the horizontal scale (10 percent of the distance traveled within the sector) is 6.5 millivolts per meter. This value, corrected to a free-space field of 100 millivolts per meter at one mile, is 21.7 millivolts per meter. The value of field strength exceeded for 50 percent of the distance within the sector of 0.5 mile (2.5 inches on the horizontal scale), is 6.0 millivolts per meter. The corrected field strength is 20.0 millivolts per meter. The corrected value exceeded for 90 percent of the distance (4.5 inches on the horizontal scale) is 4.6 x 100/30, or 15.3 millivolts per meter.

Figure 5.5. Sample Field Strength Recording.

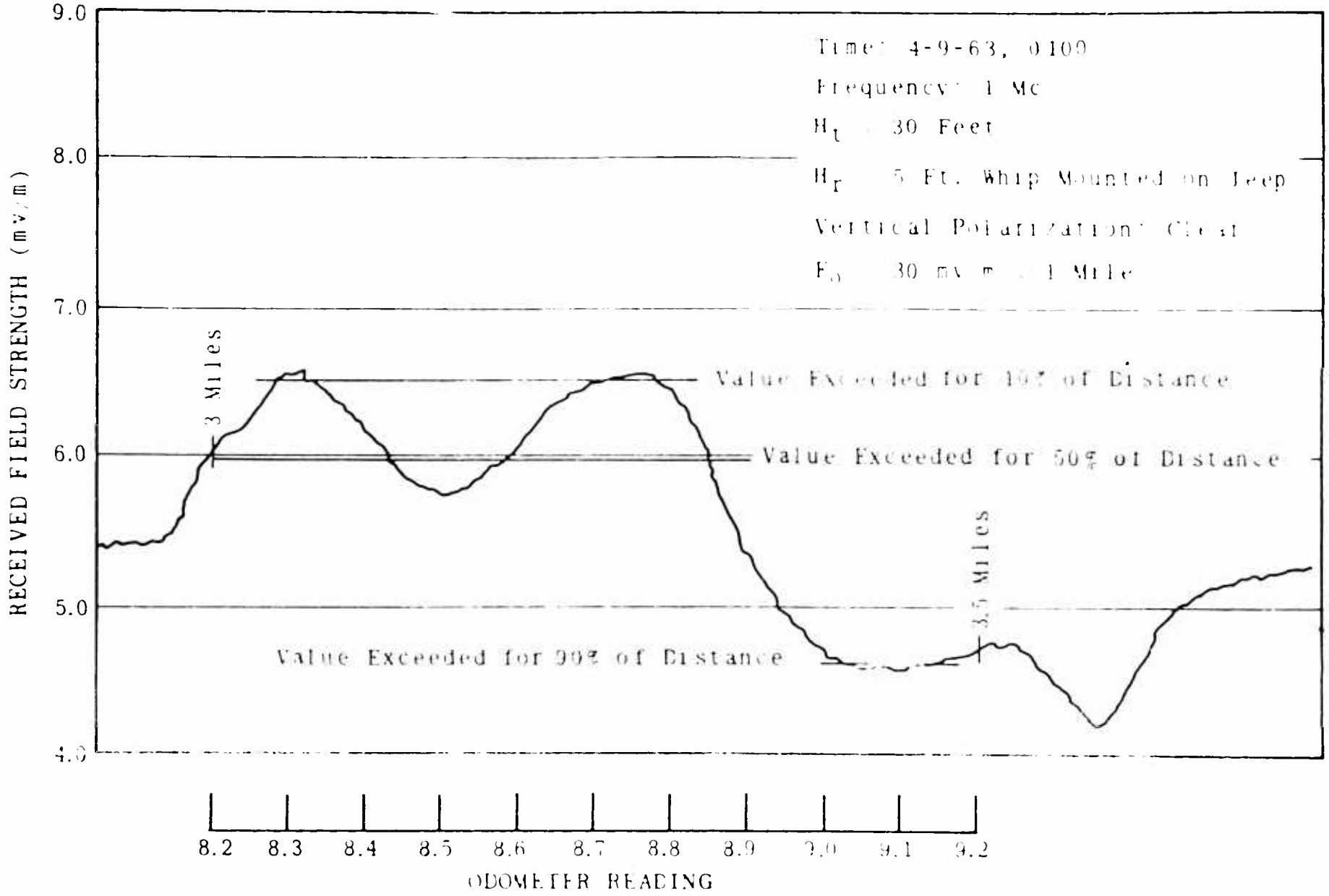

Figure 5.5. Sample Field Strength Recording.

Figure 5.6 shows the results of this type of analysis for a complete radial. To show the type of terrain along each route where the field intensity measurements were made, a curve of height in feet versus airline distance (the path profile) will be plotted for each route on the same sheet with the field intensity radial of that route. These curves will be obtained by determining the height for each sector from topographic maps and an altimeter, and plotting this height for each sector versus the distance from the transmitter location to the center of that particular sector. When the changes in elevation within any one sector are too numerous to be accurately shown by one point on the curve, the sector will be divided into smaller sectors and a height determined and plotted for each of these small subdivisions. Because the routes are not true radials, the profiles do not represent the exact contours between the transmitter and any one sector. They do, however, show the general nature of the terrain.

The second form of recording to be reduced at the Bangkok office will show the variation of field strength with receiving antenna heights at a fixed distance. These recordings will be analyzed in a manner similar to the method discussed above. However, in this case, the height will be divided into sectors (approximately 10 feet). Again, three values of field strength will be determined from the measured data: (1) the field strength value exceeded for 10 percent of the height sector, (2) the median field strength or value exceeded for 50 percent of the height sector, and (3) the value exceeded for 90 percent of the height within each interval. The data resulting from the measurements at various antenna heights will be presented in a form similar to that shown in Figure 5.7 where field strength values have been plotted at the center of the height sectors.

ELEVATION

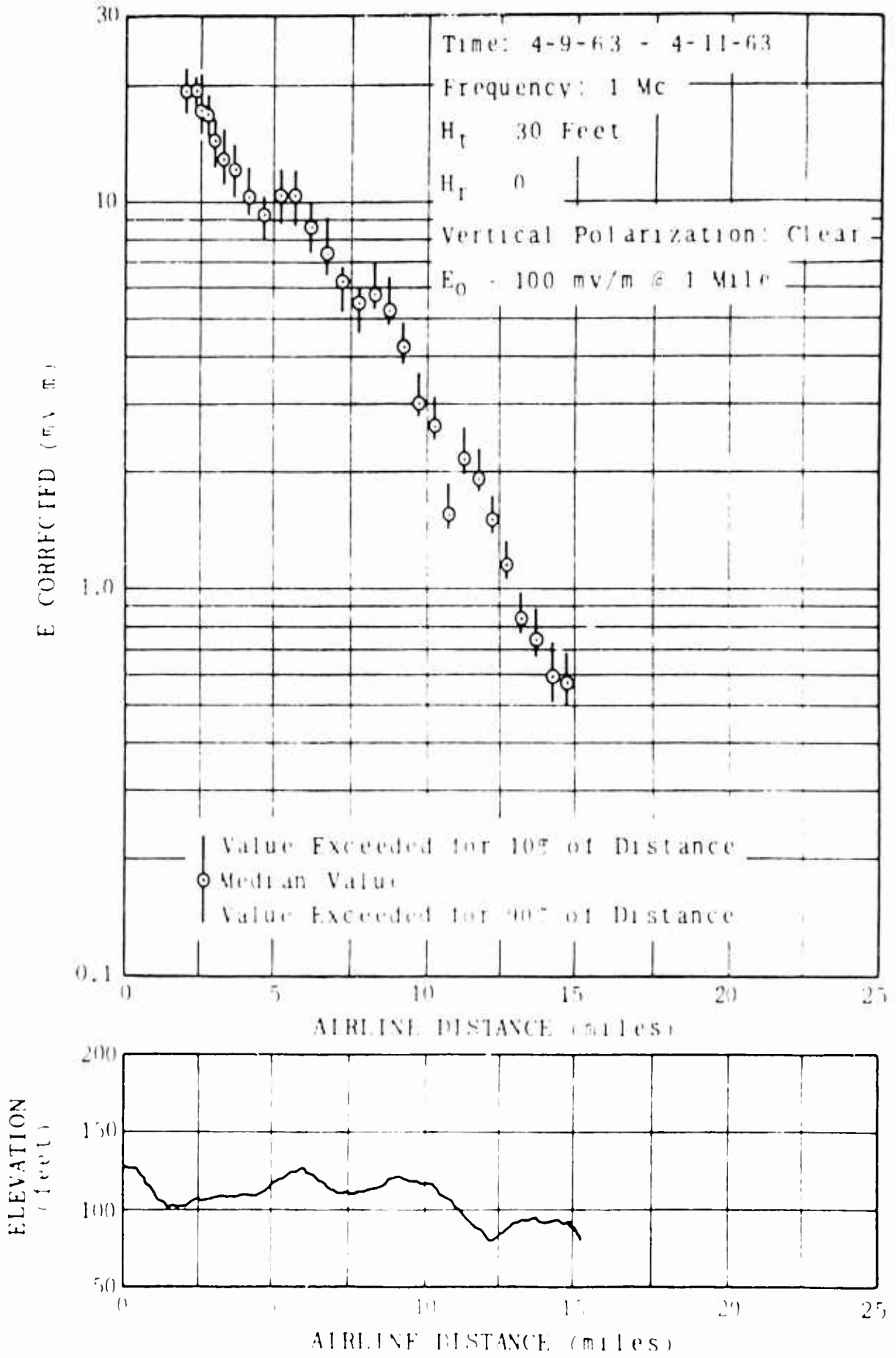

Figure 5.6. Variation of Field Strength with Distance.

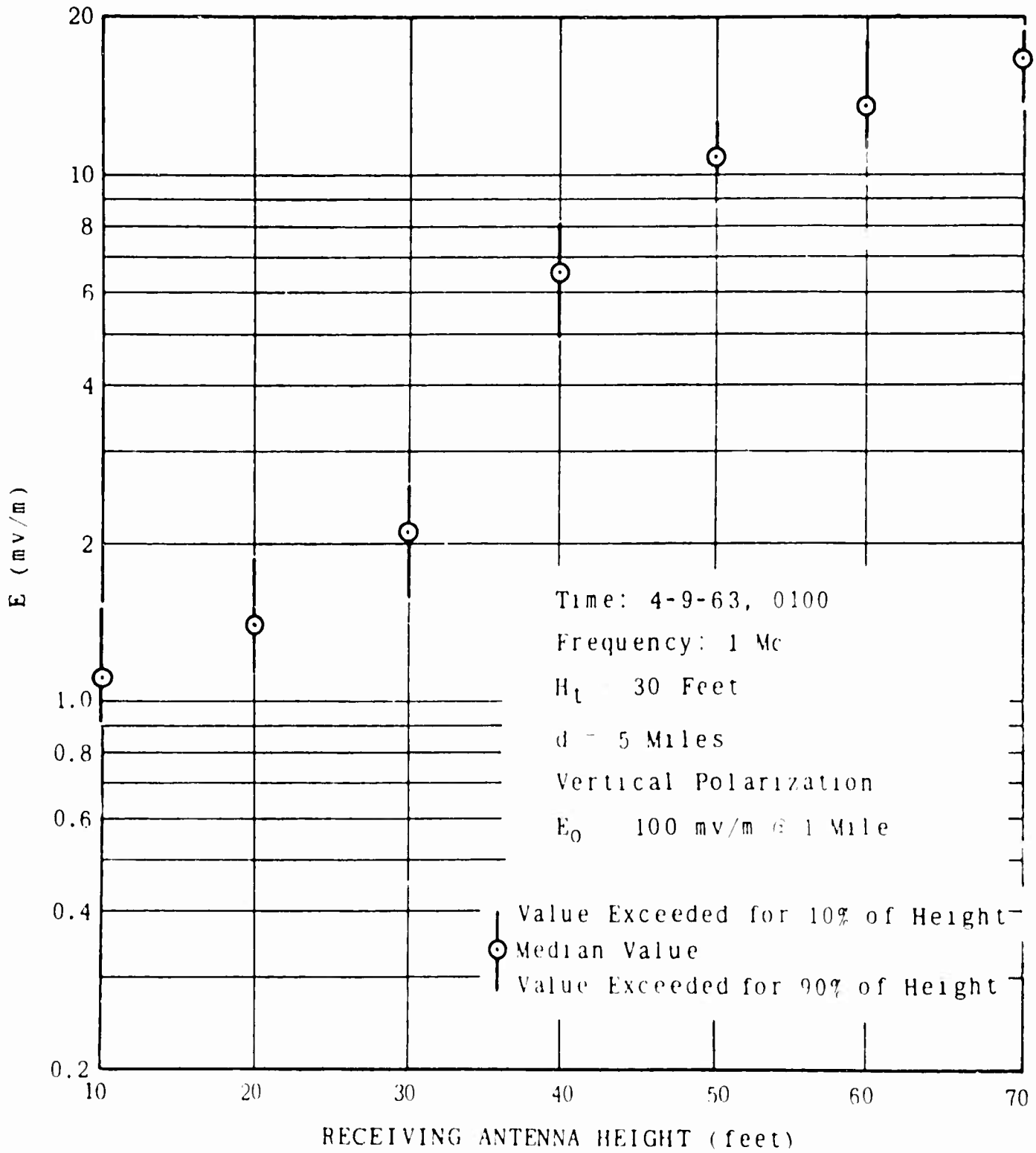

Figure 5.7. Variation of Field Strength with Receiving Antenna Height.

6.0 DATA ANALYSIS

Although the majority of time during this reporting period has been devoted to the preparation of the "Tropical Propagation Research Primary Field Test Plan", some work pertaining to the data analysis procedures has been started. Figure 6.1 shows the contemplated data analysis procedures. The over-all objective of the analysis is to devise a method of predicting the basic transmission loss (L_b) and its statistical distribution over irregular terrain covered by jungle foliage and to determine noise factors (F_a) appropriate for tropical areas. When the factors L_b and F_a are available, Equation (2.1) may be used to evaluate the applicability of new and existing communication equipment to tropical environments.

The approach to the data analysis, as outlined in Figure 6.1, is based on the assumption that foliage attenuation and rough terrain attenuation can be separated in the measured data. This will be accomplished by predicting the path loss over rough terrain in the absence of foliage for each propagation path. The difference in this predicted loss and the measured loss will be attributed to foliage attenuation. Statistical methods will then be used to relate the foliage attenuation to identifiable factors which influence the attenuation.

The first two columns on the left of Figure 6.1 indicate the type of data that will be obtained from the field measurement program. Because of the large volume to be handled, each series of measurements will be coded appropriately for later identification as shown in the third column. Study effort is shown in the blocks outlined by the dot-dash lines and represent the development of methods of analysis to be applied to the field data. Three of these studies have been started during the present reporting period and will be considered in greater detail later in this section. When all the studies are completed and the field data are available, manual operations indicated in the blocks formed by the solid lines in the fourth column will be started. The blocks formed by the dashed lines indicate the operations which can readily be performed by a digital computer. The results

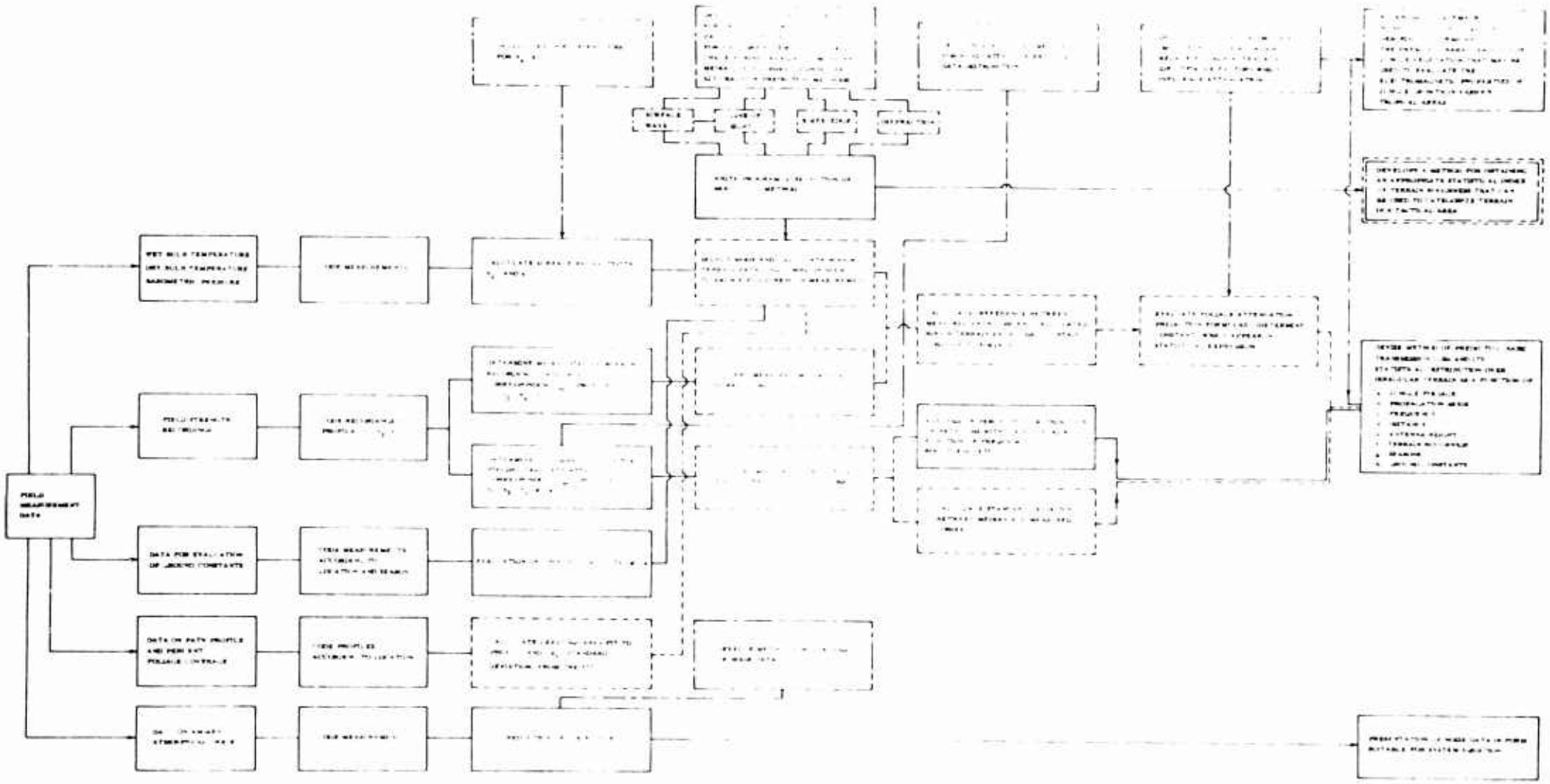

Figure . Data Analysis Procedures; Tropical Jungle Propagation Measurements.

of columns six and seven will lead to the results shown in column eight which are a summary of the over-all analysis objectives.

The three studies which have been started are

(1) Develop a method of analysis for radio refractivity N_s and the effective earth's radius factor k.

(2) Develop a mathematical model for calculating rough terrain path loss in the absence of foliage for each mode.

(3) Develop a method for obtaining an appropriate statistical index of terrain roughness that can be used to categorize terrain in a tactical area.

These studies are discussed in the following sections.

6.1 Calculation of Radio Refractivity and Effective Earth's Radius Factor

The radio refractivity is known to be a function of three basic atmospheric parameters: temperature, pressure, and water content. The relationship between these quantities is expressed as

$$N_s = (n - 1)10^6 = \left[\frac{77.6}{T}\right] p + \frac{(4810e)}{T} \qquad (6.1)$$

where the total air pressure, p, and the water vapor pressure, e, are in millibars and the temperature, T, is in degrees Kelvin.

Figure 6.2 shows a data sheet suitable for both recording the necessary data in the field and computing the radio refractivity using Equation (6.2). The first and second columns show the date and time of observation. The third, fourth, and fifth columns are used to record the dry bulb temperature, wet bulb temperature, and barometric pressure (These three parameters will be measured at least three times each day—in the morning, at noon, and in the afternoon.) The sixth column shows the atmospheric pressure expressed in inches of mercury. The seventh column is used to record the difference between the actual atmospheric pressure and the standard atmospheric pressure.

The water content in grains of water per pound of dry air (W') is obtained from a psychrometric chart as a function of

(1) Date	(2) LMT	(3) Dry Bulb Temp. FDB	(4) Wet Bulb Temp. FWB	(5) Atmos. Pressure P_a	(6) P_a	(7) ΔP_a	(8) W'	(9) W'_s
		°F	°F	mm Hg	in Hg	in Hg	Grains	Grains
Data	Data	Data	Data	Data	0.03937 (5)	(6) - 29.92	Fig ____	Fig ____

(10) ΔW	(11) W	(12) Water Vapor Pressure e	(13) CDB	(14) KDB	(15) P_a	(16) $(15) + \frac{4810\ (12)}{(14)}$	(17) N_s
Grains	Grains	Millibars	C	°K	Millibars		
Eqn ___	(8) + (10)	$\frac{(11)\ 1013.25}{4360 + (11)}$			(5) x 1.3332		$\frac{(16) \times 77.6}{(14)}$

Figure 6.2. Radio Refractivity Data Sheet.

dry bulb temperature and wet bulb temperature for a barometric pressure of 29.92 inches of mercury (see Figure 6.5). This value is recorded in the eighth column. Moisture content corrections for barometric pressures other than the standard value of 29.92 inches, Hg, are obtained using the following equation and Figures 6.3 and 6.4. The moisture content correction in grains per pound of dry air is expressed as

$$\Delta W = \Delta W'_S \left[1 - \frac{FDB - FWB}{2400} \right] \qquad (6.2)$$

where

$\Delta W'_S$ = moisture content correction of air saturated at wet bulb temperature when barometric pressure differs from standard barometer (grains per pound of dry air) and is obtained from Figures 6.3 and 6.4

FDB = dry bulb temperature in degrees Fahrenheit

FWB = wet bulb temperature in degrees Fahrenheit

The water content in grains of water per pound of dry air (W) for any barometric pressure is then

$$W = W' + \Delta W \qquad (6.3)$$

Columns 8 through 11 are used to calculate W. This value of W is then converted to water pressure, e, in millibars and recorded in Column 12. Dry bulb temperatures in degrees Centigrade and Kelvin are listed in Columns 13 and 14. The conversion from degrees Fahrenheit to degrees Centigrade may be accomplished using readily available conversion charts. Columns 15, 16, and 17 are used to perform the algebraic operations in Equation (6.1). The following example illustrates the use of the table shown in Figure 6.2.

(1) Date: 24 February 1963

(2) Time: 1200 hours

(3) FDB = 94 degrees

(4) FWB = 84 degrees

(5) P_a = 704.01 mm Hg

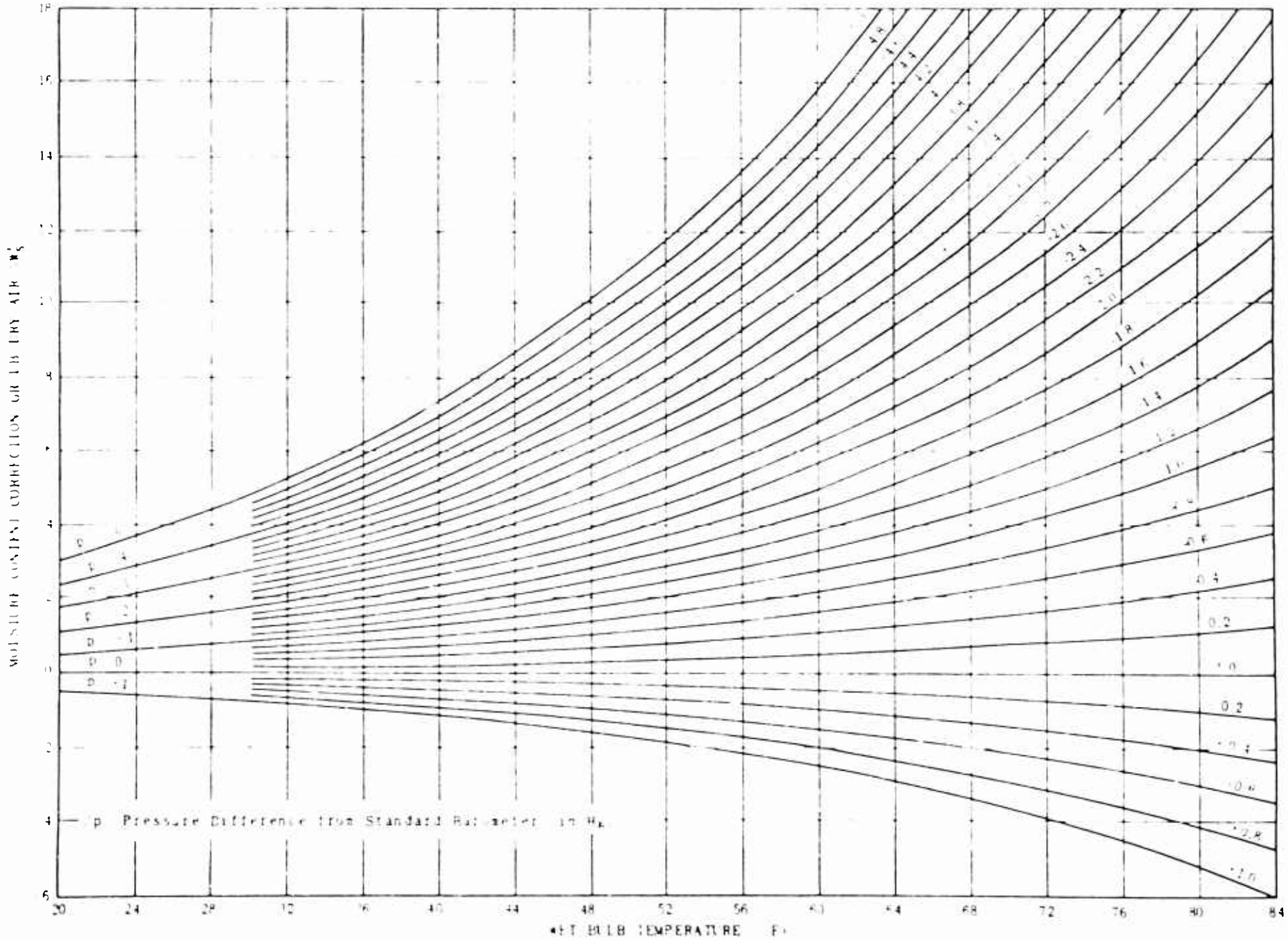

Figure 6 3. Moisture Content Correction Versus Wet Bulb Temperature.

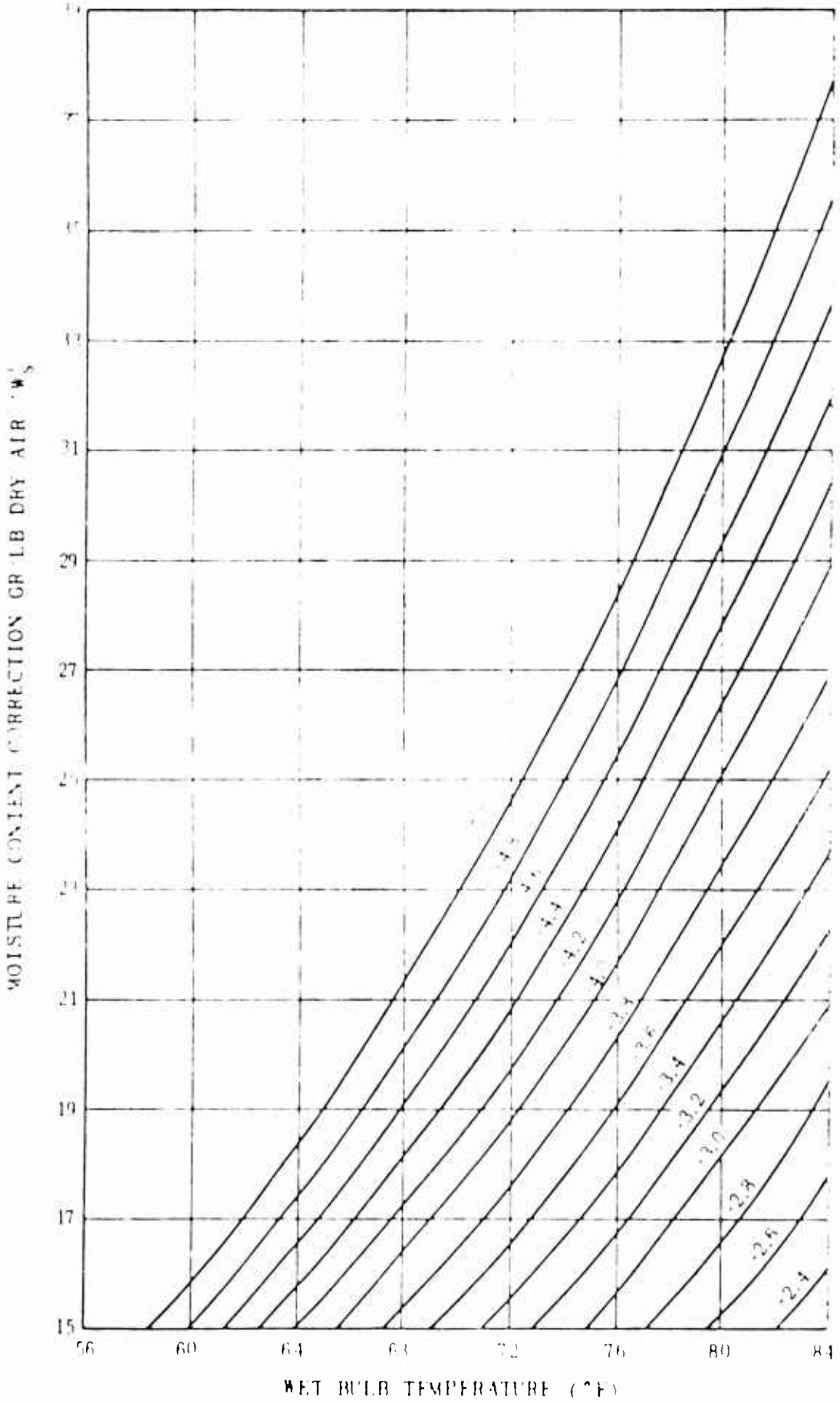

Figure 6.4. Moisture Content Correction Versus Wet Bulb Temperature.

PSYCHROMETRIC CHART

BAROMETRIC PRESSURE 29.92" MERCURY

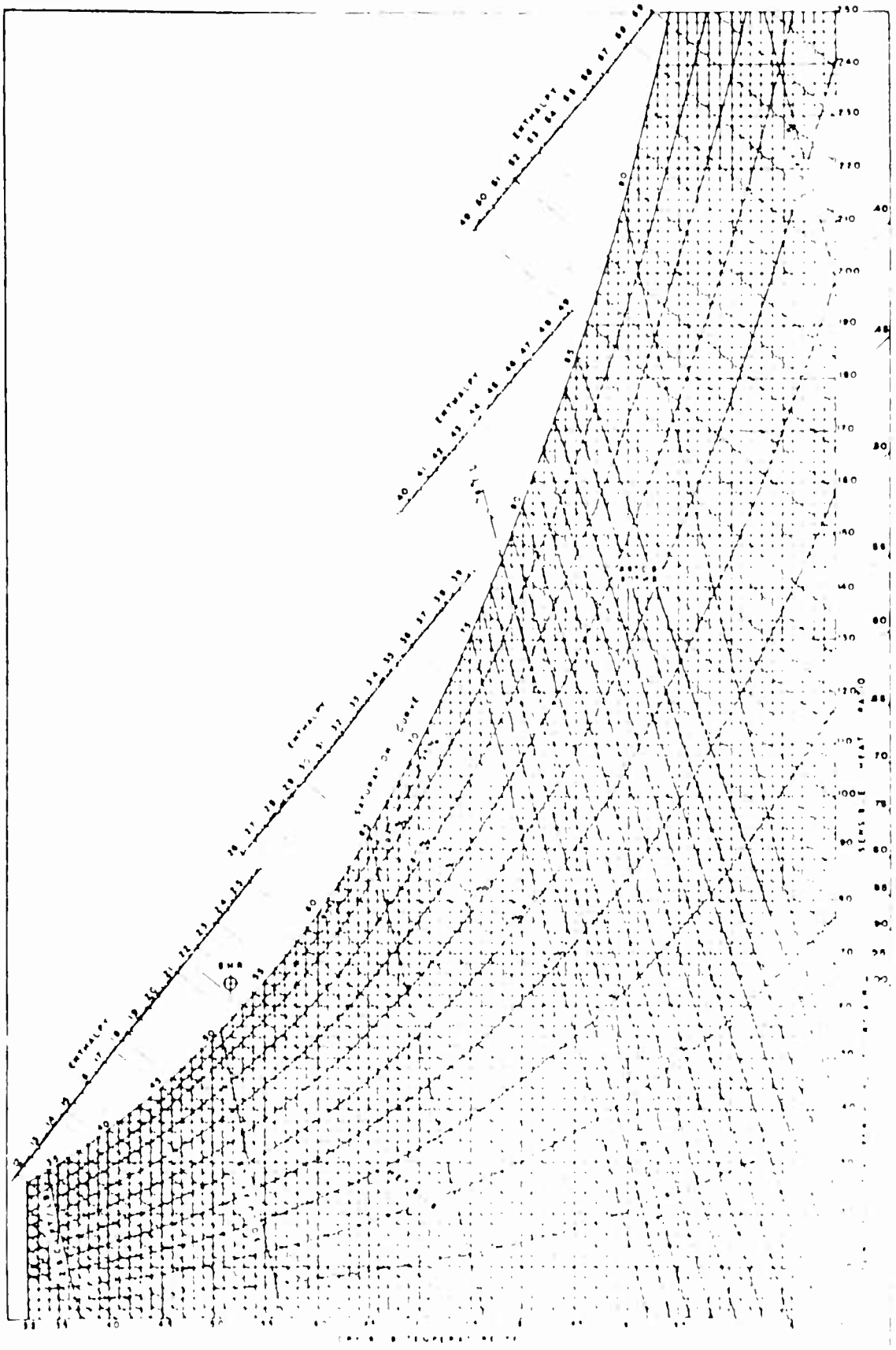

Figure 6.5

(6) P_a = 704.01 × 0.03937 = 27.72 inches, Hg

(7) ΔP_a = 27.72 - 29.92 = -2.2 inches, Hg

(8) W' = 161 grains (see Figure 6.5)

(9) $\Delta W'$ = 14.6 grains (see Figure 6.3)

(10) $\Delta W = 14.6 \left[1 - \frac{94.84}{2400}\right] = 14.5$

(11) W = 161 + 14.5 = 175.5 grains

(12) e = 175.5 × 1013.25/(4360 + 175.5) = 39.20 millibars

(13) CDB = 34.4 degrees (dry bulb temperature, degrees Centigrade)

(14) KDB = 273.2° + 34.4° = 307.6 degrees

(15) p_a = 704.01 × 1.332 = 938.59 millibars

(16) $p_a + \frac{4810e}{T} = 938.59 + \frac{4810 \times 39.20}{307.6} = 1551.72$

(17) $N_s = \left[\frac{77.6}{T}\right] \left[p_a + \frac{4810e}{T}\right] = \frac{77.6 \times 1551.72}{307.6} = 391.5$

In order to represent radio rays as straight lines, at least within the first kilometer above the earth's surface, an effective earth's radius factor (k) may be defined which is a function of the surface refractivity, N_s.

$$k = \left[1 - 0.04664 \exp (0.005577\ N_s)\right]^{-1} \qquad (6.4)$$

The effective earth's radius (a) is then given by

$$a = ka'$$

where a' is the actual radius of the earth, approximately 3960 miles. Where a would become negative, the earth is considered a plane. Figure 6.6 shows the variation of k with N_s.

The value of k which corresponds to the surface refractivity calculated in the example above is

$$k = \left[1 - 0.04665 \exp (0.005577 \times 391.5)\right]^{-1}$$

$$k = 1.707$$

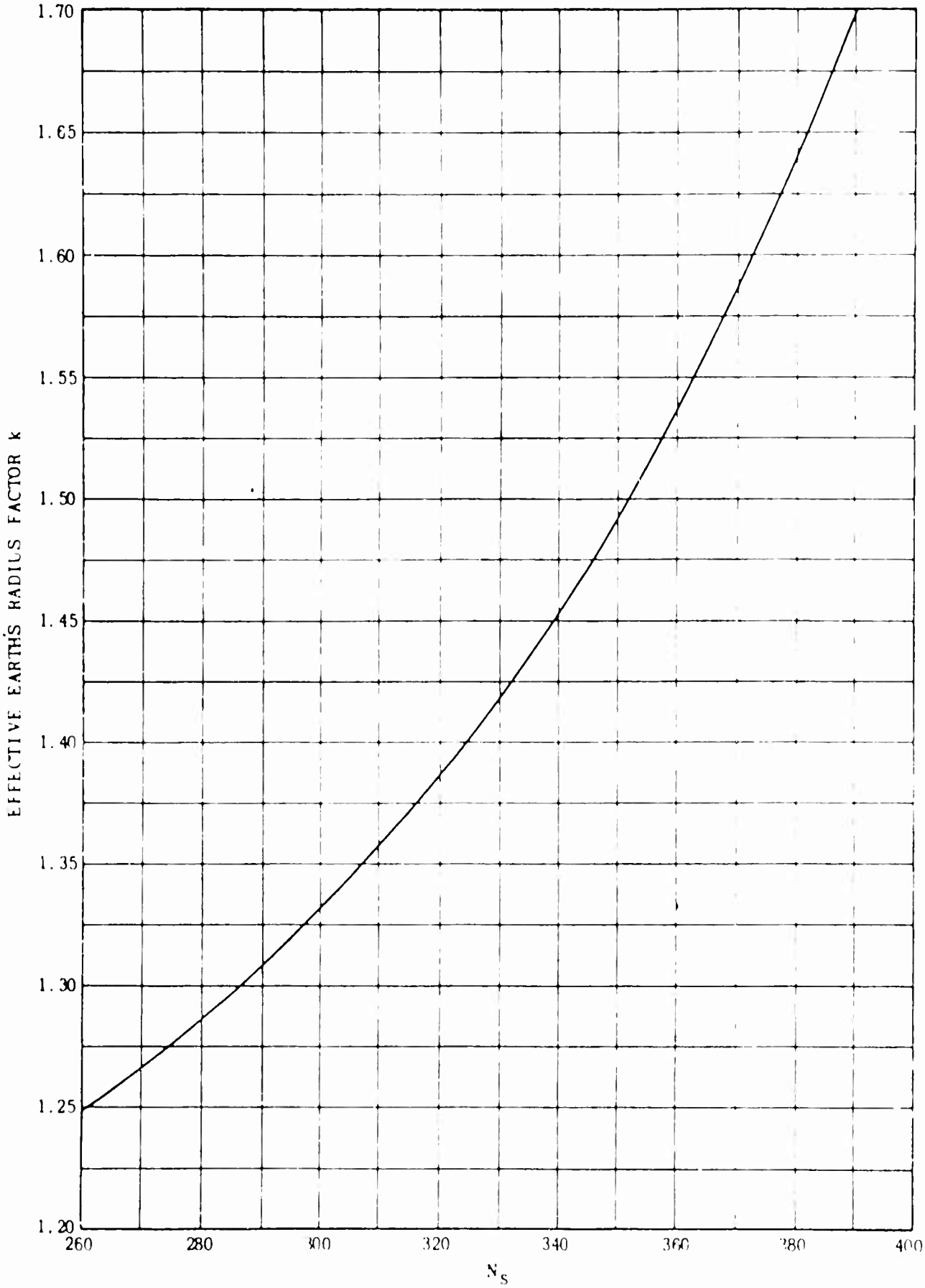

Figure 6.6. Effective Earth's Radius Factor Versus Surface Refractivity.

6.2 Prediction of Basic Transmission Loss Over Line-of-Sight Paths

The following method[1] for predicting the basic transmission loss over line-of-sight paths has been proposed by Phillip L. Rice. In this prediction procedure the actual terrain profile existing between the transmitter and receiver is replaced by a smooth curve which is statistically determined as a least square fit to the actual profile. The conventional interference field prediction formulas are then used after the earth reflection coefficient is modified by a factor which depends upon the terrain roughness.

A modified terrain profile is plotted on linear graph paper, see Figure 6.7, by modifying the actual terrain elevations to include the average effect of the curvature of a radio ray path relative to the earth's surface. The modified elevation y_i is given by

$$y_i = h_i - \frac{2x_i^2}{3k} \text{ feet}$$

where h_i is the actual elevation, in feet, at a distance x_i, in miles, from the transmitter and k is the effective earth's radius factor which corresponds to the measured value of surface radio refractivity N_s obtained at the field test site. That part of the path profile which is adjacent to either antenna and not visible from the antenna is eliminated from any further consideration. The remainder of the path is divided into n equidistant points (x_0, x_1, ... x_n) and used to determine the least squares fit which is given by

$$h(x) = a_0 + a_1 x \text{ feet} \qquad (6.5)$$

The constants a_0 and a_1 are obtained by solving the following two simultaneous equations.

---

1. A model for "Line-of-Sight Tropospheric Propagation" by Philip L. Rice CRPL, Boulder, Colorado, as modified by Dr. H. R. Reed and W. G. Richards for use in the Tropical Propagation Research Program.

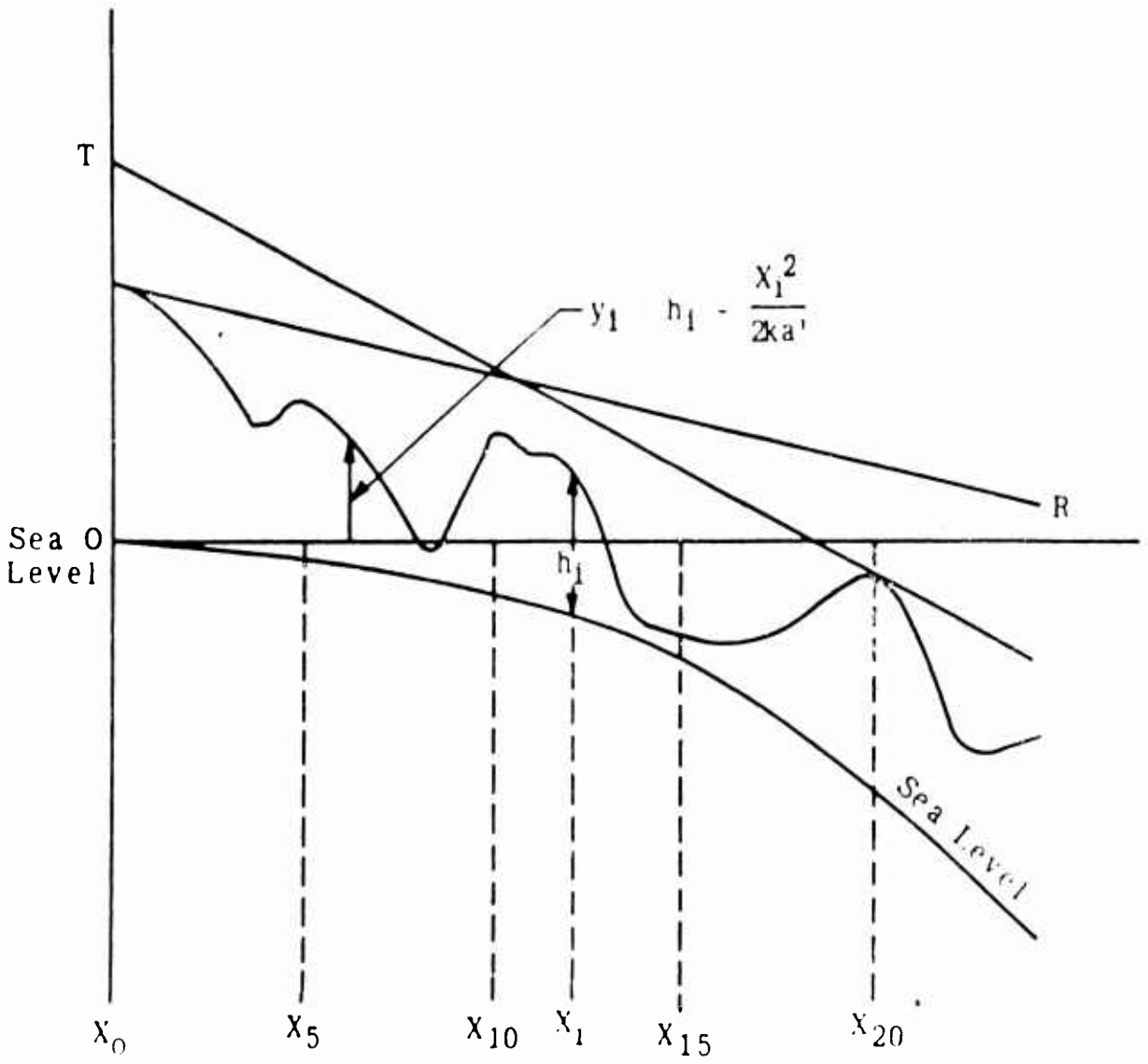

Figure 6.7. Plot of Terrain Profile.

$$\sum h_i = na_o + a_1 \sum x_i \qquad (6.6)$$

$$\sum x_i\, h_i = a_o \sum x_i + a_1 \sum x_i^2$$

The effective antenna heights at the transmitter (h_{te}) and the receiver (h_{re}) are the antenna heights above the curve given by Equation 6.5.

$$h_{te} = h_1 = h_{ts} - h(0) \qquad (6.7)$$

$$h_{re} = h_2 = h_{rs} - h(d) \qquad (6.8)$$

where h_{ts} = height of the transmitting antenna above sea level
and h_{rs} = height of the receiving antenna above sea level.

The distance, d_1, from the transmitter to the geometrical reflection point is determined by solving the following cubic equation.

$$d_1^3 - \frac{3}{2} d_1^2\, d + \frac{1}{2} d^2 - \frac{3}{4}(h_1 + h_2)\, k\, d_1 + \frac{3}{4} k\, h_1\, d = 0 \qquad (6.9)$$

For an analytic solution[2], determine

$$c = \frac{h_1 - h_2}{h_1 + h_2} \qquad (6.10)$$

and

$$m = \frac{d_{mi}^2}{3k(h_1 + h_2)_{ft}} \qquad (6.11)$$

The distances d_1 and d_2 are given by

$$d_1 = \frac{d}{2}(1 + b) \qquad (6.12)$$

$$d_2 = \frac{d}{2}(1 - b) \qquad (6.13)$$

where b is determined from a nomogram similar to Figure 6.8.

---

2. H. R. Reed, "Propagation Data for Interference Analysis," Jansky and Bailey Division of Atlantic Research Corporation, Contract No. AF 30(602) - 1934, Jan. 1962, pp. 80-87.

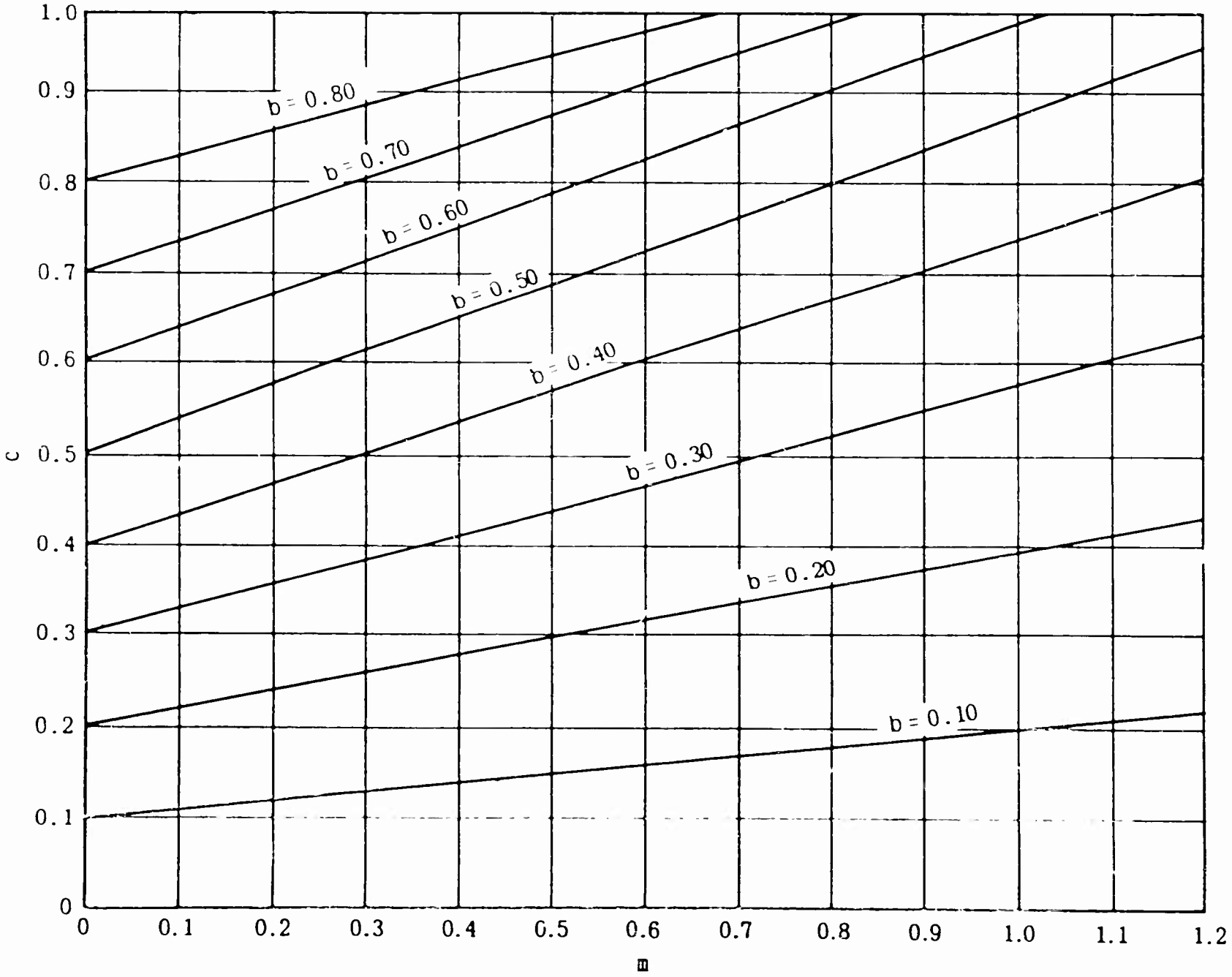

Figure 6.8. Nomogram for Determining d_1 from Cubic Equation.

The path length difference θ is determined as

$$\theta = \frac{1.385 \times 10^{-4} \; h_1' \; h_2' \; f_{mc}}{d_{mi}} \tag{6.14}$$

where

$$h_1' = h_1 - \frac{2d_1^2}{3k} \tag{6.15}$$

$$h_2' = h_2 - \frac{2d_2^2}{3k} \tag{6.16}$$

The grazing angle, ψ, at the reflection point is given by

$$\psi = \tan^{-1} \frac{h_1 - \frac{2d_1^2}{3k}}{5280 \; d_1} \tag{6.17}$$

The reflected ray path lengths, r_1 and r_2, are given by

$$r_{1,2} = \left[(3960k \sin \psi)^2 + \frac{h_{1,2}}{5280}\left(7920 \; k + \frac{h_{1,2}}{5280}\right)\right]^{\frac{1}{2}} - 3960 \; k \sin \psi \tag{6.18}$$

The Fresnel ellipse cuts the propagation path at two points, x_a and x_b miles from the transmitter. These distances are given by

$$2x_{a,b}(1 + \delta) = \left[(r_1 + r_2)(1 + \delta) + (r_1 - r_2)\right] \cos \psi \pm (r_1 + r_2 + \frac{\lambda_{mi}}{2}) \; \delta \left[1 + \frac{4r_1 r_2}{(r_1 + r_2)^2 \; \delta}\right]^{\frac{1}{2}} \tag{6.19}$$

where

$$\delta = \left[\frac{0.00868}{f_{mc}^2 \; (r_1 + r_2)^2} + \frac{0.18636}{f_{mc} \; (r_1 + r_2)}\right] \frac{1}{\sin^2 \psi} \tag{6.20}$$

The standard deviation, σ_h, of the terrain elevations, $h(x_i)$, relative to the smoothed terrain $h(x)$ $(= a_0 + a_1 x)$ for values of distance x from x_a to x_b may now be obtained. If $x_a < x_c$ or $x_b > x_n$, use either x_o or x_n, respectively.

The divergence factor for energy reflected from a spherical surface, when using the ray theory, is

$$D = \left[1 + \frac{d_1 d_2}{1980 \text{ kd } \tan \psi} \right]^{-\frac{1}{2}} \qquad (6.21)$$

The effective ground-reflected coefficient, R_e, is expressed as

$$R_e = D|\bar{R}| \exp -\left(\frac{\sigma_h \sin \psi}{\lambda}\right) \qquad (6.22)$$

when isotropic antennas are assumed to exist at each terminal. ($\bar{R} = Re^{i\phi}$, the earth's reflection coefficient.) However, if R_e, as given above is less than sin ψ, and at the same time less than 0.5, then use

$$R_e = \sqrt{\sin \psi} \qquad (6.23)$$

Simplified procedures for evaluating the plane earth reflection coefficient, $\bar{R}e^{i\phi}$, are readily available[2] and will not be considered here

The basic transmission loss is given by

$$L_b = 36.57 + 20 \log f_{mc} + 20 \log d_{mi} + A \qquad (6.24)$$

where

$$A = -10 \log \left[1 + R_e^2 + 2R_e \cos (\theta - \phi) \right] \qquad (6.25)$$

EXAMPLE: The following example is based on data for a transmission path over rough terrain for which measured data are available

The path profile is shown in Figure 6.9. In this case, x_0 and x_{21} are the end points of the path.

---

2. Ibid.

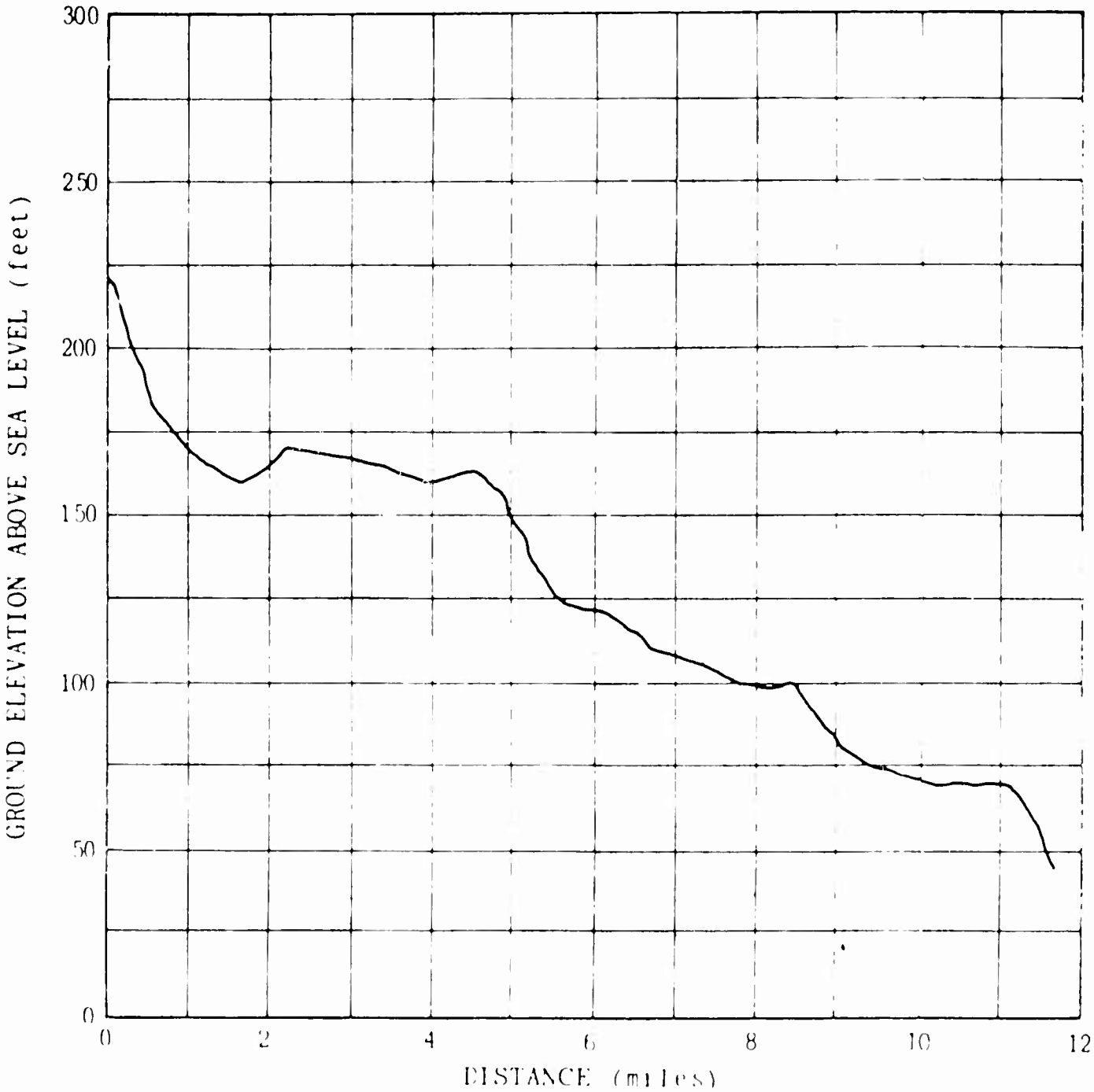

Figure 6.9. Profile of Propagation over Rough Terrain.

PROFILE DATA

i	h_i	x_i	i	h_i	x_i
0	220	0	11	120	6.2
1	182	0.6	12	110	6.7
2	165	1.1	13	105	7.3
3	160	1.7	14	100	7.8
4	170	2.2	15	100	8.4
5	168	2.8	16	82	9.0
6	164	3.4	17	50	9.5
7	160	3.9	18	70	10.1
8	162	4.5	19	70	10.6
9	150	5.0	20	70	11.1
10	125	5.6	21	47	11.6

The coefficients to the least square fit are determined by solving for a_0 and a_1 from the following simultaneous equations:

$$22\ a_0 + 129.1\ a_1 = 2750$$

$$129.1\ a_0 + 1031.93\ a_1 = 12{,}686.6$$

The resulting least squares fit is then

$$h(x) = 198.81 - 12.58x \text{ feet.}$$

It follows that

$$h(0) = 198.8 \text{ feet}$$

$$h(d) = h(11.6) = 53.39 \text{ feet}$$

The antenna heights, h_{ts} and h_{rs}, will be assumed at 363 feet and 200 feet, respectively, since measured data at 40.5 Mc are available for these heights. Then

$$h_t = h_1 = 363 - 198.8 = 164.2 \text{ feet}$$

$$h_r = h_2 = 200 - 53.4 = 146.6 \text{ feet}$$

The values of d_1 and d_2 will be determined by the analytical method as follows:

$$c = \frac{164.2 - 146.6}{164.2 + 146.6} = 0.056$$

$$m = \frac{(11.6)^2}{4(164.2 + 146.6)} = 0.107$$

The corresponding value of b is 0.05. Thus,

$$d_1 = \frac{11.6}{2}(1 + 0.05) = 6.07$$

$$d_2 = \frac{11.6}{2}(1 - 0.05) = 5.49$$

Also,

$$h_1' = 164.2 - \frac{1}{2}(6.07)^2 = 145.8$$

$$h_2 = 146.6 - \frac{1}{2}(5.49)^2 = 131.5$$

$$\tan \cdot = \frac{164.2 - \frac{(6.07)^2}{2}}{(5280)(6.07)} = 0.00455$$

$$r_1 = \left[(5280 \times 0.00455)^2 + \frac{164.2}{5280}\, 2 \times 5280 + \frac{164.2}{5280}\right]^{\frac{1}{2}} - 5280 \times 0.00455$$

$r_1 = 6.068$ miles

$r_2 = 5.478$ miles

$$\theta = \frac{1.385 \times 10^{-4} \cdot 145.8 \times 131.5 \times 40.5}{11.6} = 9.3^\circ$$

$$\delta = \left[\frac{.00868}{(40.5)^2\ (6.068 + 5.478)^2} + \frac{0.1864}{(40.5)(6.068 + 5.478)}\right]$$

$$\frac{1}{(.00455)^2} = 19.250$$

$$2x_{a,b}(1 + 19.250) =$$

$$(6.068 + 5.478)(1 + 19.250) + (6.068 - 5.478)\Big] \cos 0.2°$$

$$\pm (6.068 + 5.478)(19.250)\left[1 + \frac{4(6.068)(5.478)}{(6.068 + 5.478)^2 (19.250)}\right]^{\frac{1}{2}}$$

$$x_a = 0.16$$

$$x_b = 11.42$$

The standard deviation, σ_h, of the terrain elevations $h(x_i)$ relative to the smoothed terrain $h(x)$ is determined from the data shown in the table below.

DATA REQUIRED FOR EVALUATING STANDARD DEVIATION OF TERRAIN

i	x_i	h_i	$h(x)$	$\lvert h_i - h(x) \rvert$
0	0	220	198.81	21.19
1	0.6	182	191.26	9.3
2	1.0	165	184.97	20.0
3	1.7	160	177.42	17.4
4	2.2	170	171.13	1.1
5	2.8	168	163.59	4.4
6	3.4	164	156.04	8.0
7	3.9	160	149.75	10.3
8	4.5	162	142.20	19.8
9	5.0	150	135.91	14.1
10	5.6	125	128.36	3.4
11	6.2	120	120.81	0.8
12	6.7	110	114.52	4.5
13	7.3	105	106.98	2.0
14	7.8	100	100.69	.7
15	8.4	100	93.14	6.9
16	9.0	82	85.59	3.6
17	9.5	50	79.30	29.3
18	10.1	70	71.75	1.75
19	10.6	70	65.46	4.5
20	11.1	70	59.17	10.8
21	11.6	47	52.88	5.9

The standard deviation obtained from these twenty-two values of $|h_i - h(x)|$ is 11.96 feet.

The divergence factor, D, is

$$D = \left[1 + \frac{2(6.07)(5.49)}{5280\ (11.6)(0.00455)}\right]^{-\frac{1}{2}} = 0.898$$

The reflection coefficient for horizontal polarization is approximately $1\ e^{-i\pi}$. Thus, the reflection coefficient for the rough terrain is

$$R_e = (0.89803)(1)\ \exp\ \frac{-(11.96)(0.00455)(40.5)}{(984)} = 0.896$$

$$\cos(\theta - \phi) = \cos(9.3 + 180) = -0\ 987$$

The value of A, the loss in excess of free space, is

$$A = -10 \log\ 1 + (0.89605)^2 + 2(.89605)(-0.98686) = 14.54 \text{ db}$$

and the basic transmission loss is

$$L_b = 36.57 + 20 \log 40.5 + 20 \log 11.6 + 14.65$$

$$= 104\ 63 \text{ db}$$

The measured value of loss over this path for the parameters selected for this example is 106.3 db, a difference of 1.7 db from the predicted value.

Additional measured data are available for this and other paths at various frequencies. A comparison between the measured loss values and values predicted by the procedure given above is shown in the following table. The standard deviation for the following calculated versus measured data is 4.2 db, which represents very good correlation.

	Frequency (Mc)	L_b (calculated)	L_b (measured)
Path A d = 11.6 miles	40.5	104.6	106.3
	75.5	106.8	105.8
	165.2	108.7	113.5
	455.0	110.2	117.3

	Frequency (Mc)	L_b (calculated)	L_b (measured)
Path B			
d = 17.0 miles	40.5	106.7	116.1
	75.5	111.0	115.0
	165.2	116.1	114.6
	455.0	120.4	123.1
Path C			
d = 7.4 miles	40.5	94.4	94.4
	75.5	96.4	96.0
	165.2	98.5	101.7
	455.0	102.3	99.0

6.3 Prediction of Basic Transmission Loss Over Paths Beyond the Line-of-Sight

A major undertaking which arises in conjunction with the tropical propagation problem is that of predicting the field strength over rough terrain paths with the receiving antenna located within the diffraction field of the transmitting antenna. The problem arises, because in order to determine the loss due to tropical vegetation over a given path, the loss over a tree-less path having the same path profile must be predictable. A mathematical model is available for making such calculations, but the method is rather long and tedious to carry out. The question arose as to whether or not it would be possible to foreshorten the labor of calculation by devising some sort of an equation which would yield the path loss but at a saving in labor over previous mathematical models.

A hypothetical profile was then set up in which diffraction calculations could be made in which the distance d_{Lt} (or d_{Lr}) could be varied as well as the angle θ_{e_1} while keeping all other parameters, h_{ts}, h_{tr}, and θ_{e_2}, and total distance d at fixed values.

In Figure 6.10 is plotted the results of such a series of calculations in which A (the loss in excess of free space loss) is plotted versus θ_{e_1} for different discrete values of d_{Lt}. The distance d_{Lt}, for the profile chosen, varies in increments of 5 miles from 5 to 40 miles. The result is a family of curves.

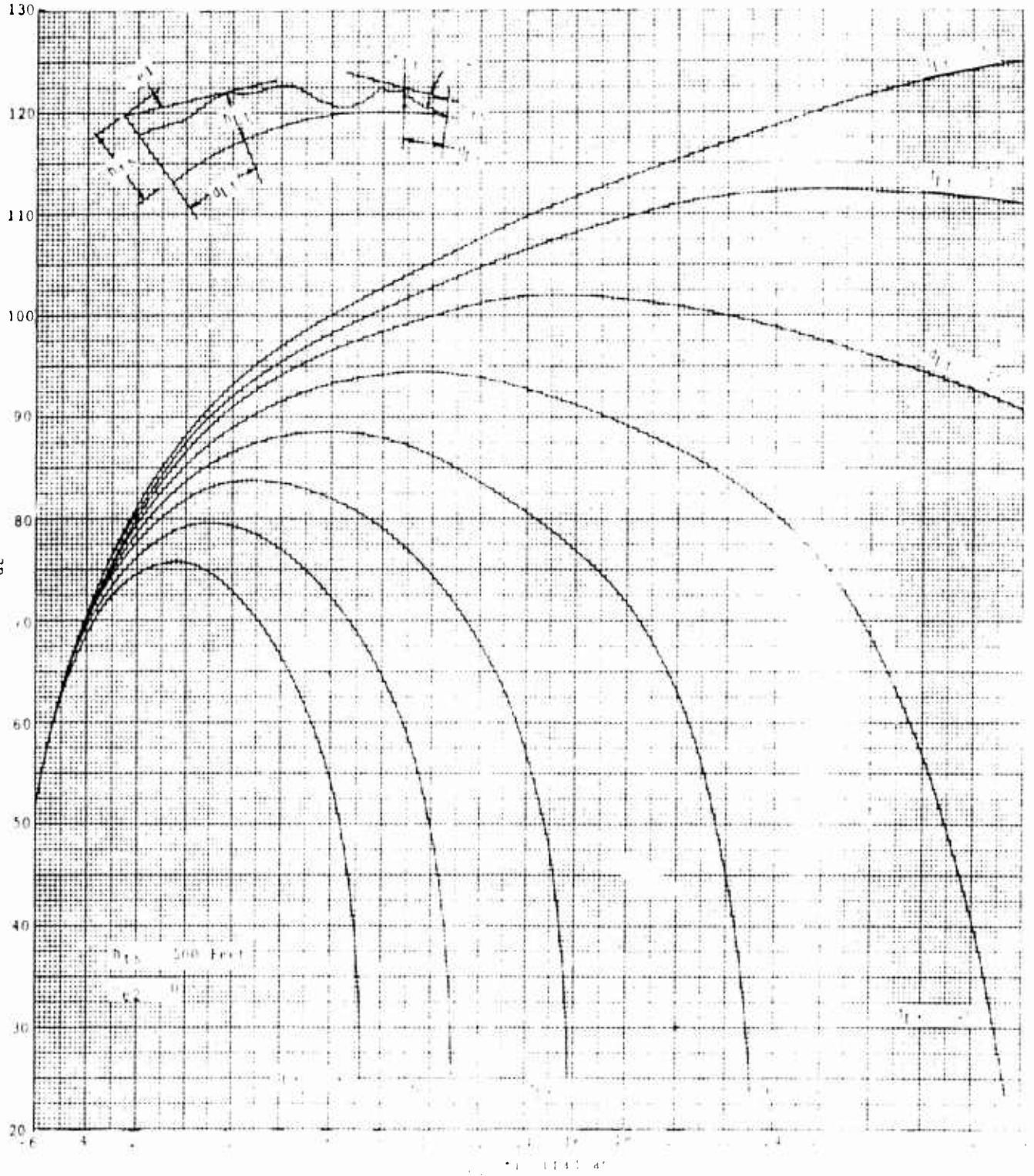

Figure 6-10 Variation of the Loss in Excess of Free Space Versus θ_1 the Angle Between a Horizontal Ray and the Horizontal

The curves of Figure 6.10 are for a transmitting antenna height above sea level, h_{ts}, of 500 feet and a θ_{e_2} of 0°, meaning that at the receiver the incident ray is approaching tangential to the curvature of the earth. Can a single equation be obtained to represent the family of curves? Is this equation accurate, and can it be readily manipulated?

An equation which represents the family of curves shown in Figure 6.10 is presented in the following, but said equation has two sets of numerical coefficients depending upon whether θ_{e_1} is ≤ 0 or ≥ 0.

The loss A, in excess of free space loss, is given by,

$$A_{db} = a_0 + a_1 x + a_2 x^2 + a_3 x^3 + a_4 y + a_5 y^2 + a_6 y^3 + a_7 xy + a_8 x^2 y + a_9 x^3 y + a_{10} xy^2 + a_{11} x^2 y^2 + a_{12} x^3 y^2 + a_{13} xy^3 + a_{14} x^2 y^3 + a_{15} x^3 y^3$$

where $x = \theta_{e_1}$ in milliradians

$y = d_{Lt}$ in miles

and

	a_0	a_1	a_2	a_3
$x \leq 0$	90.740967	4.890625	0.3015625	0.12859375
$x \geq 0$	95.894356	3.0886478	-0.007671547	-0.0000432968
	a_4	a_5	a_6	a_7
	-0.53771973	0.02284546	-0.00047348	-0.20585937
	-1.1418571	0.04000263	-0.000593486	-0.44184112
	a_8	a_9	a_{10}	a_{11}
$x \leq 0$	-0.02640625	-0.001125	0.00984375	0.00153906
$x \geq 0$	-0.005365143	0.0000176773	0.026052398	0.0008807898
	a_{12}	a_{13}	a_{14}	a_{15}
	0.00008828	-0.00018921	-0.000027539	-0.00000146
	0.00000312996	-0.000435627	-0.000026002	-0.000000640335

It is quite evident at the present writing that the above equation is not satisfactory for the purpose for which it was intended. Much more work should be done on it if time permits, otherwise the original mathematical model will be used to determine the

loss in excess of free space over diffraction paths.

A final equation for A should also include the factors h_{ts} and θ_{e_2} where θ_{e_2} can be either positive or negative.

6.4 Terrain Roughness Factors

A problem which has been foremost in the minds of propagation engineers is that of determining some sort of roughness factor which will permit rapid calculation of field strength over rough terrain. Such a factor whould have to be based on a rather large amount of statistics and the procedure envisioned has been described earlier in Monthly Report No. 2.

In short, the method proposed was to lay out at random a number of paths from zero to 30 miles in length, over the country involved, calculate the loss for these paths, and then correlate these losses with a roughness factor. If there could be found a correlation factor then it would be possible to take certain simple measurements from the map of the path, refer to a curve or a simple mathematical model, and quickly predict the path loss. This prediction process would apply to the many possible modes of propagation over rough earth paths.

To test the theory, a number of paths over rough terrain within the Eglin Air Force Base were chosen since quite accurate measured data were available. Calculations were made on five paths for frequencies ranging from 40 Mc to 10,000 Mc, and the plotted results of one of these path calculations are shown in Figure 6.11, namely, the so-called Wagner path.

In the process of calculation using a modified form of the Rice model[3] a factor such as

$$e^{-\frac{\sigma_h \sin \psi}{\lambda}}$$

---

3. Refer to Section 6.2

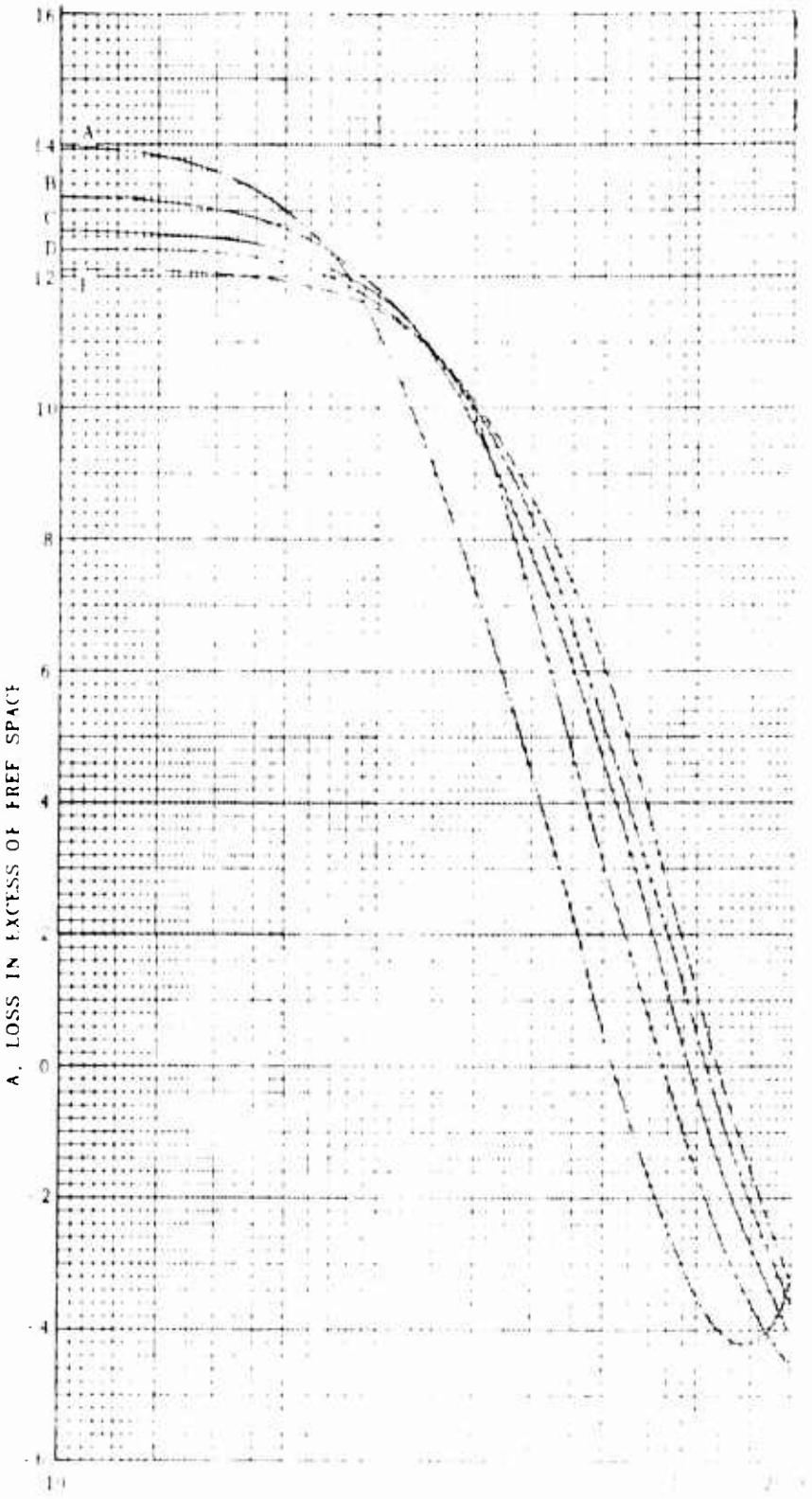

Figure 6-[illegible] Excess Frequency [illegible]

appears. The exponent, namely,

$$\frac{\sigma_h \sin \psi}{\lambda}$$

is known as the Rayleigh criterion of roughness, where

σ_h is the standard deviation of roughness relative to an equivalent smooth earth,

ψ is the grazing angle of the reflected ray,

λ is wavelength of the radiated carrier frequency.

The curves of Figure 6 11 show the relation between A, the loss in excess of free space loss, and frequency for the five different transmitting heights. The curves are relatively smooth out to about 1500 Mc and then show marked frequency effects. The original intent of the problem is to obtain equations for these variations (which is possible out to 1500 Mc) and from these equations ascertain whether a roughness factor can be obtained. The work on this phase is continuing.

7.0 PROJECT PERSONNEL

Figure 7.1 shows the Jansky & Bailey personnel who have been employed on Signal Corps Contract DA 36-039 SC-90889 during the present reporting period.

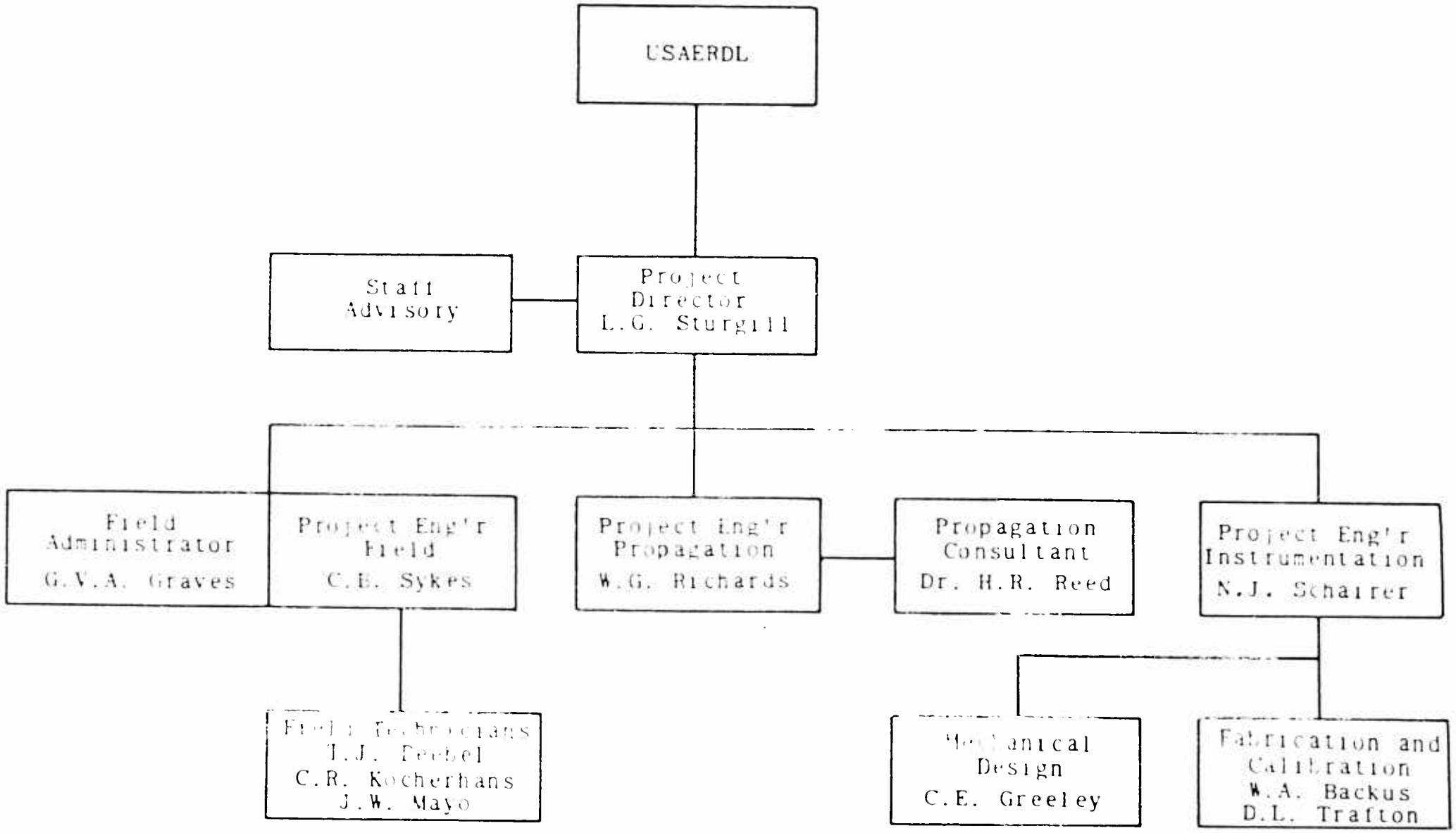

Figure 7.1. Project Personnel.

8.0 FUTURE WORK PLANS

During the next six month reporting period most of the effort will be devoted to implementing the ideas presented in the test plan. This work will include testing and modifying GFE and commercial equipment as required when it is received, packing the equipment in the shelters, and preparing the shelters for shipment to Thailand. Photographs acquired from the aerial survey will be assembled into mosaics so that trail and foliage information may be transferred from these photographs to topographic maps. Mathematical models for calculating rough terrain path loss in the absence of foliage for each mode will be developed. Finally, it is expected that the precise location of the operations site will be selected and construction of the semi-permanent buildings will be initiated.

9.0 MEETINGS AND CONFERENCES

A chronological listing of the major meetings and conferences held during this reporting period, as well as a brief description of the topics discussed, is given in this section.

Conferences were held at the Jansky & Bailey facility with USAELRDL Technical Representatives on 5 July and 26 July 1962. The technical objectives of this program were discussed in considerable detail during these conferences.

A conference was held at Fort Monmouth, New Jersey, on 21 August 1962, to discuss both technical and contractual questions relating to this program. The results of this conference led to the issuance of a contract Change Order dated 29 August 1962. This Change Order, Signal Corps Technical Requirement SCL-4379A, dated 13 July 1962, supersedes Signal Corps Technical Requirement SCL-4379, dated 5 February 1962. Among other changes, the new Technical Requirement specifies that the primary field tests in this program shall be conducted in Southeast Asia.

A technical conference with the COTR was held at USAELRDL, Fort Monmouth, New Jersey, on 20 October 1962. During this conference the contractor outlined the preliminary field test plan thus far developed, and many technical aspects of this plan were informally discussed.

A joint meeting of ARPA, USAELRDL, Jansky & Bailey personnel, and other interested agencies, was held at the ARPA offices in the Pentagon on 11 October 1962. The Program Manager of SEACORE presented a discussion of the entire program and explained the overall objectives to be accomplished through the Combat Development Technical Center (CDTC) in Thailand. The various ways in which the results of the Jansky & Bailey program would provide technical support to the CDTC were discussed.

A meeting with the Contracting Officer was held at FMPO on 17 October 1962 to discuss the contractor's response to Change Order, Modification No. 1 and related contractual matters. With respect to the schedule of technical reports, it was mutually agreed that eighteen monthly reports would be submitted for the months of

October 1962 through March 1965. Also, three semi-annual reports are to be submitted covering the periods July through December 1962, January through June 1964, and July through December 1964

A joint meeting between the COTR, Fort Monmouth, ARPA, Jansky & Bailey, and a representative from Stanford Research Institute was held at the Jansky & Bailey facility on 18 October 1962. The purpose of this meeting was to familiarize Jansky & Bailey and SRI each with the others program and to further coordinate the technical objectives of both programs.

Appendix A

An Analysis of the Quadrant Dipole Antenna

Prepared by

H. R. Reed, Ph. D
Warren Richards
William Munson

AN ANALYSIS OF THE QUADRANT DIPOLE ANTENNA

The purpose of this appendix is to present an analysis of the quadrant dipole antenna by deriving the formulas necessary to calculate the far field patterns. It will be shown that the quadrant dipole has virtually an omnidirectional pattern in azimuth and a high gain directivity factor at large radiation angles when elevated to certain heights above ground. With such characteristics, the antenna has many possible uses, one of which is in short distance skywave circuits. Several typical patterns are shown at the end of this section for selected antenna lengths and heights to illustrate these characteristics.

The retarded vector potential, $\bar{A}$, at any point P is given by

$$\bar{A} = \frac{1}{4\pi} \int_V \frac{\bar{I}\left(t - \frac{r}{v}\right)}{r} \, dV \qquad (1)$$

where

$\bar{I}\left(t - \frac{r}{v}\right)$ is current density or charge as a function of $\left(t - \frac{r}{v}\right)$

r is the space displacement between $\bar{A}$ and the time varying current

v is the velocity of propagation of the radiated wave, and integration is over the volume enclosing the charge.

Assume the current densities in the two radiators shown in Figure 1 to be given by

$$\bar{I} = \bar{a}_x I_o \sin \frac{2\pi}{\lambda} (\ell - \xi) \cos \omega t \qquad (2)$$

$$\bar{I} = -\bar{a}_y I_o \sin \frac{2\pi}{\lambda} (\ell - \eta) \cos \omega t \qquad (3)$$

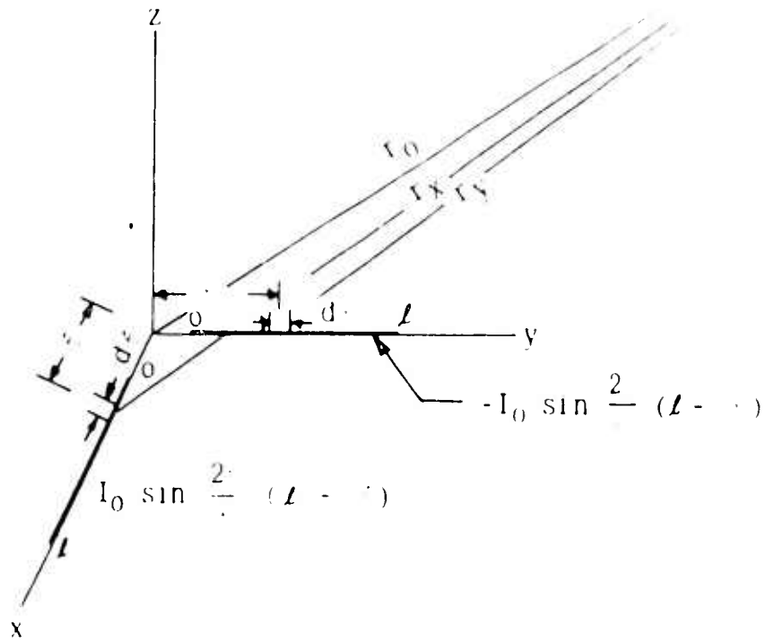

Figure A-1. Quadrant Dipole.

where it is further assumed that the excitation current is a cosine function of time. Then

$$\bar{A}_x = \frac{\bar{a}_x I_o}{4\pi} \int_o^{\ell} \frac{\sin(\beta\ell - \beta\xi)\, \cos(\omega t - \beta r_x)}{r_x}\, d\xi \qquad (4)$$

since $\frac{2\pi}{\lambda} = \beta$ and also since $\frac{\omega}{v} = \beta$

$$\cos\, \omega\left(t - \frac{r}{v}\right) = \cos(\omega t - \beta r)$$

where λ is the wavelength of the carrier frequency.

The volume integral is an integration over the cross-sectional area and length of the wire, and since the wire is of small diameter

$$\int_V \bar{I} dV = \int_o^{\ell} \frac{I_o \sin(\beta\ell - \beta\xi)\, \cos(\omega t - \beta r)}{a}\, a\, d\xi$$

The r_x appearing in Equation 4 designates that the displacement between $\bar{A}$ and the time-varying current is measured relative to the radiator oriented on the x-axis.

Similarly it is seen that

$$\bar{A}_y = -\frac{\bar{a}_y I_o}{4\pi} \int_o^{\ell} \frac{\sin(\beta\ell - \beta\eta)\, \cos(\omega t - \beta r_y)}{r_y}\, d\eta \qquad (5)$$

where r_y is the displacement between $\bar{A}$ and the time-varying current oriented on the y-axis.

From Figure 2a, which represents a point, P, in space in a combined cartesian-spherical coordinate system, and from Figure 2b, which represents a portion of the plane formed by

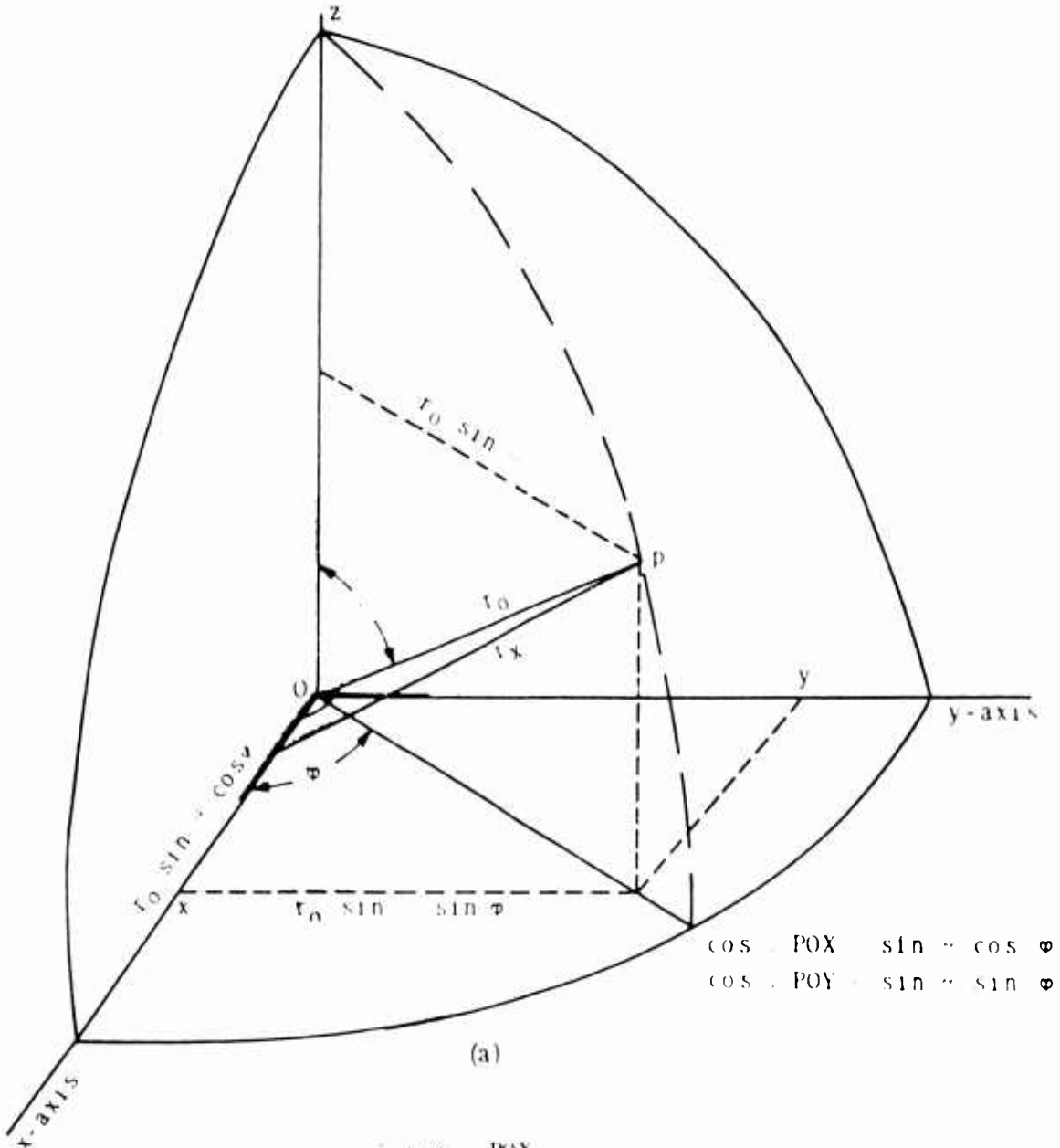

(a)

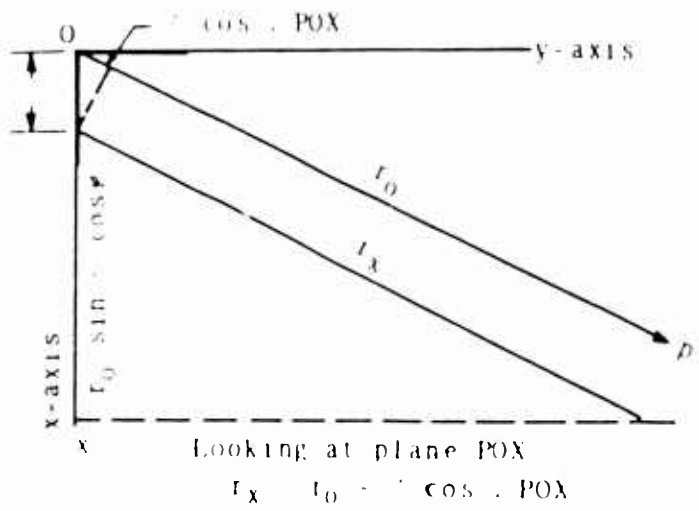

(b)

Figure A-2. Cartesian-Spherical Coordinate System.

the radius OP and the x-axis it is seen that

$$r_x = r_o - \xi \cos \angle POX \tag{6}$$

where it is further assumed that r_o and r_x represent parallel rays since the point, P, is very far removed from the origin, O.

From Figure 2a it is seen that

$$\cos \angle POX = \sin \theta \cos \varphi \tag{7}$$

$$\cos \angle POY = \sin \theta \sin \varphi \tag{8}$$

and

$$r_x = r_o - \xi \sin \theta \cos \varphi \tag{9}$$

Similarly,

$$r_y = r_o - \eta \cos \angle POY$$

$$= r_o - \eta \sin \theta \sin \varphi \tag{10}$$

Substitution of Equation 9 into Equation 4 yields

$$\bar{A}_x = \frac{\bar{a}_x I_o}{4\pi} \int_o^{\ell} \frac{\sin(\beta\ell - \beta\xi) \cos(\omega t - \beta r_o + \beta\xi \sin \theta \cos \varphi)}{r_o - \xi \sin \theta \cos \varphi} d\xi \tag{11}$$

When the distance from the antenna center, O, to point P is large the $\xi \sin \theta \cos \varphi$ term in the denominator may be neglected relative to r_o, but not so in the numerator. Then removing the r_o outside the integral sign and dropping the subscript, o, with r_o, Equation 11 becomes

$$\bar{A}_x = \frac{\bar{a}_x I_o}{4\pi r_o} \int_o^{\ell} \sin(\beta\ell - \beta\xi) \cos(\omega t - \beta r + \beta\xi \sin \theta \cos \varphi) d\xi \tag{12}$$

Now make use of the trigonometric relationship

$$\sin A \cos B = \frac{1}{2} \sin(A + B) + \frac{1}{2} \sin(A - B)$$

and

$$\sin(\beta\ell - \beta\xi)\cos(\omega t - \beta r + \beta\xi \sin\theta\cos\varphi) =$$

$$\frac{1}{2}\sin\left[(\beta\ell - \beta r + \omega t) - \beta\xi\,(1 - \sin\theta\cos\varphi)\right]$$

$$+ \frac{1}{2}\sin\left[(\beta\ell + \beta r - \omega t) - \beta\xi\,(1 + \sin\theta\cos\varphi)\right]$$

$$\bar{A}_x = \frac{\bar{a}_x I_o}{8\pi r_o}\left[\int_o^{\ell}\sin\left[(\beta\ell - \beta r + \omega t) - \beta\xi\,(1 - \sin\theta\cos\varphi)\right]d\xi\right.$$

$$\left. + \int_o^{\ell}\sin\left[(\beta\ell + \beta r - \omega t) - \beta\xi\,(1 + \sin\theta\cos\varphi)\right]d\xi\right]$$

$$= \frac{\bar{a}_x I_o}{8\pi r_o}\left\{\frac{\cos\left[(\beta\ell - \beta r + \omega t) - \beta\xi\,(1 - \sin\theta\cos\varphi)\right]}{\beta(1 - \sin\theta\cos\varphi)}\right]_o^{\ell}$$

$$+ \left.\frac{\cos\left[(\beta\ell + \beta r - \omega t) - \beta\xi\,(1 + \sin\theta\cos\varphi)\right]}{\beta(1 + \sin\theta\cos\varphi)}\right]_o^{\ell}\right\}$$

$$A_x = \frac{\bar{a}_x I_o}{8\pi r_o \beta}\left\{\frac{\cos\left[\omega t - \beta r + \beta\ell\sin\theta\cos\varphi\right] - \cos\left[\omega t - \beta r + \beta\ell\right]}{1 - \sin\theta\cos\varphi}\right.$$

$$\left. + \frac{\cos\left[-\omega t + \beta r - \beta\ell\sin\theta\cos\varphi\right] - \cos\left[-\omega t + \beta r + \beta\ell\right]}{1 + \sin\theta\cos\varphi}\right\}$$

Since $\cos \alpha = \cos (-\alpha)$

$$\cos \left[\omega t - \beta r + \beta \ell \sin \theta \cos \varphi\right]$$

$$= \cos \left[- \omega t + \beta r - \beta \ell \sin \theta \cos \varphi\right]$$

$$\bar{A}_x = \frac{\bar{a}_x I_o}{8\pi r_o \beta} \left\{ \frac{\cos \left[\omega t - \beta r + \beta \ell \sin \theta \cos \varphi\right] - \cos \left[(\omega t - \beta r) + \beta \ell\right]}{1 - \sin \theta \cos \varphi} \right.$$

$$\left. + \frac{\cos \left[\omega t - \beta r + \beta \ell \sin \theta \cos \varphi\right] - \cos \left[-(\omega t - \beta r) + \beta \ell\right]}{1 + \sin \theta \cos \varphi} \right\}$$

$$= \frac{\bar{a}_x I_o}{4\pi r_o \beta} \left\{ \frac{\cos \left[(\omega t - \beta r) + \beta \ell \sin \theta \cos \varphi\right]}{1 - \sin^2 \theta \cos^2 \varphi} \right.$$

$$\left. - \frac{\cos (\omega t - \beta r) \cos \beta \ell}{1 - \sin^2 \theta \cos^2 \varphi} + \frac{\sin (\omega t - \beta r) \sin \beta \ell \sin \theta \cos \varphi}{1 - \sin^2 \theta \cos^2 \varphi} \right\}$$

$$= \frac{\bar{a}_x I_o}{4\pi r_o \beta (1 - \sin^2 \theta \cos^2 \psi)} \left\{ \cos(\omega t - \beta r) \left[\cos(\beta \ell \sin \theta \cos \varphi) - \cos \beta \ell\right] \right.$$

$$\left. + \sin (\omega t - \beta r) \left[\sin \beta \ell \sin \theta \cos \varphi - \sin (\beta \ell \sin \theta \cos \varphi)\right] \right\} \quad (13)$$

By the symmetrical relationship that exists between Equations 4 and 5 and the relations of Equations 9 and 10, the retarded vector potential $\bar{A}_y$ may be written, using Equation 13, as

$$\bar{A}_y = \frac{-\bar{a}_y I_0}{4\pi r_0 \beta (1 - \sin^2\theta \sin^2\varphi)} \left\{ \cos(\omega t - \beta r) \left[\cos(\beta \ell \sin\theta \sin\varphi) - \cos \beta \ell \right] \right.$$

$$\left. + \sin(\omega t - \beta r) \left[\sin \beta \ell \sin\theta \sin\varphi - \sin(\beta \ell \sin\theta \sin\varphi) \right] \right\} \quad (14)$$

For simplification write the scalar value of $\bar{A}_x$ as

$$A_x = \frac{k_1}{r} \left[k_2 \cos(\omega t - \beta r) + k_3 \sin(\omega t - \beta r) \right] \quad (15)$$

and

$$A_y = \frac{k_4}{r} \left[k_5 \cos(\omega t - \beta r) + k_6 \sin(\omega t - \beta r) \right] \quad (16)$$

Now, transfer from cartesian to spherical coordinates using the transformations

$$A_r = A_x \sin\theta \cos\varphi + A_y \sin\theta \sin\varphi$$

$$A_\theta = A_x \cos\theta \cos\varphi + A_y \cos\theta \sin\varphi$$

$$A_\varphi = -A_x \sin\varphi + A_y \cos\varphi \quad (17)$$

together with Equations 15 and 16. Then

$$A_r = \frac{k_1}{r} \left[k_2 \cos(\omega t - \beta r) + k_3 \sin(\omega t - \beta r) \right] \sin\theta \cos\varphi$$

$$+ \frac{k_4}{r} \left[k_5 \cos(\omega t - \beta r) + k_6 \sin(\omega t - \beta r) \right] \sin\theta \sin\varphi \quad (18)$$

$$A_\theta = \frac{k_1}{r} \left[k_2 \cos(\omega t - \beta r) + k_3 \sin(\omega t - \beta r) \right] \cos\theta \cos\varphi$$

$$+ \frac{k_4}{r} \left[k_5 \cos(\omega t - \beta r) + k_6 \sin(\omega t - \beta r) \right] \cos\theta \sin\varphi \quad (19)$$

$$A_\varphi = -\frac{k_1}{r} \left[k_2 \cos(\omega t - \beta r) + k_3 \sin(\omega t - \beta r) \right] \sin\varphi$$

$$+ \frac{k_4}{r} \left[k_5 \cos(\omega t - \beta r) + k_6 \sin(\omega t - \beta r) \right] \cos\varphi \quad (20)$$

Now $\overline{H} = \nabla \times \overline{A}$

and from Maxwell's equations

$$\nabla \times \overline{H} = \epsilon \frac{\partial \overline{E}}{\partial t}$$

in a region in which free charges do not exist. Then

$$\nabla \times \nabla \times \overline{A} = \epsilon \frac{\partial \overline{E}}{\partial t}$$

and

$$\overline{E} = \frac{1}{\epsilon} \int \nabla \times \nabla \times \overline{A} \, dt \tag{21}$$

In this derivation the assumption has been made that the point, P, is very remote from the antenna location and, hence, r is very large. In the expression for $\nabla \times \nabla \times \overline{A}$ all terms but two contain $1/r$ or $1/r^2$. Since r is large, these latter terms soon become negligible with respect to the other two terms and, for this case,

$$\nabla \times \nabla \times \overline{A} = \overline{a}_r(0) - \overline{a}_\theta \frac{\partial^2 A_\theta}{\partial r^2} - \overline{a}_\varphi \frac{\partial^2 A_\varphi}{\partial r^2} \tag{22}$$

From Equation 21 it can be seen that $E_r = 0$ since the r component of $\nabla \times \nabla \times \overline{A} = 0$.

For the θ component of $\nabla \times \nabla \times \overline{A}$ from Equation 22,

$$\nabla \times \nabla \times \overline{A} \Big|_\theta = - \frac{\partial^2 A_\theta}{\partial r^2} \tag{23}$$

Taking the second derivation of Equation 19 and again neglecting all terms containing $1/r^2$ and higher powers of r, it is found that

$$-\frac{\partial^2 A_\theta}{\partial r^2} = \beta^2 A_\theta \tag{24}$$

For the φ component, one obtains by a similar treatment of Equation 20

$$-\frac{\partial^2 A_\varphi}{\partial r^2} = \beta^2 A_\varphi \tag{25}$$

Then,

$$E_\theta = \frac{1}{\epsilon}\int \nabla \times \nabla \times \bar{A}\, dt\Big]_{-\theta} = \frac{1}{\epsilon}\beta^2 \int A_\theta dt \tag{26}$$

and

$$E_\varphi = \frac{1}{\epsilon}\int \nabla \times \nabla \times \bar{A}\, dt\Big]_{-\varphi} = \frac{1}{\epsilon}\beta^2 \int A_\varphi dt \tag{27}$$

$$E_\theta = \frac{\beta^2 k_1}{\epsilon r}\left[\frac{k_2}{\omega}\sin(\omega t - \beta r) - \frac{k_3}{\omega}\cos(\omega t - \beta r)\right]\cos\theta\cos\varphi$$

$$+ \frac{\beta^2 k_4}{\epsilon r}\left[\frac{k_5}{\omega}\sin(\omega t - \beta r) - \frac{k_6}{\omega}\cos(\omega t - \beta r)\right]\cos\theta\sin\varphi$$

$$E_\theta = \frac{I_0 \beta}{4\pi\omega\epsilon r_0}\left(\frac{\cos\theta\cos\varphi}{1 - \sin^2\theta\cos^2\varphi}\right)\left\{\left[\cos(\beta\ell\sin\theta\cos\varphi) - \cos\beta\ell\right]\sin(\omega t - \beta r)\right.$$

$$\left. - \left[\sin\beta\ell\sin\theta\cos\varphi - \sin(\beta\ell\sin\theta\cos\varphi)\right]\cos(\omega t - \beta r)\right\}$$

$$- \frac{I_0 \beta}{4\pi\omega\epsilon r_0}\left(\frac{\cos\theta\sin\varphi}{1 - \sin^2\theta\sin^2\varphi}\right)\left\{\left[\cos(\beta\ell\sin\theta\sin\varphi) - \cos\beta\ell\right]\sin(\omega t - \beta r\right.$$

$$\left. - \left[\sin\beta\ell\sin\theta\sin\varphi - \sin(\beta\ell\sin\theta\sin\varphi)\right]\cos(\omega t - \beta r)\right\} \tag{28}$$

$$E_\varphi = \frac{-\beta^2 k_1}{\omega \epsilon r_0}\left[k_2 \sin(\omega t - \beta r) - k_3 \cos(\omega t - \beta r)\right]\sin\varphi$$

$$+ \frac{\beta^2 k_4}{\omega \epsilon r_0}\left[k_5 \sin(\omega t - \beta r) - k_6 \cos(\omega t - \beta r)\right]\cos\varphi$$

$$E_\varphi = \frac{-\beta I_0}{4\pi\omega\epsilon r_0}\left(\frac{\sin\varphi}{1 - \sin^2\theta\cos^2\varphi}\right)\left\{\left[\cos(\beta\ell \sin\theta\cos\varphi) - \cos\beta\ell\right]\sin(\omega t - \beta r)\right.$$

$$\left. - \left[\sin\beta\ell \sin\theta\cos\varphi - \sin(\beta\ell \sin\theta\cos\varphi)\right]\cos(\omega t - \beta r)\right\}$$

$$- \frac{\beta I_0}{4\pi\omega\epsilon r_0}\left(\frac{\cos\varphi}{1 - \sin^2\theta\sin^2\varphi}\right)\left\{\left[\cos(\beta\ell \sin\theta\sin\varphi) - \cos\beta\ell\right]\sin(\omega t - \beta r)\right.$$

$$\left. - \left[\sin\beta\ell \sin\theta\sin\varphi - \sin(\beta\ell \sin\theta\sin\varphi)\right]\cos(\omega t - \beta r)\right\} \qquad (29)$$

To simplify the mechanics of further calculations, let

$$A = \cos(\beta\ell \sin\theta\cos\varphi)$$

$$B = -\left[\sin\beta\ell \sin\theta\cos\varphi - \sin(\beta\ell \sin\theta\cos\varphi)\right]$$

$$C = \cos(\beta\ell \sin\theta\sin\varphi)$$

$$D = -\left[\sin\beta\ell \sin\theta\sin\varphi - \sin(\beta\ell \sin\theta\sin\varphi)\right] \qquad (30)$$

The above factors are common to both E_θ and E_φ.

$$\text{Let } E = \frac{\sin\varphi}{1 - \sin^2\theta\cos^2\varphi} \qquad G = \frac{\cos\theta\cos\varphi}{1 - \sin^2\theta\cos^2\varphi}$$

$$F = \frac{\cos\varphi}{1 - \sin^2\theta\sin^2\varphi} \qquad H = \frac{\cos\theta\sin\varphi}{1 - \sin^2\theta\sin^2\varphi} \qquad (31)$$

Substitution of Equations 30 and 31 into Equations 29 and 28 yields

$$|E_\varphi| = \left| \frac{\beta I_o}{4\pi\omega\epsilon r_o} \left\{ (E) \left[A \sin(\omega t - \beta r) + B \cos(\omega t - \beta r) \right] + F \left[C \sin(\omega t - \beta r) + D \cos(\omega t - \beta r) \right] \right\} \right|$$

$$= \left| \frac{\beta I_o}{4\pi\omega\epsilon r_o} \left\{ (EA + FC) \sin(\omega t - \beta r) + (EB + FD) \cos(\omega t - \beta r) \right\} \right|$$

$$= \sqrt{(EA + FC)^2 + (EB + FD)^2} \quad \frac{\beta I_o}{4\pi\omega\epsilon r_o} \tag{32}$$

$$|E_\theta| = \left| \frac{\beta I_o}{4\pi\omega\epsilon r_o} \left\{ G\left[A \sin(\omega t - \beta r) + B \cos(\omega t - \beta r) \right] - H\left[C \sin(\omega t - \beta r) + D \cos(\omega t - \beta r) \right] \right\} \right|$$

$$= \left| \frac{\beta I_o}{4\pi\omega\epsilon r_o} \left\{ (GA - HC) \sin(\omega t - \beta r) + (GB - HD) \cos(\omega t - \beta r) \right\} \right|$$

$$= \sqrt{(GA - HC)^2 + (GB - HD)^2} \quad \frac{\beta I_o}{4\pi\omega\epsilon r_o} \tag{33}$$

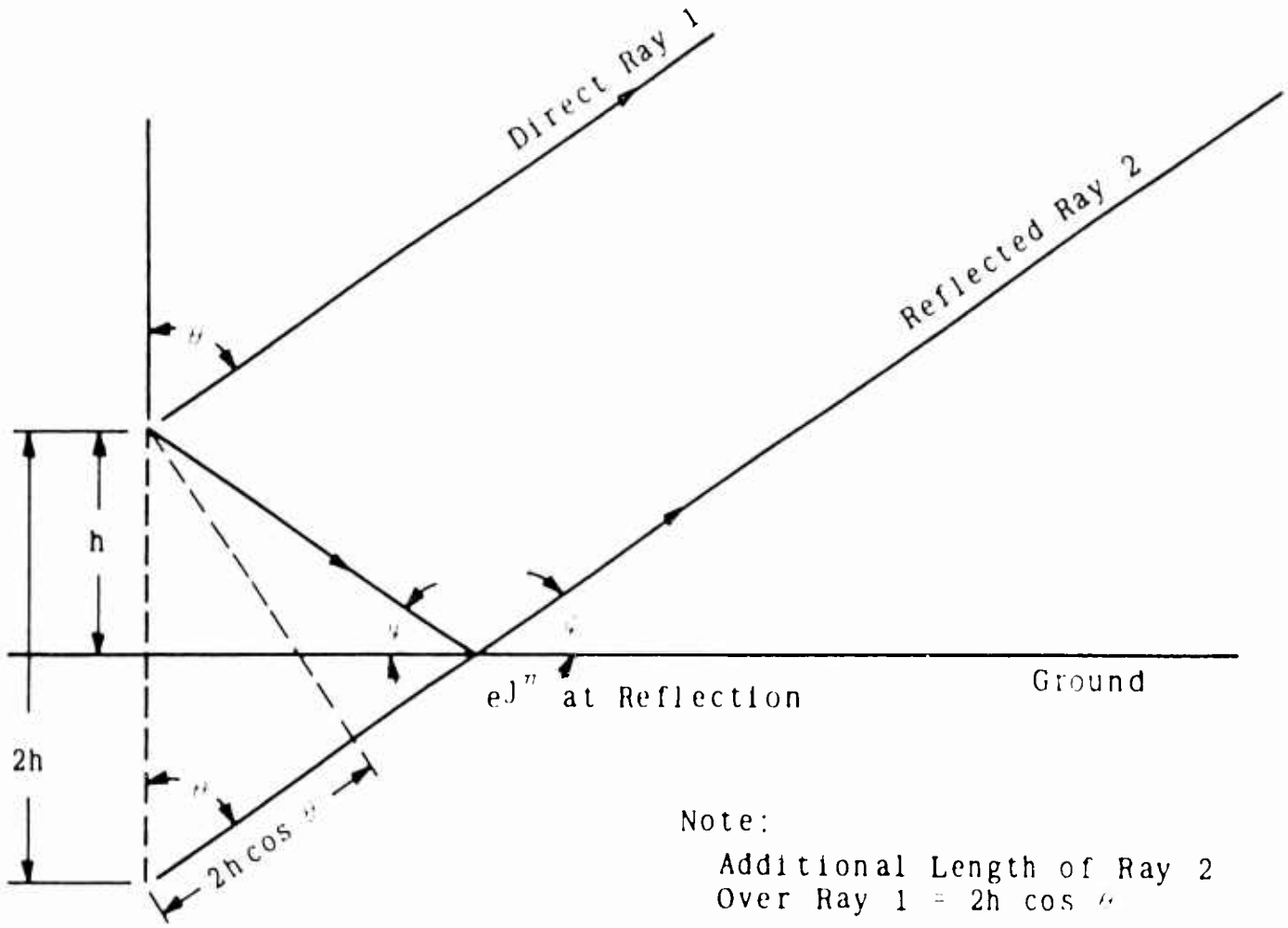

Note:

Additional Length of Ray 2
Over Ray 1 = 2h cos

Figure A.3. Path Length Difference.

When the angle is θ for the direct ray, it is $180° - \theta$ for the reflected ray.

$$\sin(180° - \theta) = \sin \theta$$

$$\cos(180° - \theta) = -\cos \theta$$

$$\cos(\theta + 180°) = -\cos \theta$$

Examination of Equations 30 and 31 shows that for the reflected ray,

A is again A B is again B C is again C

D is again D E is again E F is again F

but G is now -G and H is now -H

and reference to Equations 28 and 29 shows that

E_θ reflected = $-E_\theta$ direct

E_φ reflected = E_φ direct

$$\text{Now } E_{res\ \varphi} = E_\varphi\sqrt{1 + \overline{DR}^2 + 2DR\cos(\theta' - \phi)} = E_\varphi\sqrt{1 + D^2 - 2D\cos\theta'} \quad (R = -1)$$

$$= E_\varphi\sqrt{2 - 2\cos\theta'} = \sqrt{2}\,E_\varphi\sqrt{1 - \cos\theta'} = 2E_\varphi \sin\frac{\theta'}{2} \quad (D \doteq 1)$$

In which θ' is the path length difference between the direct and the reflected rays and as shown in Figure 3 is, in radians, $2h\cos\theta\left(\frac{2\pi}{\lambda}\right)$ or in degrees is $2h\cos\theta\left(\frac{360^\circ}{\lambda}\right)$. Then

$$E_{res\ \varphi} = 2E_\varphi \sin\left(\frac{2\pi}{\lambda} h\cos\theta\right) \tag{34}$$

For the E_θ component, there is an additional 180° phase shift to be considered for the reflected ray, so

$$E_{res\ \theta} = E_\theta\sqrt{1 + \overline{DR}^2 + 2DR\cos(\theta' - \varphi - 180^\circ)}$$

$$= E_\theta\sqrt{1 + D^2 + 2D\cos\theta'}$$

$$= E_\theta\sqrt{2 + 2\cos\theta'}$$

$$= 2E_\theta\cos\frac{\theta'}{2}$$

$$= 2E_\theta\cos\left(\frac{2\pi h}{\lambda}\cos\vartheta\right) \tag{35}$$

The total value of E horizontally polarized is

$$T^{E_H} = \sqrt{E_\varphi{}^2{}_{res} + E_\theta{}^2{}_{res}\cos^2\theta}$$

or

$$ {}_{T}E_{H} = \sqrt{\left[2E_{\varphi} \sin\left(\frac{2\pi h}{\lambda} \cos\theta\right)\right]^2 + \left[2E_{\theta} \cos\left(\frac{2\pi h}{\lambda} \cos\theta\right)\cos\theta\right]^2} $$

$$ = 2\sqrt{E_{\varphi}^2 \sin^2\left(\frac{2\pi h}{\lambda} \cos\theta\right) + E_{\theta}^2 \cos^2\left(\frac{2\pi h}{\lambda} \cos\theta\right)\cos^2\theta} \qquad (36) $$

Let $\frac{2\pi h}{\lambda} \cos\theta = \alpha$

Then,

$$ {}_{T}E_{H} = 2\sqrt{E_{\varphi}^2 \sin^2\alpha + E_{\theta}^2 \cos^2\alpha \cos^2\theta} $$

$$ = 2\sqrt{(E_{\varphi}^2 - E_{\theta}^2 \cos^2\theta) \sin^2\alpha + E_{\theta}^2 \cos^2\theta} \qquad (37) $$

The total value of E vertically polarized is obtained in a similar manner. However, in this case, the vertical component, E_{θ}, is assumed to be reflected from the ground with zero phase shift. Thus

$$ {}_{T}E_{V} = E_{\theta} \sin\theta \left[1 + \overline{DR}^2 + 2DR \cos(\theta' - 180°)\right]^{\frac{1}{2}} $$

$$ = E_{\theta} \sin\theta \left[2 - 2\cos\theta'\right]^{\frac{1}{2}} $$

$$ {}_{T}E_{V} = 2E_{\theta} \sin\theta \cos\left(\frac{2\pi h}{\lambda} \cos\theta\right) $$

A measure of the energy radiated in a given direction is given by

$$ E_{Q} = \sqrt{{}_{T}E_{V}^2 + {}_{T}E_{H}^2} $$

Example:

$$ \ell = \frac{\lambda}{4} \qquad h = \frac{\lambda}{8} \qquad \beta\ell = \frac{\pi}{2} $$

$$ \alpha = \frac{2\pi h}{\lambda} \cos\theta = \frac{\pi}{4} \cos\theta = 43.5° $$

$\theta = 15°$ $E_\theta = 0$ $\varphi = 45°$ $E_\varphi = 1.411$

$\sin 43.5° = 0.688$ $\quad {}_TE_H = 2\sqrt{1.411^2 \times 0.688^2} = 1.942K$

${}_TE_V = 0$ $\quad E_Q = 1.942K$

$\theta = 15°$ $E_\theta = 0.961$ $\varphi = 90°$ $E_\varphi = 1.0$

$\cos\theta = \cos 15° = 0.965$

${}_TE_H = 2\sqrt{(1.0^2 - 0.961^2 \times 0.965^2) \times 0.688^2 + 0.961^2 \times 0.965^2}$

$= 1.920K$

${}_TE_V = .342$ $\quad E_Q = 1.971K$

$\theta = 15°$ $E_\theta = 1.355$ $\varphi = 135°$ $E_\varphi = 0.147$

$\cos\theta = 0.965$

${}_TE_H = 2\sqrt{(0.147^2 - 1.355^2 \times 0.965^2) \times 0.688^2 + 1.355^2 \times 0.965^2}$

$= 1.906$

${}_TE_V = 0.481$ $\quad E_Q = 1.971K$

where

$$K = \frac{\beta I_o}{4\pi\omega\epsilon r_o}$$

Values of E_Q have been plotted in Figures 4 through 16 as a function of the angles θ and φ. Figures 4 through 7 show the virtually omnidirectional pattern obtained for $\ell = 0.25\lambda$ ($\beta\ell = \frac{\pi}{2}$) and $h = 0.125\lambda$. Figures 4, 8, 9 and 10 illustrate the effect of changing the antenna height. These figures show that the omnidirectional trend occurs when the height is an odd multiple of $\lambda/8$.

Patterns for $\ell = 0.1\lambda$ and $h = 0.5\lambda$ are shown in Figures 11 through 14. The omnidirectional trend for heights which are odd

multiples of $\lambda/8$ is again illustrated in Figure 15 where patterns for $\theta = 15°$, $\ell = 0.1\lambda$ have been plotted as a function of h/λ. Figure 16 shows a typical vertical radiation pattern.

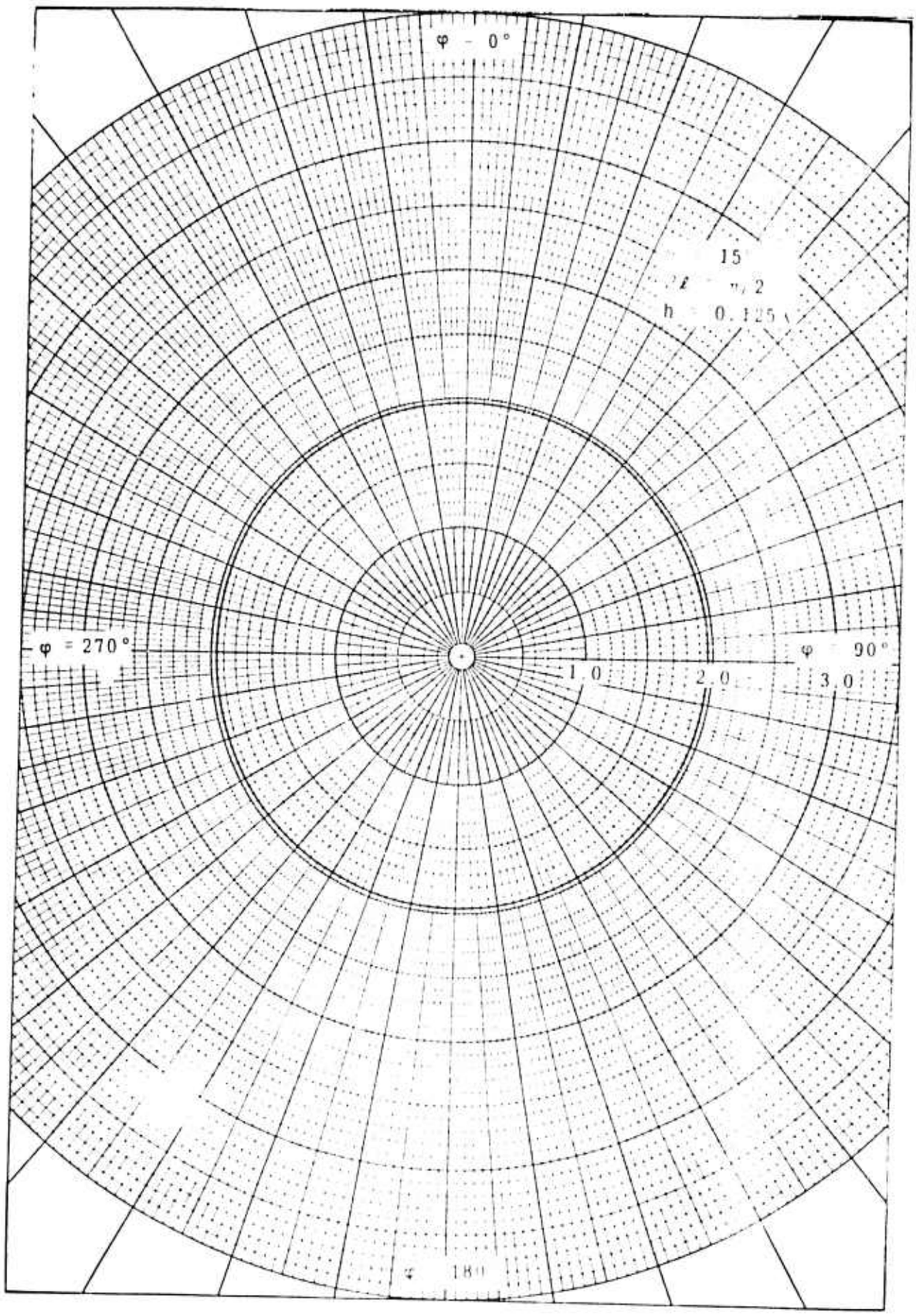

Figure A.4 E_Q Versus φ.

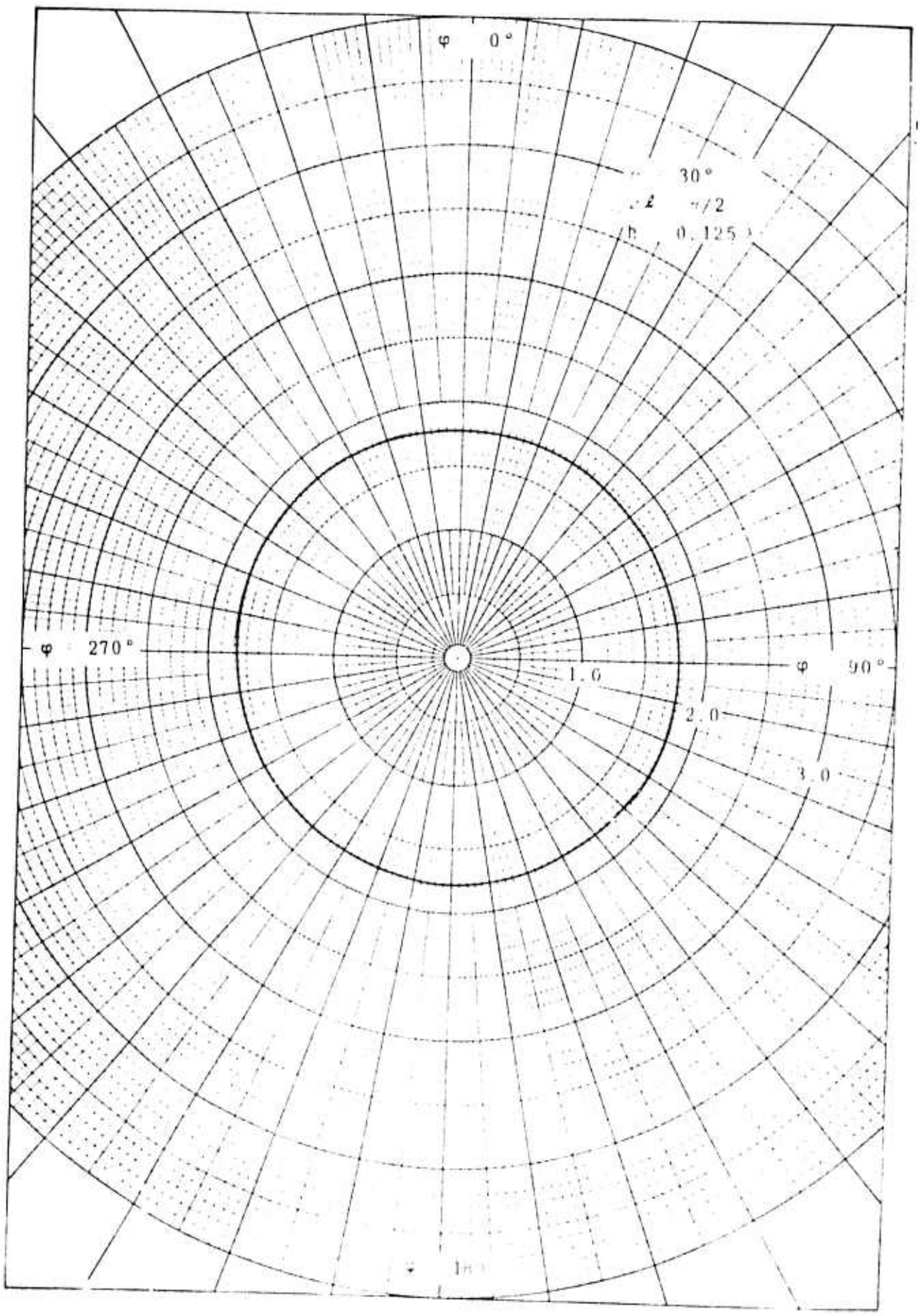

Figure A.5. E_Q Versus φ.

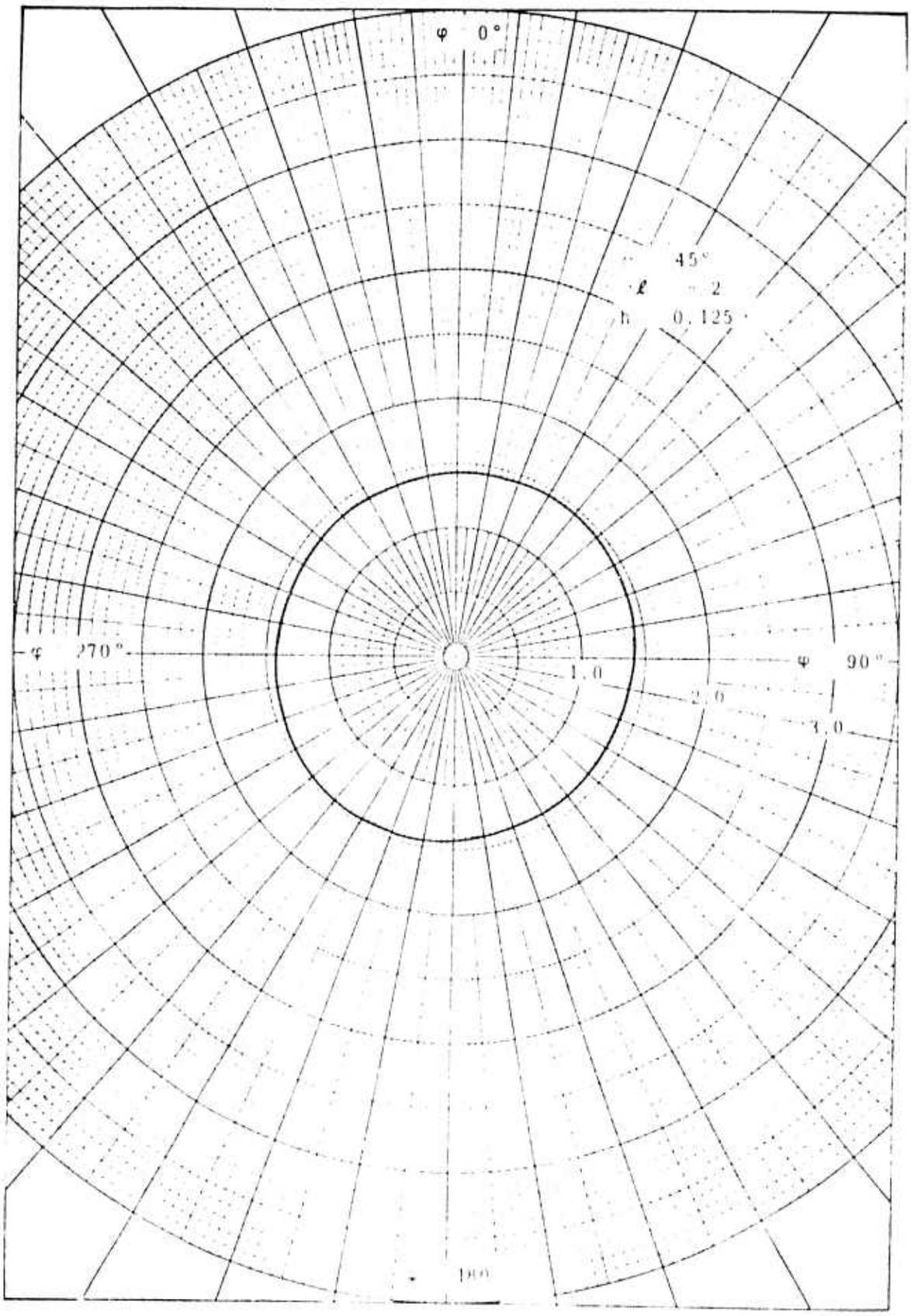

Figure A.6. E_Q Versus φ.

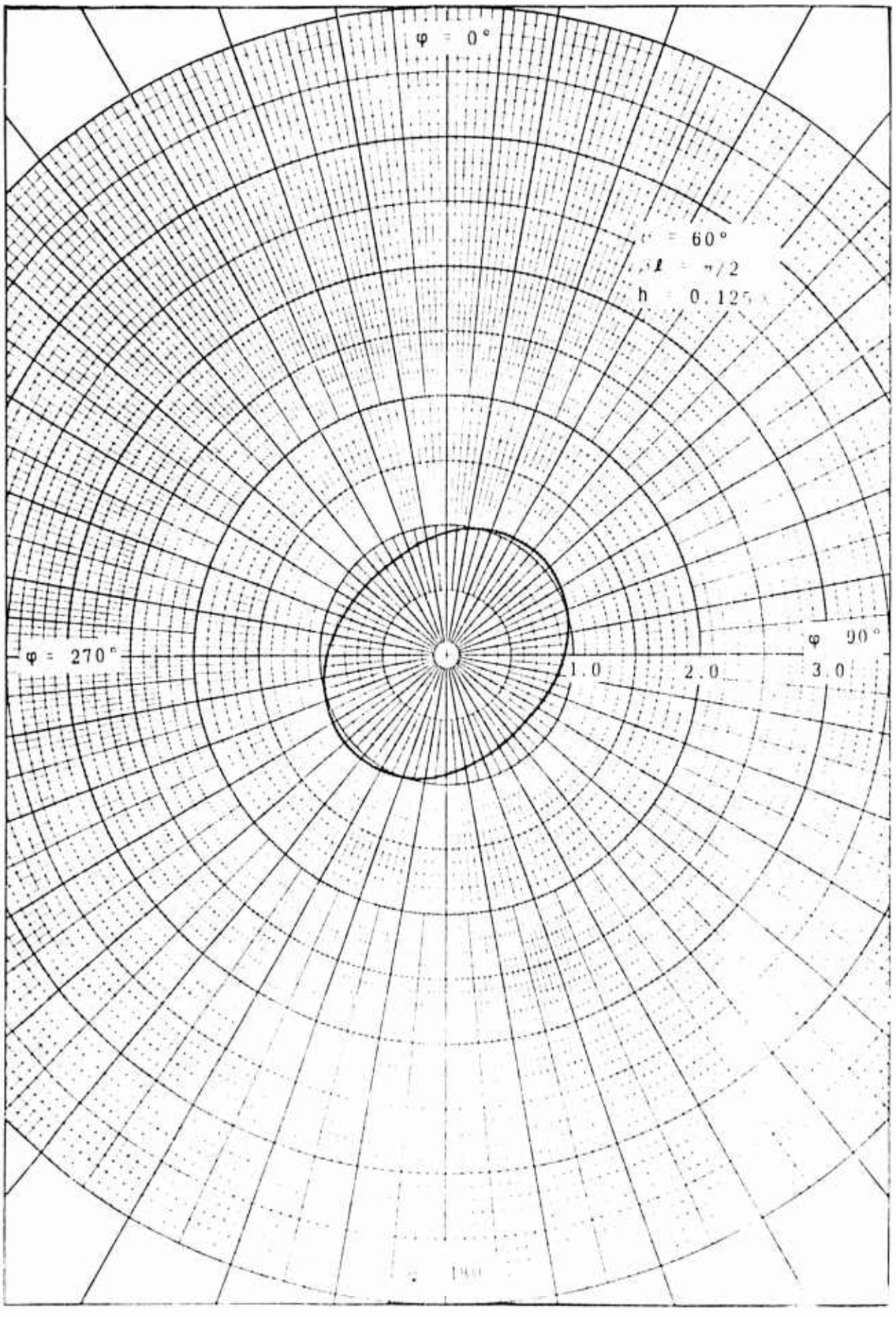

Figure A.7. E_Q Versus φ.

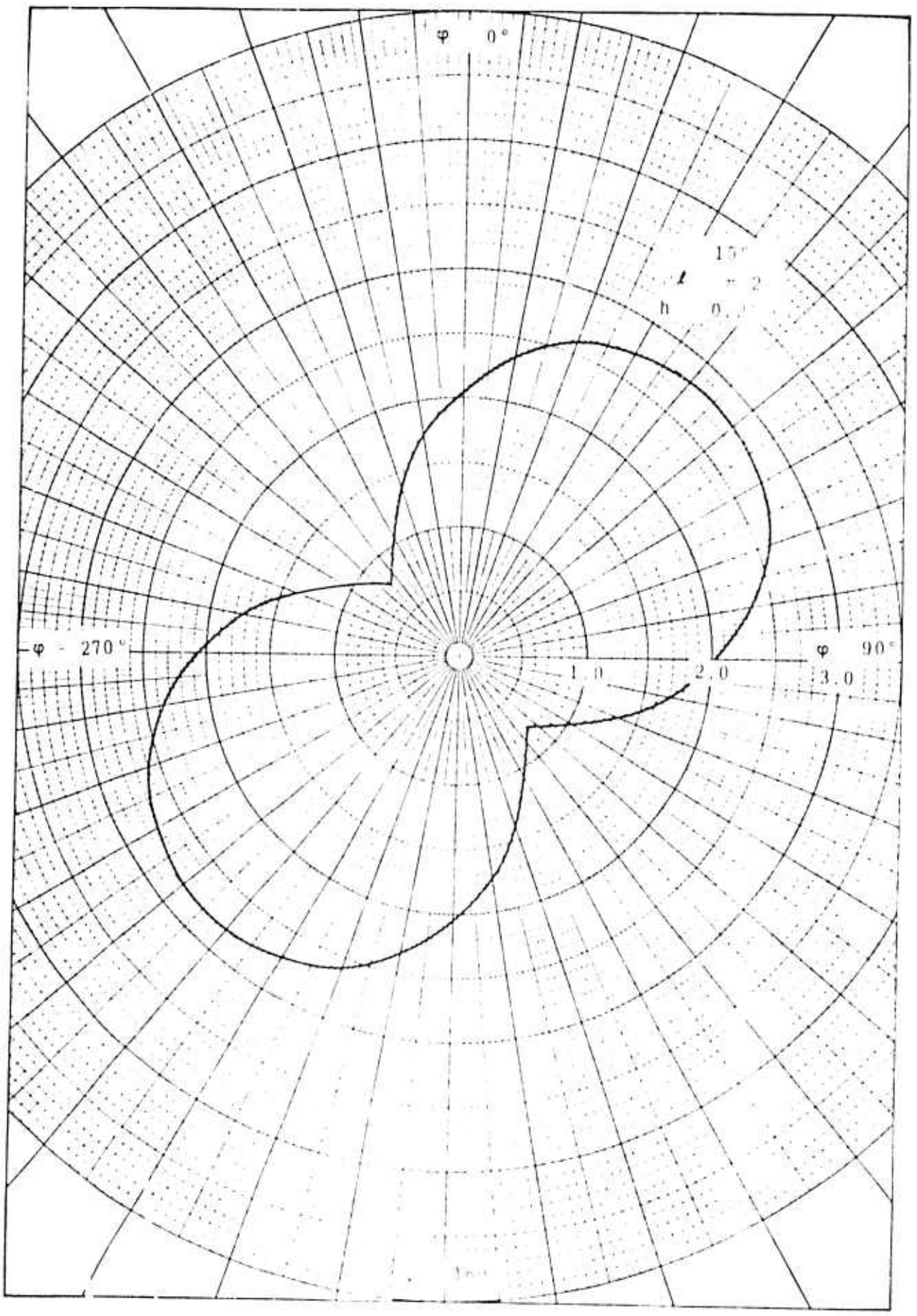

Figure A 8 F_Q Versus φ

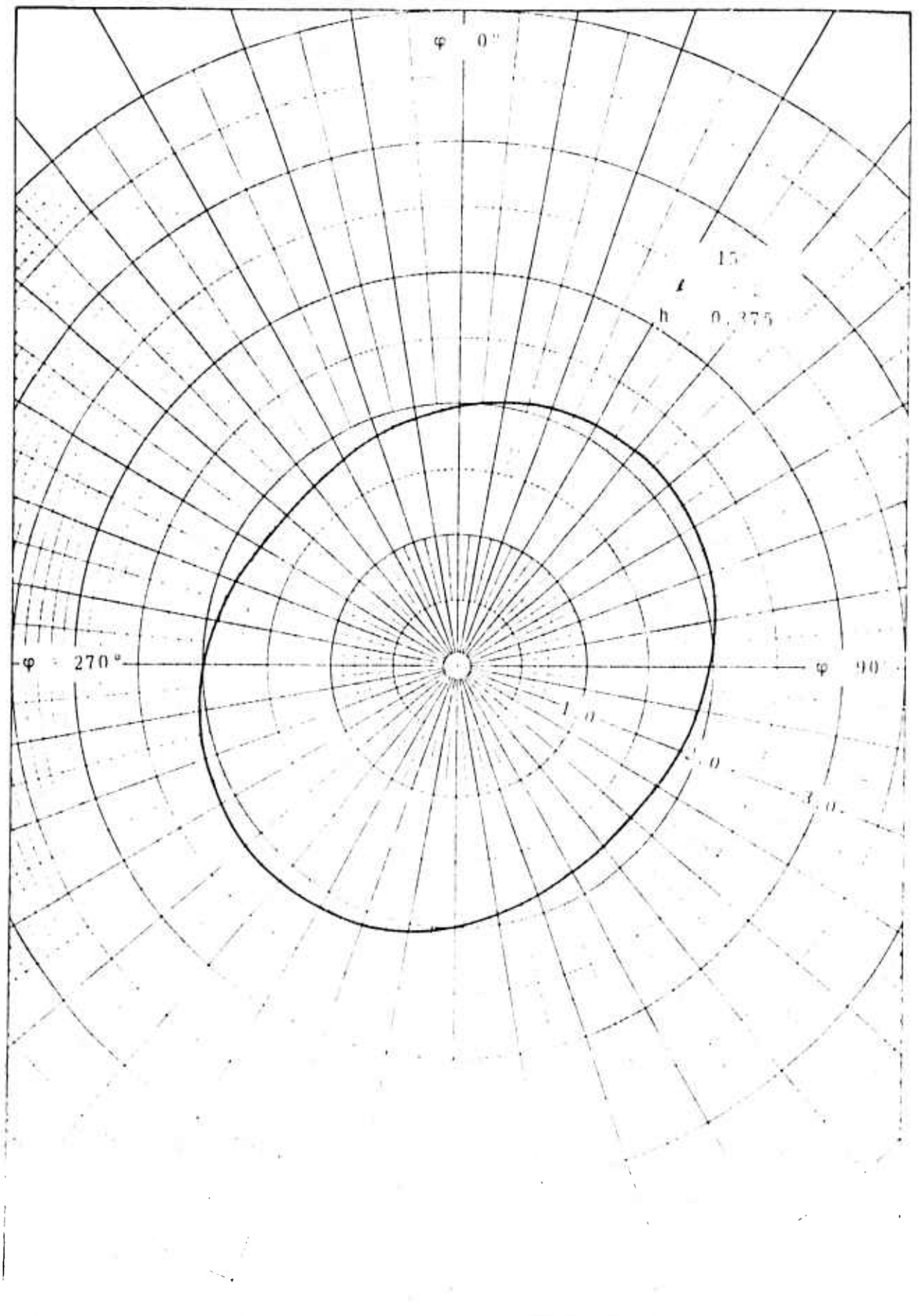

Figure A.9 E_Q Versus φ.

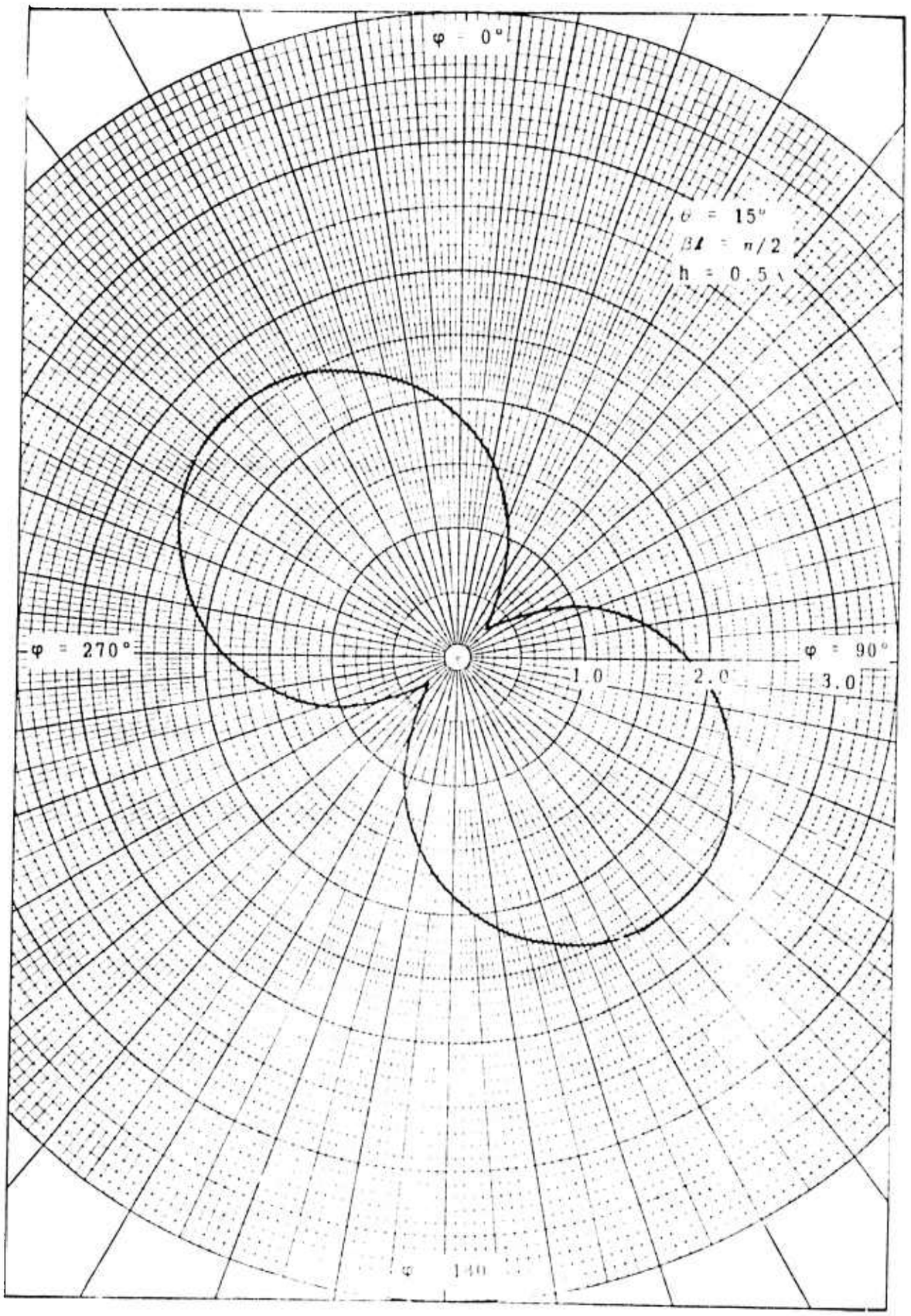

Figure A.10 E_Q Versus φ.

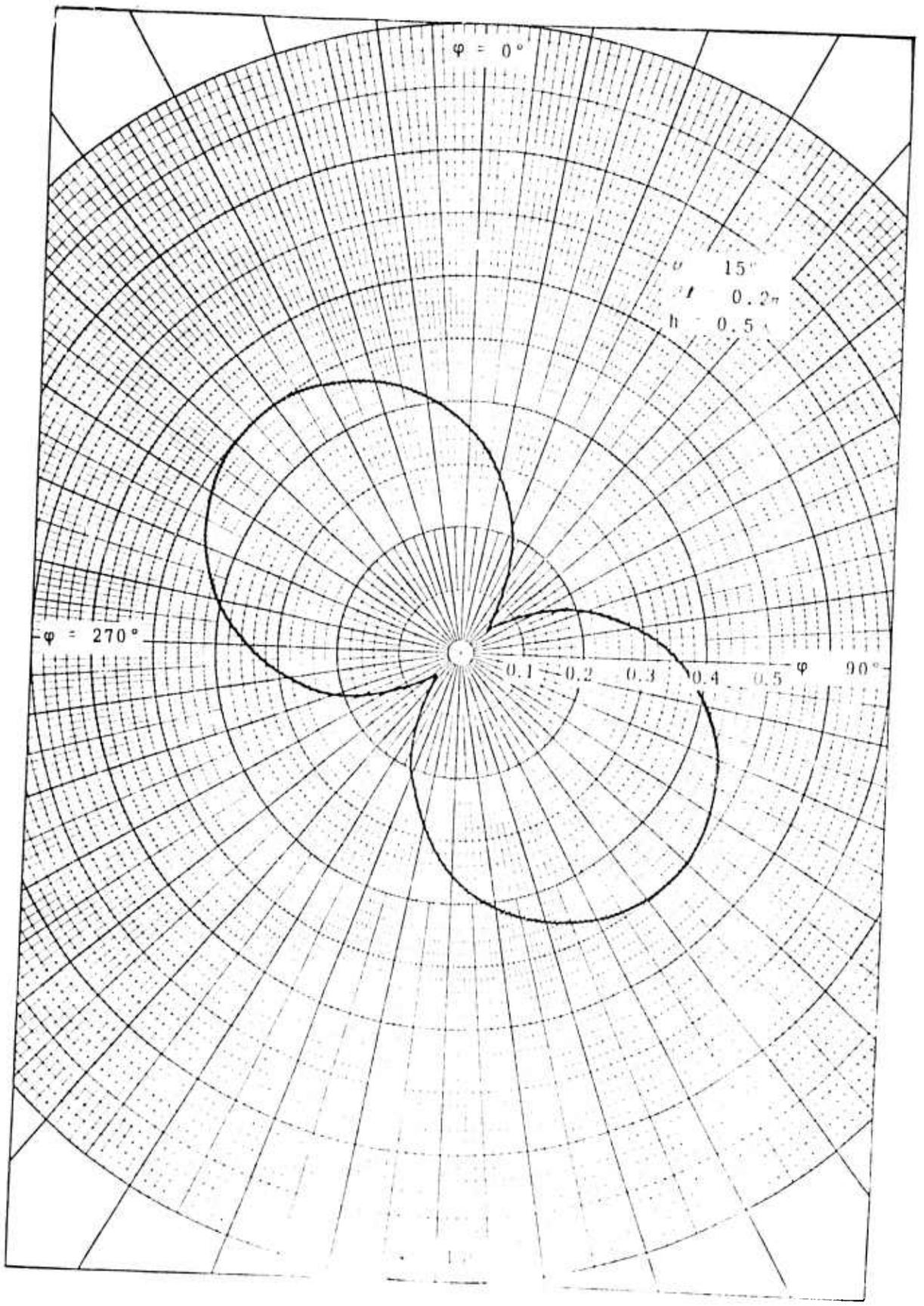

Figure A.11 E_Q Versus φ

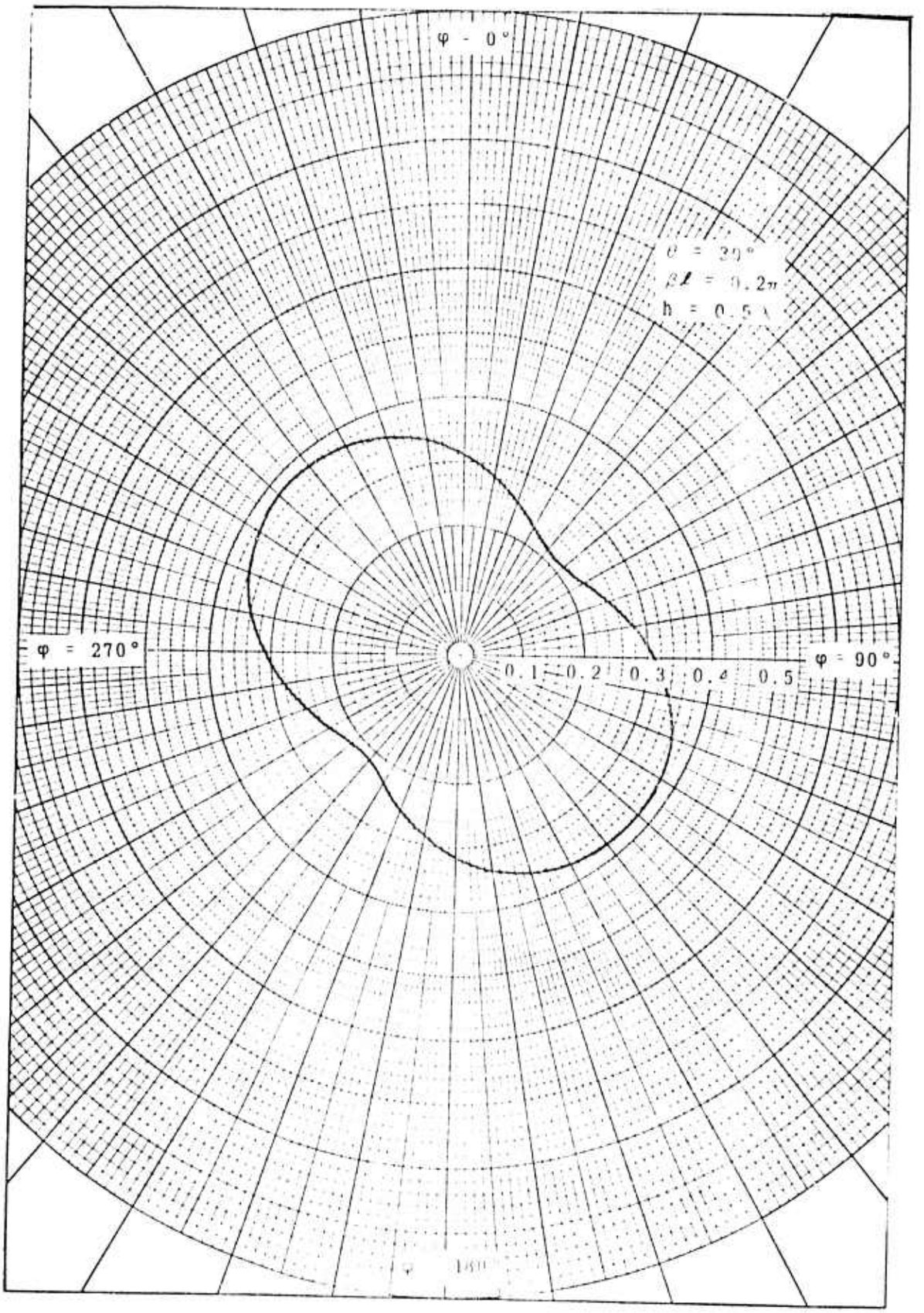

Figure A.12 E_Q Versus φ.

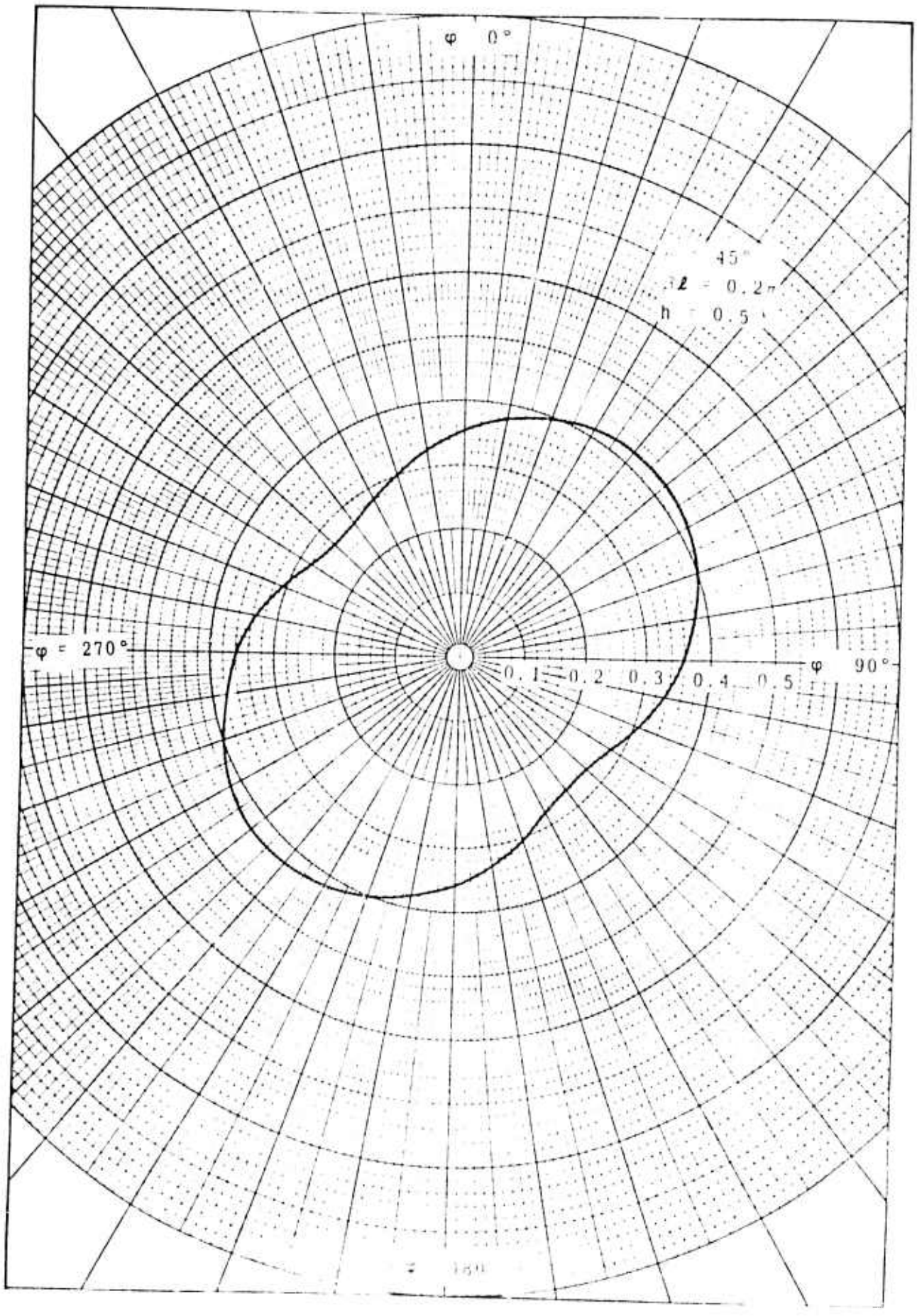

Figure A 13 E_Q Versus φ.

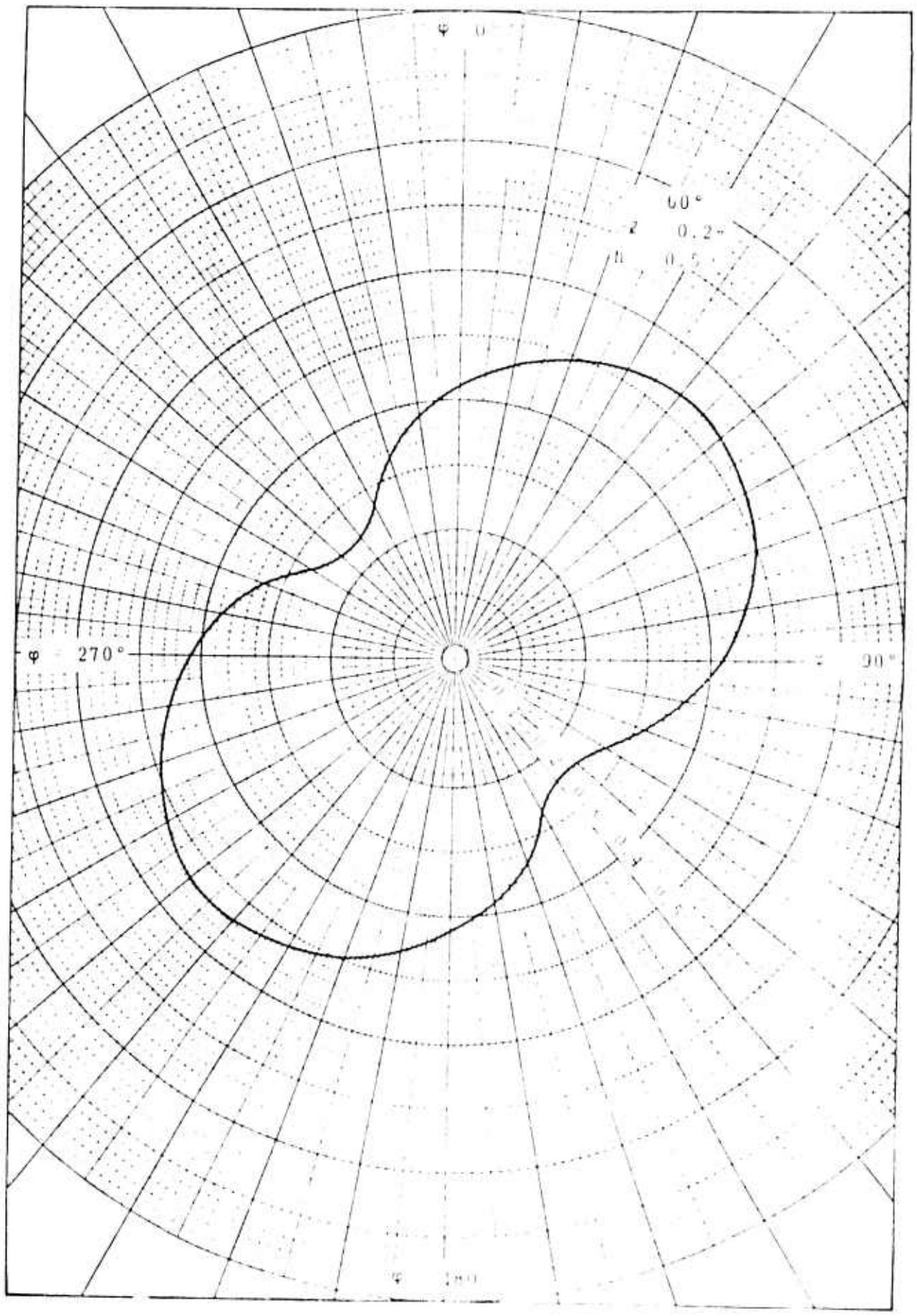

Figure A 14 E_Q Versus φ.

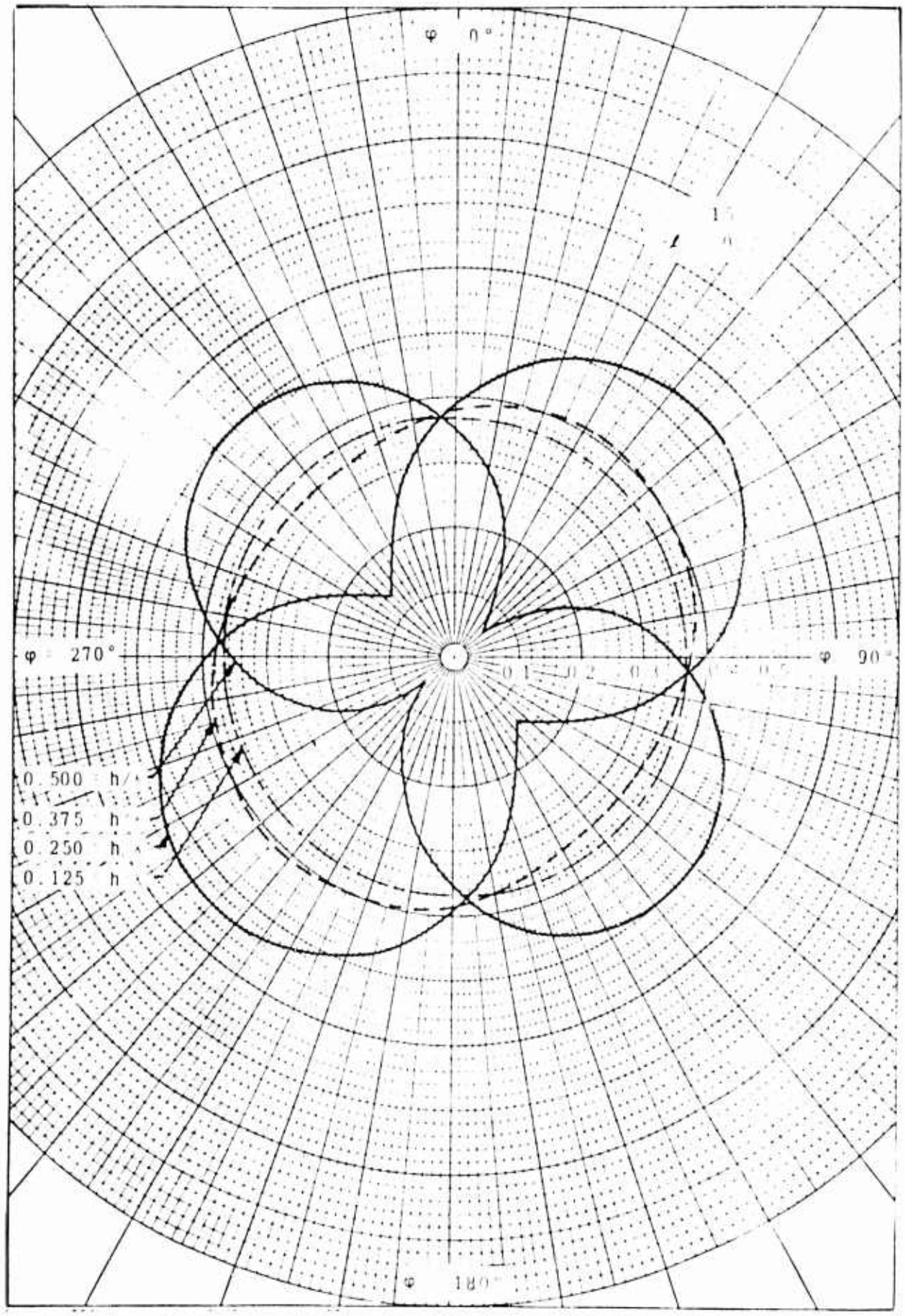

Figure A.15. E_Q Versus φ.

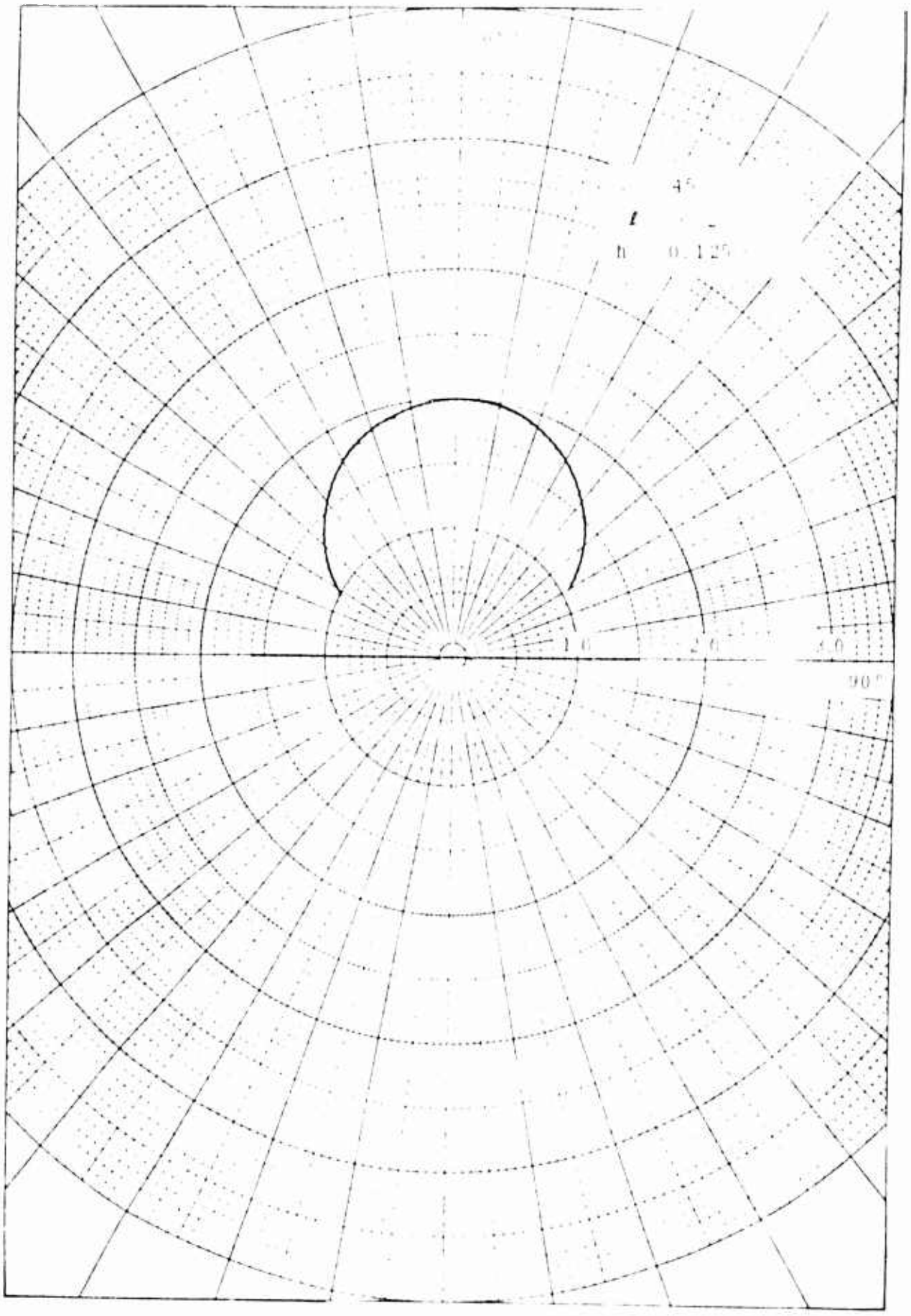

Figure A 16 E_Q Versus